CHARACTERIZATION OF YIELD AND YIELD COMPONENTS USING BI-PARENTAL AND ASSOCIATION MAPPING OF TEXAS POPULAR CULTIVARS AND SYNTHETIC WHEAT

A Dissertation

by

YAN YANG

Submitted to the Office of Graduate and Professional Studies of
Texas A&M University
in partial fulfillment of the requirements for the degree of

DOCTOR OF PHILOSOPHY

Chair of Committee,	Shuyu Liu
Co-Chair of Committee,	Amir M. H. Ibrahim
Committee Members,	Jackie C. Rudd
	Qingwu Xue
	Dirk Hays
	Xuejun Dong
Head of Department,	David D. Baltensperger

August 2018

Major Subject: Plant Breeding

ABSTRACT

Defining genetic architecture of complex traits is a fundamental step towards marker-assisted selection (MAS) for wheat improvement. Quantitative trait loci (QTL) studies provide prime information on the action, number and effect of QTL/genes controlling quantitative traits. The objective of this study was to use a saturated genetic map, derived from 90K single nucleotide polymorphic (SNP) array and genotype-by-sequence (GBS) markers, to map QTL associated with stripe rust resistance, grain yield, yield components, and other agronomic traits including test weight, height, and heading date. A mapping population of 124 F_6 recombinant inbred lines (RILs) developed from the cross 'TAM 112'/'TAM 111' was developed. A set of 9928 markers were used for QTL analyses. The largest and most consistent stripe rust resistance QTL was identified on the long arm of chromosome 2B. Five tightly linked SNP markers were converted to Kompetitive allele specific PCR (KASP) markers for high throughput screening. The corresponding diagnostic markers should be applied through marker-assisted breeding. The same mapping population was used to identify and characterize QTL for yield and yield components for which data was obtained from eight Texas environments. QTL analysis was performed using the three different software based on individual environment and three mega-environments. Four unique and consistent QTL regions with pleiotropic effects were identified after comparing different models, which were distributed on chromosome fragment 1D2, 2D1, 4D, and 7D1. Synthetic derived wheat (SDW) has been reported to produce more yield than conventional bread wheat. To understand the genetics of marker-trait associations underlying yield performance in SDW, field trials were conducted at nine locations over three years. Yield, yield components, and other agronomic traits were measured on a panel of 419 SDW lines. We

employed GBS to identify the genetic loci for yield traits though genome wide association studies (GWAS). All accessions, which were derived from synthetic spring lines crossed with TAM 111 or TAM 112, clustered into two subgroups, which were highly consistent with their pedigrees. The results of this study uncovered 45 loci associated with yield, yield components, and agronomic traits in individual environment based on best linear unbiased predication values. Candidate genes co-localized with such QTL, thereby providing potential targets for selection.

DEDICATION

Dedicated to my dearest mother, Canxia Shi, my beloved husband, Shumao Zhang, and my incoming newborn.

ACKNOWLEDGEMENTS

I would like to express my deepest gratitude to my Ph.D. advisors, Dr. Shuyu Liu and Dr. Amir M. H. Ibrahim, for their tremendous support and guidance throughout my research at Texas A&M University. Their continuous intense training, guidance, and inspiration educated me into a professional researcher in wheat molecular breeding. Their enthusiasm and devotion to academic work always invigorated me to engage in the chase of science. I am fortunate to have their knowledgeable advice which was carefully aimed in the direction of my professional and my research life.

I would like to express my sincere appreciation to Dr. Jackie C. Rudd, Dr. Qingwu Xue, Dr. Dirk B. Hays, and Dr. Xuejun Dong for serving as my committee members and offering many profound comments and suggestions on my research. Their precious time is invaluable to me.

My heartfelt appreciation also goes to my previous and current colleagues in wheat breeding lab, Dr. Bharath Reddy, Dr. Silvano Ocheya, Dr. Sarah Ajayi, Dr. Geraldine Opena, Mr. Bryan Simoneaux, Mr. Smit Dhakal, Mr. Hussam Alawadi, Miss Jordanna Tadlock, Mr. Anil Adhikari, Mr. Mahendra Bhandari and Mr. Brandon Gerrish, for their support of my research work and their friendship beyond the academic life. I thank Miss Lisa Garza, Ms Maria Pilar Fuentealba, Mr. Chor Tee Tan, Miss Hangjin Yu, Miss Jackie Avila, Miss Kila Andrews, Mr. Julio Rocha, Mr. Cameron Skees, Mr. Jason Baker, Mr. Kirk Jessup, and Dr. Ravindra Devkota for developing the population in the present study and for their support in phenotypic evaluation in Texas, USA. I also than Dr. Charlie D. Johnson, Dr. Richard Metz, Dr. Shichen Wang for helping my project on GBS data analysis. I am indebted to my colleagues and the

entire wheat breeding and genetics lab team who made my research studies achievable and this dissertation possible.

My sincere gratitude goes to the Monsanto's Beachell-Borlaug International Scholars program for the financial support of my doctorate studies. I am indebted to Dr. Edward Runge, the chair of the MBBIS Judging Committee for his continued support and encouragement throughout my studies. Thanks to partial funding from Tecas A&M AgriLife Research and Texas Wheat Producer Board to Dr. Shuyu Liu.

I am grateful to the administrative staff at the Department of Soil and Crop Sciences and Texas A&M AgriLife Research for their support and facilitation of my doctoral research program. Thanks also go to my friends and colleagues and the department faculty and staff for making my time at Texas A&M University a great experience.

Thanks to my mother for her encouragement and to my husband, Shumao Zhang for his patience and love.

CONTRIBUTORS AND FUNDING SOURCES

This work was supervised by a dissertation committee consisting of Dr. Shuyu Liu, (advisor), Dr. Amir M. H. Ibrahim (co-advisor), Dr. Jackie C. Rudd, Dr. Qingwu Xue, Dr. Dirk Hays, and Dr. Xuejun Dong of the Department of Soil and Crop Sciences. All work for the dissertation was completed independently by the student.

Graduate study was supported by a scholarship from the Monsanto's Beachell Borlaug International Scholarship Program (MBBISP), a fellowship from the Tom Slick Senior Graduate Research Fellowship Program by Texas A&M University, Texas A&M AgriLife Research and Texas Wheat Producer Board.

TABLE OF CONTENTS

Page

ABSTRACT ii

DEDICATION iv

ACKNOWLEDGEMENTS v

CONTRIBUTORS AND FUNDING SOURCES vii

TABLE OF CONTENTS viii

LIST OF FIGURES x

LIST OF TABLES xi

CHAPTER I INTRODUCTION 1

CHAPTER II DEVELOPING KASP MARKERS FOR A MAJOR STRIPE RUST RESISTANCE QTL IN TAM 111 USING 90K ARRAY AND GENOTYPING-BY-SEQUENCING 4

2.1 Introduction 4
2.2 Materials and methods 6
2.3 Results 10
2.4 Discussion 25
2.5 References 33

CHAPTER III ANALYSIS OF QTL ASSOCIATED WITH YIELD AND YIELD COMPONENTS IN TAM111 AND TAM112 AND THEIR INTERACTIONS WITH ENVIRONMENTS 40

3.1 Introduction 40
3.2 Materials and methods 42
3.3 Results 46
3.4 Discussion 67
3.5 References 74

CHAPTER IV GENOME-WIDE ASSOCIATION MAPPING FOR YIELD COMPONENTS IN SYNTHETIC DERIVED WHEAT LINES 84

4.1 Introduction 84

4.2 Materials and methods 86
4.3 Results 90
4.4 Discussion 111
4.5 References 115

CHAPTER V SUMMARY AND CONCLUSIONS 119

LIST OF FIGURES

Page

Figure 1. Stripe resistance for stripe resistance QTL detected based on a single trait multi-environment QTL mapping model of GenStat, (a) disease severity (DS) and (b) infection type (IT). 13

Figure 2. Linkage maps of SNPs associated with *QYr.tamu-2BL* on previous reported paper and in this study on chromosome 2B and their corresponding physical map locations on chromosome 2B of Chinese Spring. (A) Genetic map for 2BL with associated *QYr.tamu-2BL* for DS average by using DArT markers (Basnet et al., 2014), (B) Linkage group 2B89 with associated *QYr.tamu-2BL* for DS and IT by using 90K and GBS markers†, (C) Linkage group 2B7 in this study, (D) Fragment of wheat chromosome 2B reference map showing the physical location of the SNPs mapped on the high-resolution genetic map. 28

Figure 3. Three Mega-environments (MEs)† clustered by using principle component analysis (PCA) analysis..... 60

Figure 4. Manhattan plot for significant SNP associated with yield in different environments... 94

Figure 5. Manhattan plot for significant SNP associated with thousand kernel weight in different environments. 98

Figure 6. Manhattan plot for significant SNP associated with kernel spike^{-1} in different environments. 100

Figure 7. Manhattan plot for significant SNP associated with spikes m^{-2} in different environments. 102

Figure 8. Manhattan plot for significant SNP associated with harvest index in different environments. 104

LIST OF TABLES

Page

Table 1. The number of each type of mapped marker within each chromosome (Chrom), number of linkage groups (LGs) within each chromosome, the length of each chromosome in centimorgans (cM) and the marker density in cM of each chromosome for the genetic map construct from 124 RILs of a cross between TAM 112 and TAM 111. 12

Table 2. QTL associated with disease severisty (DS) and infection type (IT) for single environment analysis by using MapQTL software. 14

Table 3. QTL detected using single trait multi-environment QTL composite interval mapping model of GenStat. 17

Table 4. Additive by environment interaction for QTL associated with DS and IT by using QTLNetwork software. 20

Table 5. Epistatic and epistatic QTL by environment interactions for stripe rust resistance from QTLNetwork software. 21

Table 6. Kompetitive Allele Specfic Polymerase Chain Reaction (KASP) single-nucleotide polymorphisms (SNPs) tightly linked to *QYr.tamu-2BL* and their primer sequences. 23

Table 7. Lines and cultivars used for validation of major QTL on 2BL linked KASP markers. 24

Table 8. The combined ANOVA, heritability, and mean performance for all traits across environments. 47

Table 9. Genetic correlation among grain yield and other traits measured in individual environments. 48

Table 10. QTL for yield and yield components detected for the model of single trait with multiple environments using GenStat. 50

Table 11. Significant additive effects and additive by environment interactions of QTL for yield and yield components detected using QTLNetwork. 53

Table 12. Significant epstasis effects and epstasis by environment interactions of QTL for yield and yield components detected using QTLNetwork. 57

Table 13. Significant additive effects QTL detected for association with multiple traits across three ME using MapQTL. 61

Page

Table 14. Significant additive effects and additive by environment interactions of QTL detected by ME analysis using QTLNetwork.....62

Table 15. Epistatic QTL and their interaction with ME analysis using QTLNetwork. 64

Table 16. Comparisons of QTL identified from three models of GenStat, QTLNetwork, and MapQTL, and for yield and major yield components. 65

Table 17. QTL for yield and yield components detected for the model of single trait with multiple environments for ME analysis using GenStat.....71

Table 18. The combined ANOVA, heritability, and mean performance for all traits across environments. 91

Table 19. Genetic correlation among yield and other traits measured in individual environments. 92

Table 20. QTL identified associated with yield and yield components from GWAS. 94

Table 21. Common QTL identified associated with yield and yield components from GWAS. 110

CHAPTER I

INTRODUCTION

Because of recent spikes of the food prices and growing threat of future supplies, food security has risen to the top of the global political agenda. Providing an adequate supply of food is a key factor to food security, together with an efficient distribution system and minimization of waste (Parry, 2012). However, guaranteeing an adequate supply of food at present time could be achieved for the current global population, whereas maintaining this into the future will be challenging due to a steadily increasing world population. In addition, global food security could be jeopardized due to a reducing availability of fertile land and water for agriculture along with climate change, particularly higher temperatures and diminishing amount of rainfall causing severe drought problem (Parry and Hawkesford, 2010; Lobell et al., 2011). Even though the advances in productivity and technology in agriculture have contributed to improved food security, food supply is expected to rise by 2-3% each year to meet the projected demand. However, it is noted that the production of the major cereals, rice (*Oryza sativa*), maize (*Zea mays* L.), and wheat (*Triticum aestivum* L.) have levelled off, increasing at less than half of its rate in the past decade. Wheat shows the lowest rate of increase in yield potential, and this stagnation requires novel approaches to break the yield barrier.

Wheat is a high impact crop contributing significant number of calories and proteins on a global scale. It is the most widely planted crop and can be processed into a multitude of products spanning different cultural backgrounds (Ray et al., 2013). The annual genetic gain in wheat is barely 1.0% and in some region yield plateau has been reported. Studies have shown that an annual increase of about 2.4% in wheat yield potential is required to reach the demand threshold

required to suffice the global population in the next few decades (Hawkesford et al., 2013). The gap between the expected and observed annual increase is primarily due to biotic and abiotic stresses acting individually or interactively to reduce yield, in addition to inability to follow sound cultural practices by low input producers.

Drought stress is one of the greatest challenges to wheat productivity in the 21st century. Drought stress complexed by drought-fueled insect pest infestation, is a major impediment to crop yield in the U.S., China and tropical regions. Insect pests that were restricted to tropical regions have extended their range through migration into other areas due to climate change. Greenbugs [GB, *Schizaphis graminum* (Rondani)] and Hessian fly [Hf, *Mayetiola destructor* (Say) (Diptera: Cecidomyiidae)] are among the primary pests that cause economic yield losses under drought stress environments in Texas. Generally insects thrive more in warmer weather. As temperatures rise, these pests eat more and reproduce more (Maxmen, 2013). Stripe (yellow) rust, caused by *Puccinia striiformis* Westend. f. sp. *tritici* Erikss. (hereafter referred to as *Pst*), is an economically important disease of wheat (*Triticum aestivum* L.) worldwide. It can cause significant reduction in wheat production in the southern Great Plains. Stripe rust can occur in most wheat areas with cool and moist weather conditions during the growing season. It is necessary to focus on developing wheat germplasm lines with multiple resistance and tolerance to biotic and abiotic stresses, respectively. Candidate genes for greenbug resistance, stripe rust resistance and drought tolerance have been studied by Texas A&M Wheat Genetic Team Led by Shuyu Liu (Reddy et al., 2013; 2014). High throughput genotyping, combined with the use of traditional and marker-assisted breeding (MAB) strategies, provides an excellent approach to potentially increase wheat production under biotic and abiotic stresses. The Texas A&M AfriLife Research has maintained a diverse set of wheat germplasm and has developed numerous wheat

cultivars in the Southern Great Plains. Success stories include the development and release of TAM 111 in 2003 (PI 631352; Lazar et al., 2004), and the recent 'TAM 112' (PI 643143; Rudd et al., 2014), released by Texas A&M AgriLife Research, both are hard red winter wheat cultivar (HRWW) with high grain yield under drought and well-watered environments and are widely planted HRWW in the U.S. High Plains. TAM 112 ranks among the top drought tolerant cultivars in the Southern Great Plains of the U.S. (NASS, 2012, http://www.nass.usda.gov). It also possesses resistances to greenbug (*Gb3* gene), wheat curl mites (WCM) and powdery mildew. TAM 111 has provided a fair level of stripe rust resistance depending on the local dominant races in the US Great Plains.

In current study, single nucleotide polymorphism (SNPs) markers were used for genetic mapping and detecting QTL for yield, yield components in addition agronomic traits and end-use quality characteristics. In addition to SNPs linked to genes identified in previous Texas wheat mapping populations (Liu et al., 2014), genotyping-by-sequencing (GBS) (Elshire et al., 2011; Poland et al., 2012) was used to genotype the recombinant inbred lines (RILs). Genome-wide high resolution genetic maps were constructed and QTL for yield, its components, end-use quality, and pest resistances were analyzed. Tightly linked SNPs were converted to KASP markers (Tan et al., 2015; LGC Genomics, Beverly, MA, USA) for high throughput screening, which can be used to estimate the effects of these genes/QTLs and applied in MAB in the current TAMU as well as other breeding programs in the U.S. and worldwide. The identification and characterization of QTL and expressed genes for drought tolerance and pest resistance provide novel molecular tools for understanding genetic mechanisms and the development of new germplasm lines with tolerance to multiple stresses.

CHAPTER II

DEVELOPING KASP MARKERS FOR A MAJOR STRIPE RUST RESISTANCE QTL IN TAM 111 USING 90K ARRAY AND GENOTYPING-BY-SEQUENCING

2.1 Introduction

Stripe (yellow) rust, caused by *Puccinia striiformis* Westend. f. sp. *tritici* Erikss. (hereafter referred to as *Pst*), is an economically important disease of wheat (*Triticum aestivum* L.) worldwide. It can cause significant reduction in wheat production in the southern Great Plains. Stripe rust can occur in most wheat areas with cool and moist weather conditions during the growing season. Genetic resistance is the most economical, effective and environment-friendly approach of stripe rust management. Resistance to *Pst* can be categorized as either race-specific, which is controlled by genes with major effects for all-stage resistance, or race-nonspecific-type, which is often expressed at the adult stage of growth (Lagudah, 2011).

In 2010, a dominant race of *Pst* broke down the long-time effective *Yr 17* resistance in the US Great Plains. However, a few cultivars, including TAM 111, remained resistance against the *Yr 17* virulent race (Basnet et al., 2014). Since then, TAM 111 has provided a fair level of stripe rust resistance depending on the local predominant races and weather conditions in the US Great Plains. Integrated deployment of major seedling resistance genes in conjunction with adult plant resistance is an effective strategy to combat stripe rust resistance (Liu et al., 2014). To date, there are 80 stripe rust resistance loci derived from *Triticum* and related genera or species, have been formally named (https://shigen.nig.ac.jp/wheat/komugi/genes/symbolClassListAction.do?geneClassificationId=222, accessed on October 27, 2017). Among these genes, five *Yr* genes, *Yr5*, *Yr7*, *Yr43*, *Yr44*, and

Yr53 have been reported to be mapped on the long arm of chromosome 2B (Macer, 1966; Johnson et al., 1969; Cheng and Chen, 2010; Sui et al., 2009; Xu et al., 2013). In addition, Basnet et al. (2014) mapped a major QTL associated with resistance to stripe rust on the chromosome 2BL in TAM 111, and placed this QTL on the genetic position 45, 35, 23 and 10 cM from *Yr5*, *Yr44*, *Yr53*, *Yr43*, respectively.

Basnet et al. (2014) conducted Diversity Arrays Technology (DArT) genotyping (Akbari et al., 2006) of the two parents and 92 randomly selected recombinant inbred lines (RILs) developed by TAM 111 and TAM 112, which are both popular hard red winter wheat (HRWW) cultivars. 294 genetic markers were retained for linkage map construction with approximately 937 cM in total genetic distance and 3.1 cM for average map density. However, the genetic distance for marker loci greatly differ across different mapping populations, making it difficult to apply for marker-assisted selection (MAS). High-density genetic markers development for high-resolution mapping is a precursor for QTL-to-gene era. Therefore, Mapping the QTL for stripe rust resistance using high-density 90,000 single nucleotide polymorphism (SNP) array (Wang et al., 2014) and genotyping-by-sequencing (GBS) (Poland et al., 2012) may help to place the causal genes in narrow genetic intervals and more efficiently identify closely linked markers which can be applied in high-throughput screening with Kompetitive Allele Specific PCR (KASP) markers.

The genome of bread wheat consists of tetraploid wheat (*Triticum turgidum* L., AABB) and the wild diploid relative, *Aegilops tauschii* Coss. (DD), which makes it a larger size (~17 Gb) (Iehisa et al., 2014). The complicated composition of wheat genetic pool and huge genome size caused the difficulties to construct high resolution of linkage map. With the advancement of DNA sequencing technologies, it is well established that single nucleotide polymorphism (SNP)

are the most common and the smallest unit of genetic variation among members of a species, providing nearly unlimited resources for markers. The wheat 90K SNP iSelect assay developed by Illumina is another useful genetic tool for tagging marker-associated traits. Using eight biparental mapping populations, Wang et al. (2014) mapped 40,267 SNPs out of the 91,829 (90K) SNPs and used them to constructed genetic map, which serves as an invaluable resource for QTL mapping studies in wheat. More recently, GBS appears to be a promising alternative and can be readily used for either de novo discovery or whole genome wide sequence of large populations at low cost (Poland et al., 2012). GBS or double digestion restriction enzyme associated DNA sequencing (ddRADseq) (Elshire et al., 2011; Peterson et al., 2012) target the genomic sequence flanking restriction enzyme sites to produce a reduced representation of the genome. GBS has been applied effectively to create high-density genetic maps for identifying many important traits associated QTL or candidate genes in wheat (Li et al., 2015; Lin et al., 2015; Saintenac et al., 2013). The objective of this study was to constructing a saturated genetic map from a large number of array and GBS SNPs using RILs from TAM 112/TAM 111 to reanalyze QTL for stripe rust resistance in a popular cultivar TAM 111. The closely linked markers were converted to KASP markers for high throughput screening of advanced breeding lines in many breeding programs in the US Great Plains.

2.2 Materials and methods

2.2.1 Plant materials and phenotypic data

A mapping population of 124 F_6 RIL derived from the cross TAM 112/TAM 111 was developed by the single-seed decent method. TAM 111 is resistant to most of the prevalent *Pst* races of the south-central states, and TAM 112 is moderately susceptible. Both cultivars are hard

red winter wheat (HRWW) cultivars released by Texas A&M AgriLife Research (Lazar et al., 2004; Rudd et al., 2014), which are very popular in the south-central Great Plains of the United States. Six wheat lines (TAM 113, TAM 114, TAM 204, Duster, Iba, Joe, and CO960293), five Texas elite lines (TX05A001822, TX12A001044, TX12A001078, TX12M4068, and TX13A001069) and four synthetic lines (Synthetic derived line: AMPSY # 3, 77, 515, and 588) were used for validation of the markers closely linked to major QTL.

All phenotypic data used in this study have been borrowed from previously published study by Basnet et al. (2014). The two parents and 124 RILs were evaluated for stripe rust response during the three growing seasons in 2010, 2011 and 2012 at six locations: Castroville, TX in 2010 (CAS10), Pullman and Mt. Vernon, WA in 2010 and 2011 (PULL10 and PULL11 and MTV10 and MTV11), Yuma, AZ in 2010 (AZ10), Etter, TX in 2012 (ET12), and Fayetteville, AR in 2012 (AR12). Disease severity (DS) reading was used with 0 to 100% representing complete resistance and susceptibility, respectively. Multiple DS scores were taken in the MTV10, MTV11, and AR12 experiments at stages of booting (BT), flowering (FLR), and dough (DH). Two readings were performed at Castroville, TX, 2010 (CAS10_R1 and CAS10_R2). Single evaluation of DS was performed during flowering to early maturity stage in Arizona, and Pullman experiments (PULL10, PULL11, and AZ10). The infection type (IT) data was recorded at PULL10, PULL11, MTV10_BT, MTV10_FLR, MTV11_BT, AR12_BT, AR12_FLR, and ET12. Parents and the RILs were also tested for reaction to race PST-100 at seedling and adult plant stages in the greenhouse located at USDA-ARS, hard winter wheat genetics research unit, Manhattan, KS (APGHDS, APGHIT, and SDLGHIT). In this study, best linear unbiased prediction (BLUP) for each genotype were computed using restricted maximum likelihood (REML) adapted to META-R macro (Gregorio et al., 2015). Average coefficient of

infection (ACI) was calculated according to Saari and Wilcoxson (1974) by multiplying of disease severity (DS) and constant values of infection type (IT) for AR12. The constant values for infection types were used based on: R = 0.2, MR = 0.4, M = 0.6, MS = 0.8 and S = 1.0. The CI was used for validation of the KASP markers applied in breeding lines for MAS.

2.2.2 Genotyping and linkage map construction

The 124 recombinant inbred lines (RILs) and two parents were genotyped with the Infinium iSelect 90K SNP array, which was conducted at the USDA Agriculture Research Service Bioscience Research Laboratory in Fargo, ND. For genotyping, the DNA sample from the RIL and two parents was extracted according to the CTAB methods with minor modifications (Liu et al., 2013). The genotype data were analyzed using Illumina's GenomeStudio Genotyping Module version 2011.1. The parents were replicated four times and only SNPs with a consistent genotype in at least three parental sets were included to constructed linkage maps. ddRADseq was done in the Genomics and Bioinformatics Center at Texas A&M University (http://www.txgen.tamu.edu/). Initially, 50K SNPs and indels with < 50% missing data were used. Imputation was done then to reduce the missing data. SNP calling was done by the following filter steps: First, monomorphic SNPs were eliminated. Second, missing value for either parent was adjusted based on the allele specificity. Third, the 124 RILs SNP scores were converted to "A" of female parent and to "B" of male parent no matter their polymorphic type. "Not called (NC)" was assigned to missing value. Fourth, the SNPs with A/B ratios within the range of 0.25 – 4.00 and missing value < 20% were kept (Liu et al., 2016). After filtering, a set of 11,839 GBS, 20 SSR and STS markers linked to *Glu-D1*, *1AL.1RS*, *Gb3* and a set of 4869 SNPs from the 90K array were used for map construction. Each marker was tested for Mendelian

segregation distortion using χ^2-analysis with the software program JoinMap 4 (Van Ooijen, 2006). The logarithm of odds (LOD) score ranging from 3.0 to 30, genetic distance < 30 cM, and the Kosambi mapping function (Kosambi 1944) were employed for constructing a map.

2.2.3 QTL Mapping

QTL mapping was performed using MapQTL (Van Ooijen, 2009) with composite interval mapping multiple QTL mapping (MQM) analysis for single environment. The LOD threshold of 2.5 was used to select significant QTL. Significant QTL were graphically visualized using the software MapChart 2.2 (Voorrips, 2002). Single significant QTL and A × E analysis were also confirmed in GenStat based on a linear mixed model (LMM) framework as outlined by several authors (Boer et al., 2007; Van Eeuwijk et al., 2010). Under the LMM framework, multi-environment QTL mapping was implemented in a stepwise process commencing with simple interval mapping (SIM) followed by two or more successive rounds of composite interval mapping (CIM) using QTL identified in SIM to control the genetic background. The QTL for all positions that were significant in the restricted CIM scan were included in the mixed model. QTL with non-significant effects were removed using Wald tests (conditional on all other QTL), and those with significant effects were included to reach a final QTL model. QTLNetwork 2.0 was used to analyze the main additive (A), epistatic effects (A × A) and interaction effects of QTL and environments (A × E, A × A × E) across all tested environments (Yang et al., 2008). Two traits (DS and IT) were assessed. A 1,000-permutation test was used to calculate critical F-values for an experiment-wise significance level of 0.05. Tests to detect QTL were conducted at 1-cM intervals with a window size of 10 cM (Yang et al., 2008). A Monte Carlo Markov Chain approach was used to estimate QTL effects.

2.2.4 KASP Assay

The genetic consensus maps and physical maps of those tightly linked SNPs were compared across Chromosome Survey Sequence (CSS) of Chinese Spring, W7984 and NRgene Pseudo Molecular physical map of Chinese Spring. A total of six consistent and representative SNPs tightly linked to *QYr.tamu-2BL* were converted to the KASP platform. Sequences from the 90K array-based SNPs and GBS markers flanking *QYr.tamu-2BL* were used to design KASP markers using Primer3 software (http://biotools.umassmed.edu/bioapps/primer3_www.cgi). Sequences of allele-specific and common primers were designed and tested. Each KASP reaction was performed in a volume of 10 µL with 5 mL DNA and 5 mL of the prepared genotyping mix (2 × KASP master mix and primer mix). Protocols for the preparation and running of KASP reactions are given in the KASP manual (http://www.kbioscience.co.uk). Amplification was performed using the ABI 7500 instrument (Applied Biosystems, Foster City, CA), starting with 15 min at 94°C, followed by 40 cycles of 94°C for 20 s and 60°C for 1 min. Endpoint detection of the fluorescence signal was acquired for 1 min at 30°C using ABI 7500 real time PCR (Tan et al., 2017). The KASP assay was validated to detect and distinguish resistant and susceptible alleles for the major QTL on 2BL.

2.3 Results

2.3.1 Genetic linkage map construction using 90K array SNPs and GBS

For 90K array SNPs filtering, more details are in Liu et al. (2016). After GBS filtering, a set of 11,839 GBS with known chromosome locations based on the updated Chinese Spring reference genome were used for map construction. In addition, 20 SSR and STS markers linked

to *Glu-D1*, *1AL.1RS*, *Gb3* and $CMC_{TAM\ 112}$ and a set of 4869 SNPs from the 90K array were included with a total of 16,728 markers. After JoinMap analyses, there are 4885 identical markers, including 18 SNPs from 90K, which were excluded from further analyses. A set of 10,924 markers including 19 SSR, STS and genes, 4,846 90K SNP array, and 6,063 GBS were used to construct more than 300 linkage groups (chromosome fragments). Many of them have less than 5 GBS markers and genetic length is 0, which were not used for further QTL analyses. A set of 9928 markers, including 19 SSR and STS, 5,094 GBS, 4,815 SNPs from the 90K array , which were from 80 chromosome fragments and covering all 21 chromosomes, were used for QTL analyses.

The cumulative map length is 11,618.9 cM with an average marker density of 1.5 cM (Table 1). The length of LGs ranged from 43.8 cM (chromsome 5D) to 892.3 cM (chromosome 1A), with an average of 553.3 cM. A total of 3,923 markers were from the A genome with the length of 4547.1 cM and average marker density of 1.2 cM; 4554 markers from the B genome which has the total length of 4359 cM and average marker density around 1.0 cM and 1451 markers from the D genome. Two chromosomes exhibited markers less than 100 (4D and 5D with 85 and 13 markers, respectively). The markers from the 90K SNP array mapped on A, B, and D genomes accounted for 43.2%, 42.5%, and 14.4% of the total SNP markers, respectively. Similarly, the A, B, and D genome have 36.2%, 49.1%, and 14.7% of the total mapped GBS markers.

Table 1. The number of each type of mapped marker within each chromosome (Chrom), number of linkage groups (LGs) within each chromosome, the length of each chromosome in centimorgans (cM) and the marker density in cM of each chromosome for the genetic map construct from 124 RILs of a cross between TAM 112 and TAM 111.

Chorm	No.LGs	No. SNP	No.GBS	No. SSR	No. total markers	Length of Chrom (cM)	Marker density (cM)
1A	4	631	471	1	1103	892.3	0.81
1B	6	415	600	1	1016	649.2	0.64
1D	2	289	156	1	446	629.5	1.41
2A	5	215	346	0	561	749.3	1.34
2B	5	492	535	5	1032	874	0.85
2D	3	54	64	0	118	252.6	2.14
3A	8	242	187	1	430	661.5	1.54
3B	3	156	239	0	395	439	1.11
3D	2	100	126	0	226	463.1	2.05
4A	4	119	143	0	262	308	1.18
4B	1	114	133	0	247	415.6	1.68
4D	2	34	51	0	85	144.1	1.7
5A	4	304	212	0	516	655.1	1.27
5B	6	133	185	1	319	667.6	2.09
5D	1	4	9	0	13	43.8	3.37
6A	4	285	228	0	513	692.6	1.35
6B	4	432	432	0	864	645.6	0.75
6D	4	99	156	2	257	447.6	1.74
7A	4	283	255	0	538	588.3	1.09
7B	5	302	379	0	681	668	0.98
7D	3	112	187	7	306	732.1	2.39
Total	80	4815	5094	19	9928	11618.9	1.5

2.3.2 Significant QTL additive effects and their interaction with environments

Significant QTL for DS and IT were detetced based on the single trait multiple environment model of GenStat. Genome-wide scan for QTL effects in multiple environments trials revealed significant QTL associated with DS on the linkage group 1A1, 1A4, 2A1, 2BL, 7B1, and 7D3 (Figure 1a), and associated with IT are mapped on 1A1, 2A1, 2BL, and 6B2 (Figure 1b). Those QTL showed consistent map locations in single environment analysis from

MQM mapping of MapQTL (Table 2). Most of the QTL associated with stripe rust resistance are from TAM 111, except the ones for DS on chromosome 1A and 7B. The variation among the same color code shows different QEI effect. The darker the color is, the bigger the effect is. By using the QTL identified in SIM as co-variant, CIM revealed six QTL for DS and four QTL for IT in the final model to investigate the QEI effect. The estimated QTL effects are given in Table 1. Only the significant QEI effects are displayed below each QTL.

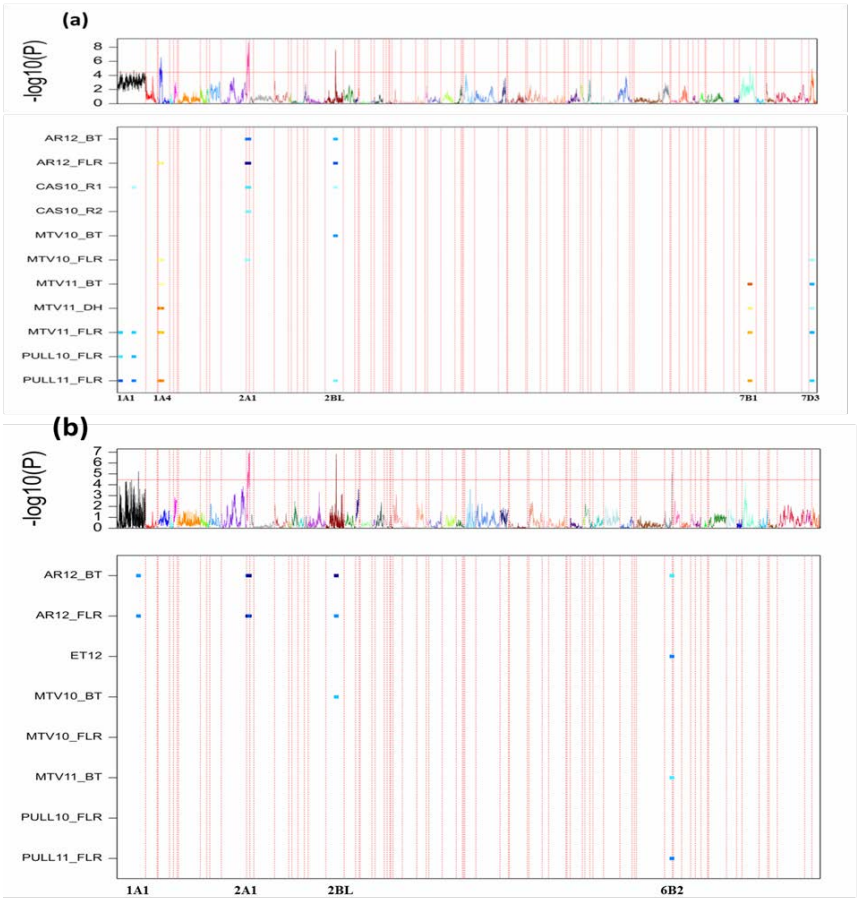

Figure 1. Stripe resistance for stripe resistance QTL detected based on a single trait multi-environment QTL mapping model of GenStat, (a) disease severity (DS) and (b) infection type (IT).

Table 2. QTL associated with disease severisty (DS) and infection type (IT) for single environment analysis by using MapQTL software.

QTL name[†]	QTL ID	Trait[‡]	Environments[§]	Chromosome	Position (cM)	linked markers	LOD	R^2 (%)[¶]	Additive	HVA[#]
QYr.tamu-1A1.2	16	IT	PULL10_FLR	1A1	65.4	GBS3926916	3.34	11.7	0.45	TAM 111
QYr.tamu-1A1.2	16	DS	PULL11_FLR	1A1	65.9	GBS3929350	2.94	10.3	3.90	TAM 111
QYr.tamu-1A1.4	17	IT	ET12	1A1	112.4	GBS3922087	4.49	15.4	0.36	TAM 111
QYr.tamu-1A1.3	18	DS	PULL10_FLR	1A1	291.7	IWB64585	2.73	9.6	2.72	TAM 111
QYr.tamu-1A1.1	7	DS	CAS10_R1	1A1	387.6	GBS3933603	3.11	10.9	0.93	TAM 111
QYr.tamu-1A1.5	9	DS	MTV11_FLR	1A1	452.5	IWB23185	2.73	9.7	1.05	TAM 111
QYr.tamu-1A1.6	19	IT	ET12	1A1	495.0	IWB31781	4.73	16.1	0.37	TAM 111
QYr.tamu-1A2	20	DS	MTV11_FLR	1A2	2.9	IWB27332	2.56	9.1	1.02	TAM 111
QYr.tamu-1A4.1	1	IT	MTV10_FLR	1A4	28.9		2.66	9.4	-0.24	TAM 112
QYr.tamu-1A4.1	1	DS	MTV11_DH	1A4	46.9		5.12	17.3	-3.25	TAM 112
QYr.tamu-1A4.1	1	DS	MTV11_FLR	1A4	46.9		3.94	13.6	-1.27	TAM 112
QYr.tamu-1A4.1	1	DS	MTV11_BT	1A4	55.4	IWB22882	2.82	10	-1.15	TAM 112
QYr.tamu-1A4.3	15	DS	PULL11_FLR	1A4	99.0	IWB54198	3.79	13.1	-4.39	TAM 112
QYr.tamu-1D1	21	DS	CAS10_R2	1D1	128.5		2.65	9.4	-0.90	TAM 112
QYr.tamu-2A1	2	DS	AR12_FLR	2A1	36.8		7.95	25.6	13.28	TAM 111
QYr.tamu-2A1	2	IT	AR12_FLR	2A1	36.8		6.52	21.5	0.68	TAM 111
QYr.tamu-2A1	2	DS	AR12_BT	2A1	39.7		4.28	14.7	2.52	TAM 111
QYr.tamu-2A1	2	DS	AZ10	2A1	40.7		6.01	27	12.62	TAM 111
QYr.tamu-2A1	2	IT	AR12_BT	2A1	42.7		3.35	11.7	0.39	TAM 111
QYr.tamu-2A3	22	DS	MTV11_DH	2A3	161.5	GBS5201704	2.78	9.8	2.41	TAM 111
QYr.tamu-2A4	12	DS	AR12_FLR	2A4	196.0	GBS6399682	3.27	11.4	-10.39	TAM 112
QYr.tamu-2A4	12	IT	AR12_FLR	2A4	196.0	GBS6399682	3.75	13	-0.61	TAM 112
QYr.tamu-2A4	12	IT	AR12_BT	2A4	203.6		3.56	12.4	-0.47	TAM 112
QYr.tamu-2A4	12	DS	AR12_BT	2A4	204.6		3.25	11.4	-2.74	TAM 112
QYr.tamu-2A4	12	DS	AZ10	2A4	204.6		3.05	14.8	-11.42	TAM 112
QYr.tamu-2A4	12	DS	CAS10_R1	2A4	212.6		4.05	14	-1.36	TAM 112
QYr.tamu-2B5.1	23	DS	AZ10	2B5	24.6	GBS5282792	3.34	16	9.01	TAM 111
QYr.tamu-2B5.2	24	DS	AR12_FLR	2B5	55.1		3.14	11	8.90	TAM 111
QYr.tamu-2B7	25	DS	PULL11_FLR	2B7	18.1	GBS8047412	4.91	16.7	4.99	TAM 111
	25	DS	APGH	2B7	20.1	GBS8091669	7.87	25.3	14.81	TAM 111
	25	IT	APGH	2B7	21.2	IWA1489	10.37	32	1.20	TAM 111

Table 2. Continued

QTL name[†]	QTL ID	Trait[‡]	Environments[§]	Chromosome	Position (cM)	linked markers	LOD	R^2 (%)[¶]	Additive	HVA[#]
	25	IT	SDLGH	2B7	21.2	IWB47823	4.14	14.3	0.40	TAM 111
QYr.tamu-2B7	25	IT	AR12_FLR	2B7	21.3	IWB47823	3.29	11.5	0.48	TAM 111
QYr.tamu-2B7	25	DS	CAS10_R2	2B7	22.8	IWB11848	3.26	11.4	0.76	TAM 111
QYr.tamu-2B7	25	DS	AR12_BT	2B7	28.1	GBS8046492	2.99	10.5	1.98	TAM 111
QYr.tamu-2B7	25	DS	MTV10_BT	2B7	28.1	GBS8046492	4.04	13.9	5.02	TAM 111
QYr.tamu-2B7	25	IT	MTV10_BT	2B7	28.1	GBS8046492	3.48	12.1	0.41	TAM 111
QYr.tamu-2B7	25	IT	AR12_BT	2B7	48.2	GBS7966969	5.09	17.2	0.43	TAM 111
QYr.tamu-2BL.2	26	DS	CAS10_R2	2B89	91.1		2.8	9.9	0.72	TAM 111
QYr.tamu-2BL.1	3	IT	MTV10_FLR	2B89	177.4		3.07	10.8	0.27	TAM 111
	3	DS	APGH	2B89	178.4	IWB47487	21.72	55.4	22.76	TAM 111
	3	IT	SDLGH	2B89	178.4	IWB47487	10.91	33.3	0.63	TAM 111
QYr.tamu-2BL.1	3	DS	AR12_BT	2B89	180.0	IWB47487	8.06	25.9	3.11	TAM 111
QYr.tamu-2BL.1	3	IT	AR12_BT	2B89	180.0	IWB47487	20.09	52.6	0.75	TAM 111
QYr.tamu-2BL.1	3	DS	AR12_FLR	2B89	180.0	IWB47487	8.56	27.2	13.25	TAM 111
QYr.tamu-2BL.1	3	IT	AR12_FLR	2B89	180.0	IWB47487	11.25	34.1	0.82	TAM 111
QYr.tamu-2BL.1	3	DS	AZ10	2B89	180.0	IWB47487	5.89	26.5	11.73	TAM 111
	3	IT	APGH	2B89	180.57	IWB52095	37.82	75.50	1.83	TAM 111
QYr.tamu-2BL.1	3	DS	CAS10_R1	2B89	181.6		3.48	12.1	0.98	TAM 111
QYr.tamu-2BL.1	3	DS	MTV10_BT	2B89	181.6		9.45	29.6	7.35	TAM 111
QYr.tamu-2BL.1	3	IT	MTV10_BT	2B89	181.6		7.89	25.4	0.60	TAM 111
QYr.tamu-2BL.1	3	DS	PULL11_FLR	2B89	181.6		7.84	25.3	6.12	TAM 111
QYr.tamu-2BL.1	3	IT	PULL11_FLR	2B89	186.9		3.64	12.6	0.28	TAM 111
QYr.tamu-3A3.1	27	IT	PULL11_FLR	3A3	86.4	GBS4400050	2.77	9.8	0.25	TAM 111
QYr.tamu-3A3.2	28	DS	PULL11_FLR	3A3	125.3		2.92	10.3	3.91	TAM 111
QYr.tamu-3A3.3	29	DS	PULL10_FLR	3D1	129.4	GBS6858594	3.08	10.8	-2.88	TAM 112
QYr.tamu-4A5.1	4	DS	CAS10_R1	4A3_1	44.9	GBS7081733	2.56	9.1	0.86	TAM 111
QYr.tamu-4A5.1	4	DS	MTV11_FLR	4A3_1	44.9	GBS7081733	3.88	13.4	1.26	TAM 111
QYr.tamu-4A5.1	4	IT	ET12	4A3_1	48.0		2.96	10.4	0.30	TAM 111
QYr.tamu-4A5.1	4	IT	PULL10_FLR	4A3_1	74.7		3.05	10.7	0.44	TAM 111
QYr.tamu-4A5.2	30	DS	MTV11_FLR	4A3_1	142.8		3.95	13.7	1.27	TAM 111
QYr.tamu-4A5.2	30	DS	MTV11_BT	4A3_1	145.5		3.89	13.5	1.40	TAM 111
QYr.tamu-4A5.2	30	DS	AR12_BT	4A3_1	148.5	IWB60281	3.66	12.7	2.20	TAM 111

Table 2. Continued

QTL name[†]	QTL ID	Trait[‡]	Environments[§]	Chromosome	Position (cM)	linked markers	LOD	R^2 (%)[¶]	Additive	HVA[#]
QYr.tamu-4A5.2	30	DS	AR12_FLR	4A3_1	148.5	IWB60281	3.02	10.6	8.38	TAM 111
QYr.tamu-4B1234	14	DS	PULL11_FLR	4B1234	11.3		3.15	11	-4.04	TAM 112
QYr.tamu-4B1234	14	DS	MTV11_DH	4B1234	18.5		3.19	11.2	-2.87	TAM 112
QYr.tamu-4D.2	31	DS	PULL11_FLR	4D	29.0	GBS14307148	3.45	12	4.20	TAM 111
QYr.tamu-5A5	32	IT	ET12	5A2_1	56.1		2.89	10.2	-0.30	TAM 112
QYr.tamu-6A4	33	DS	MTV11_BT	6A4	141.0	IWB47346	2.69	9.5	1.12	TAM 111
QYr.tamu-6B2	8	IT	ET12	6B2	174.2		3.18	11.1	0.31	TAM 111
QYr.tamu-6B5	34	IT	ET12	6B2_1	10.4	GBS2933828	4.46	15.3	0.38	TAM 111
QYr.tamu-7B6.1	15	IT	ET12	7B1_2	54.7	IWB63589	3.39	11.8	-0.31	TAM 112
QYr.tamu-7B6.2	35	DS	MTV11_BT	7B1_2	238.6		3.05	10.7	-1.25	TAM 112
QYr.tamu-7D1	34	DS	MTV11_BT	7D1	466.6		2.82	9.9	1.20	TAM 111
QYr.tamu-7D3	6	IT	MTV11_BT	7D3	51.9		2.5	8.9	0.04	TAM 111
QYr.tamu-7D3	6	DS	MTV11_BT	7D3	52.9		3.46	12	1.27	TAM 111
QYr.tamu-7D3	6	DS	MTV11_FLR	7D3	53.1	GBS3391666	3.16	11.1	1.13	TAM 111

†QTL name including trait, institute, and linkage group; the linkage group is unique for each numbered QTL if the peak positions were less than 30 cM; within each chromosome fragment, different numbered QTL will have various chromosome fragment parts starting from the fragment name, then adding ".1, .2, …".
‡Abbreviation of traits: DS disease severity, and IT infection type.
§Abbreviation of environments: Castroville, TX in 2010 (CAS10), Pullman and Mt. Vernon, WA in 2010 and 2011 (PULL10 and PULL11 and MTV10 and MTV11), Yuma, AZ in 2010 (AZ10), Etter, TX in 2012 (ET12), and Fayetteville, AR in 2012 (AR12). Greenhouse for seedling and adult plant screening (APGH, SDLGH). Data recorded at stages of booting (BT), flowering (FLR), and dough (DH). Two readings were performed at Castroville, TX in 2010 (CAS10_R1 and CAS10_R2).
¶phenotypic variance explained by this significant QTL.
#High value allele.

All six QTL for DS showed QEI. A major QTL *QYr.tamu-2BL.1* with the largest effect was detected on the long arm of chromosome 2B with a -log10(P) value of 31.4 (Table 3). This QTL was delimited to an interval between IWB47487 and IWB29391. The proportion of phenotypic variance explained by this major QTL ranged from 3.1 to 23.9 % across all eight environments. The high value allele (HVA) is derived from paternal line TAM 111. The largest additive effect originated from AR12 at flowering stage is 12.4. For the other QTL on chromosome fragments 1A4, 2A1, 4A3, 4D, and 7D3, only the QTL on chromosome 1A4 had

Table 3. QTL detected using single trait multi-environment QTL composite interval mapping model of GenStat.

QTL name[†]	QTL ID	Position (cM)	Marker Interval	-log10(P)	Traits[‡]	QTL x E[§]	Environments[¶]	R^2 range (%)[#]	AE range[††]	HVA[‡‡]
QYr.tamu-1A4.1	1	45.9	IWB72163-IWB1256	6.9	DS	yes	AR12_FLR, MTV10_FLR, MTV11_DH, MTV11_FLR, PULL11_FLR	2.5 - 12.1	0.9 - 4.0	all TAM 112
QYr.tamu-2A1	2	35.8	GBS5258582-GBS5281750	8.5	DS	yes	AR12_BT, AR12_FLR, CAS10_R1	4.0 - 19.3	0.6 - 11.2	all TAM 111
QYr.tamu-2BL.1	3	180.6	IWB47487-IWB29391	31.4	DS	yes	AR12_BT, AR12_FLR, CAS10_R1, CAS10_R2, MTV10_BT, MTV10_FLR, MTV11_DH, PULL11_FLR, APGH	3.1 - 23.9	0.6 - 12.4	all TAM 111
QYr.tamu-4A3.1	4	46	GBS7081733-GBS7152618	4.3	DS	yes	AR12_BT, AR12_FLR, CAS10_R1, CAS10_R2, MTV11_BT, MTV11_BT, MTV11_FLR, PULL10_FLR, PULL11_FLR	3.4 - 6.7	0.4 - 4.2	all TAM 111
QYr.tamu-4D.1	5	91.5	GBS2273804-IWB3253	3.4	DS	yes	MTV11_BT, PULL11_FLR	2.9 - 4.9	0.6 - 2.7	all TAM 111
QYr.tamu-7D3	6	*53.1*	IWB17509-IWB19321	4.6	DS	*yes*	MTV10_FLR, MTV11_BT, MTV11_FLR, PULL11_FLR	3.2 - 8.2	0.9 - 2.2	all TAM 111
QYr.tamu-1A1.1	7	379.3	IWB5261-GBS3869219	4.4	IT	yes	MTV10_FLR, PULL10_FLR, PULL11_FLR	2.8 - 7.7	0.1 - 0.3	all TAM 111
QYr.tamu-2A1	2	39.7	GBS5281750-GBS8038726	8.1	IT	yes	AR12_BT, AR12_FLR, ET12	3.1 - 19.8	0.2 - 0.6	all TAM 111
QYr.tamu-2BL.1	3	180.6	IWB47487-IWB29391	33.4	IT	yes	AR12_BT, AR12_FLR, MTV10_BT, MTV10_FLR, PULL11_FLR, APGH, SDLGH	9 - 49.2	0.2 - 0.8	all TAM 111
QYr.tamu-6B2	8	127.3	GBS3043811-GBS3003285	6	IT	yes	ET12, PULL11_FLR	7.5 - 16.4	0.2 - 0.4	all TAM 111

[†]Only QTL with significant ($P < 0.05$) additive effect are present. QTL name including trait, institute, and chromosome fragment; the chromosome fragment part is unique for each numbered QTL if the peak positions were less than 30 cM; within each linkage fragment, QTL will have various chromosome fragment parts starting from the fragment name, then adding ".1, .2, …".
[‡]Abbreviation of traits: DS disease severity, and IT infection type.
[§]QTL-by-environment interaction.

HVA contributed from maternal parent TAM 112, suggesting that TAM 111 contains more favorable alleles for stripe rust resistance. Among the thirteen environments used for DS analysis in this study, *QYr.tamu-1A4.1*, on linkage group 1A4 with the flanking marker IWB72163 and

IWB1256 was detected in five environments, and the additive effect ranged from 0.9 to 4.0. The corresponding R^2 ranged from 2.5 to 12.1 %. The QTL *QYr.tamu-2A1* located on the short arm of chromosome 2A showed significant QEI effect among three environments with additive effect ranging from 0.6 to 11.2. Two GBS markers were mapped to this QTL region, which was linked closely to GBS5258582 and GBS5281750. The percentage of phenotypic variance explained by this QTL ranged from 4 to 19.3 %. *QYr.tamu-4A3.1* with the closely associated markers GBS7081733 and GBS7152618 was exhibited in eight out of the thirteen environments. The percentage of the phenotypic variance explained by this QTL was 3.4 to 6.7 %, and the additive effect ranged 0.4 - 4.2. *QYr.tamu-4D.1,* with flanking markers GBS2273804 and IWB3253, was detected in two environments MTV11 and PULL11. This QTL explained 2.9 - 4.9 % of phenotypic variance on DS, with additive effect ranging 0.6 to 2.7. *QYr.tamu-7D* was delimited to an interval between 90K SNPs *IWB17509* and *IWB19321* and explained 3.2 – 8.2 % phenotypic variance for DS. This QTL was identified in MTV10, MTV11, and PULL11.

Four QTL showed significant QEI effect for IT, which were mapped onto the chromosome fragments 1A1, 2A1, 2BL, and 6B2. The HVA for all four QTL were provided by TAM 111 (Table 3). The QTL *QYr.tamu-1A1.1* peaked at 379.3 cM on chromosome 1A1, with flanking marker IWB5261 and GBS38692195, and this QTL explained 2.8 to 7.7 % phenotypic variance for IT across three environments: MTV10, PULL10, and PULL11.The other two QTL placed on chromosome 2A1 and 2BL had the similar peak position with the ones detected in the DS analysis. The QTL *QYr.tamu-2A1* on the short arm of chromosome 2A identified in AR12 and ET12 and explained 3.1 - 19.8 % of the phenotypic variance for IT. Two GBS markers GBS5281750 and GBS8038726 were the most closely linked marker to this QTL. The major QTL *QYr.tamu-2BL.1* showed significant QEI with seven environments out of ten used for IT

analysis with the associated markers IWB47487 and IWB29391. The additive effect ranged from 0.2 to 0.3, and corresponding R^2 values were 9 - 49.2 % across the environments. The -log10 (P) value of *QYr.tamu-2BL.1* is 31.4. The largest R^2 was detected in AR12. *QYr.tamu-6B2* explained 7.5 – 16.4 % of phenotypic variance across two environments: ET12 and PULL11. The closely associated markers were GBS3043811 and GBS3003285.

From single trait with single environment analysis using MapQTL software, 27 unique QTL regions were identified except the eight QTL detected in the single trait with multiple environments results (Table 2). Seven out of eight consistent QTL were identified based on the two analyses. Only the QTL *QYr.tamu-4D.1* associated with DS wasn't detected for any environment from MapQTL. In addition, based on the model of additive by environments analysis from QTLNetwork, ten QTL on chromosome fragments 1A1, 1A4, 2A1, 2A4, 2BL, 4A3, 4B1234, 4D, 5B4, and 7B6 were identified for significant additive effects and additive by environment (A × E) interaction effects (Table 4). The major QTL on chromosome 2BL was not detected for DS in the A × E analysis. Among those QTL, only the consistent QTL *QYr.tamu-2A1* was identified for association with both DS and IT. All ten QTL were detected at the similar genetic positions of the MapQTL model.

Table 4. Additive by environment interaction for QTL associated with DS and IT by using QTLNetwork software.

QTL[†]	QTL ID	Chrom	Peak (cM)	Trait[‡]	Marker interval	Range (cM)	Additive effect[§]	Additive × Environment (A × E)[¶]
QYr.tamu-1A4.2	10	1A4	116.4	DS	IWA4897-GBS3893918	108.6-119.4	1.21	2.23(MTV11_FL)
QYr.tamu-1A4.2	10	1A4	128.2	DS	GBS3922137-IWB9993	125.1-131.2	-2.67	-2.9(MTV11_BT), -3.85(MTV11_FL), 1.7(MTV11_DH), 1.94(CAS10_R1), 2.26(PULL10_FLR)
QYr.tamu-2A1	2	2A1	33.8	DS	GBS5235477-GBS5281750	30.8-36.8	3.52	9.38(MTV11_BT), 7.54(MTV11_FL), -2.43(MTV11_DH), -3.19(CAS10_R1), -3.03(PULL10_FLR), -2.74(PULL11_FLR), -4.11(MTV10_BT)
QYr.tamu-2A4	12	2A4	209.6	DS	IWB71583-GBS5962870	203.6-216.6	-2.32	-2.58(MTV11_BT), -3.26(MTV11_FL), 1.75(CAS10_R1)
QYr.tamu-4A3.2	13	4A3	140.7	DS	GBS7167599-IWB49921	132.1-143.0	1.48	1.59(MTV11_BT)
QYr.tamu-4B1234	14	4B1234	17.3	DS	GBS4867710-IWB4336	10.7-23.3	-1.83	-1.59(MTV11_BT)
QYr.tamu-4D.2	31	4D	27.6	DS	GBS14467522-GBS14467068	24.0-33.6	1.22	1.51(APGH)
QYr.tamu-5B	36	5B4	183	DS	GBS2297010-IWB4335	177.2-185.2	-1.71	-7.67(APGH)
QYr.tamu-1A1.5	9	1A1	459.7	IT	IWB1449-IWB27624	459.5-460.7	0.07	0.18(PULL10_FLR), -0.14(AR12_BT)
QYr.tamu-2A1	2	2A1	15.7	IT	IWB57168-GBS5283411	14.8-16.7	0.12	-0.13(MTV11_BT), 0.3(AR12_FLR) -0.26(PULL10_FLR), 0.25(MTV10_BT), -0.32(MTV11_BT), 0.38(AR12_BT), 0.43(AR12_FLR), -0.33(ET12)
QYr.tamu-2BL.1	3	2B89	180	IT	IWB47487-GBS5204614	179.4-181.0	0.33	
QYr.tamu-7B6.1	15	7B6	54.7	IT	IWB63589-GBS312765	53.7-55.7	-0.11	-0.13(ET12)

†QTL name including trait, institute, and linkage group; the linkage group is unique for each numbered QTL if the peak positions were less than 30 cM; within each chromosome fragment, different numbered QTL will have various chromosome fragment parts starting from the fragment name, then adding ".1, .2, …".

‡Abbreviation of traits: DS disease severity, and IT infection type.

§Negative sign meeans the favorable allele provided by female parent TAM 112.

¶Abbreviation of environments: Castroville, TX in 2010 (CAS10), Pullman and Mt. Vernon, WA in 2010 and 2011 (PULL10 and PULL11 and MTV10 and MTV11), Yuma, AZ in 2010 (AZ10), Etter, TX in 2012 (ET12), and Fayetteville, AR in 2012 (AR12). Greenhouse for seedling and adult plant screening (APGH, SDLGH). Data recorded at stages of booting (BT), flowering (FLR), and dough (DH). Two readings were performed at Castroville, TX in 2010 (CAS10_R1 and CAS10_R2).

2.3.3 Epistasis and interaction effects between epistasis and environments

Six pairs of QTL have significant A × A epistasis for DS and all these pairs showed significant A × A × E interactions in some environment and growth stage combinations (Table 5). *QYr.tamu-2A1* was involved in two out of six A × A epistatic interactions, one of them with the major QTL *QYr.tamu-2BL.1*. Significant A × A × E interactions, existed between the two QTL *QYr.tamu-2A1* and *QYr.tamu-2BL.1*, were detected in seven of twelve environment and

Table 5. Epistatic and epistatic QTL by environment interactions for stripe rust resistance from QTLNetwork software.

Trait†	QTL1	QTL1 ID	Marker interval	Peak (cM)	QTL2	QTL2 ID	Marker interval	Peak (cM)	A× A‡	Additive × additive × Environment§
DS	*QYr.tamu-1A4.2*	10	GBS3922137-IWB9993	128.2	*QYr.tamu-4D.2*	31	GBS14467522-GBS14467068	27.6	-1.33	-1.52(AR12_FLR)
	QYr.tamu-2A1	2	GBS5235477-GBS5281750	32.8	*QYr.tamu-5B4*	new	GBS2297010-IWB4335	183	1.93	7.35(APGH)
	QYr.tamu-1A2	20	GBS3928881-GBS3904706	15.5	*QYr.tamu-2D1*	new	GBS3383067-GBS5365969	118.1	1.1	2.4(APGH)
	QYr.tamu-1D2	new	GBS1090764-GBS1895325	133.8	*QYr.tamu-6B1*	new	GBS2939009-GBS2950610	4.3	-1.18	-2.28(APGH)
										9.4(AR12_FLR), 7.77(AZ10), -2.56(CAS10_R2), -3.15(ET12_FLR), -2.84(MTV11_FLR), -
	QYr.tamu-2A1	2	GBS5235477-GBS5281750	32.8	*QYr.tamu-2B89.1*	3	IWB47487-GBS5204614	180	3.37	2.17(PULL11_FLR), 3.03(APGH)
	QYr.tamu-5B1	new	GBS10885111-GBS10797866	174.2	*QYr.tamu-7A3*	new	GBS4243020-GBS4256644	63.8	-1.33	-5.52(APGH)
IT	*QYr.tamu-2A1*	2	IWB57168-GBS5283411	15.7	*QYr.tamu-2BL.1*	3	IWB47487-GBS5204614	180	0.2	0.3(AR12_FLR), -0.2(ET12)
	QYr.tamu-2BL.1	3	GBS5244500-GBS5239202	109.5	*QYr.tamu-4A3*	new	IWA3671-IWB4258	91.7	-0.2	ns
	QYr.tamu-3A9	new	GBS2752243-GBS5341158	89.1	*QYr.tamu-6A2*	new	GBS4345853-GBS4344367	261.5	ns	0.3(PULL10_FLR)

†Abbreviation of traits: DS disease severity, and IT infection type.

‡ Additive × additive effect. Negative sign indicates the epistasis interaction decreases the trait. Positive sign indicates the epistasis interaction increases the trait.

§Abbreviation of environments: Castroville, TX in 2010 (CAS10), Pullman and Mt. Vernon, WA in 2010 and 2011 (PULL10 and PULL11 and MTV10 and MTV11), Yuma, AZ in 2010 (AZ10), Etter, TX in 2012 (ET12), and Fayetteville, AR in 2012 (AR12). Greenhouse for adult plant screening (APGH). Data recorded at stages of booting (BT), flowering (FLR), and dough (DH). Two readings were performed at Castroville, TX in 2010 (CAS10_R1 and CAS10_R2).

growth stage combinations, and they had the largest epistasis effect. The effect for epistasis by environment ranged from 2.2 to 9.4. AR12_FLR had the largest effect for epistasis by environment interaction. It suggests that the major QTL *QYr.tamu-2BL.1* would show great effect on stripe rust resistance under specific environments.

For IT, three pairs of QTL had significant A × A epistasis but only two showed significant A × A × E interactions. The major QTL *QYr.tamu-2BL.1* on chromosome 2BL showed a significant epistasis interaction with the QTL *QYr.tamu-2A1* on 2A. The previous QTL *QYr.tamu-2A1* on chromosome 2A involved in epistasis interaction with *QYr.tamu-2BL.1* for DS at 28 cM, and for IT, *QYr.tamu-2A1* peaked at 15.7 cM genetic distance. Therefore, this pair

QTL interaction was showed in both DS and IT analysis. However, one epistasis between *QYr.tamu.2BL.1* and *QYr.tamu.4A3* did not have interactions with environment and growth stage combinations. The positive epistatic interaction suggested that this interaction provided greater than expected resistance to stripe rust. The pair of *QYr.tamu-3A9* and *QYr.tamu-6A2* showed A × A × E interactions with environment PULL10.

2.3.4 KASP marker development and validation for QYr.tamu-2BL.1

The associated marker with *QYr.tamu-2BL.1* was IWB47487. The genetic positions of 30 closely mapped markers with IWB47487 were compared with Chromosome Survey Sequence (CSS) for Chinese Spring, combined with the reference sequence of W7984 and NRgene Pseudo Molecular physical map of Chinese Spring. The sequences of six SNP, GBS5245415, IWB47487, IWB52095, IWB32069, IWB26631, and IWB29391, closely linked to *QYr.tamu-2BL.1* were converted to KASP assays (Table 6), and these KASP markers were used to genotyped 16 advanced breeding lines and cultivars. Three markers, IWB47487, IWB26631, and IWB29391 differentiated the resistant and susceptible alleles in the mapping population and were mapped back. The KASP SNPs for these three diagnostic markers replaced array-based and GBS SNPs to reconstructed the genetic map of *QYr.tamu-2BL.1* using the 124 RILs of the TAM 112/TAM 111 population. The results showed that the genotypic data obtained from the KASP assays were consistent with the genotypic data of array SNP and GBS data from the 124 RILs. The newly generated genetic map with 13 closely linked SNPs spanned a genetic distance of 14.2 cM with an average density of 1.1 cM. In this high-resolution map, IWB29391 was 1.7 cM distal and IWB26631 was 2.2 cM proximal from IWB47487 that was at the stripe resistance QTL peak.

Table 6. Kompetitive Allele Specfic Polymerase Chain Reaction (KASP) single-nucleotide polymorphisms (SNPs) tightly linked to *QYr.tamu-2BL* and their primer sequences.

SNP name	KASP primers	Primer sequence (without tail sequences)
5245415_2bs:4872	GBS5245415_T	5'-GGAGCATAACAGAATAAGT-3'
	GBS5245415_C	5'-GGAGCATAACAGAATAAGC-3'
	Common reverse	5'-GGACTCCGTCGACTACAAGC-3'
IWB26631	IWB26631_T	5'-CTCCATCCTCACCAAGCAGT-3'
	IWB26631_C	5'-CTCCATCCTCACCAAGCAGC-3'
	Common reverse	5'-CCAAGTTTAGCGGTTTACGG-3'
IWB29391	IWB29391_T	5'-GTCACAAGACCAGGGGATTT-3'
	IWB29391_G	5'-GTCACAAGACCAGGGGATTG-3'
	Common reverse	5'-CCTGGGGCCTTGTTACACTA-3'
IWB32069	IWB32069_A	5'-ATGTACTTTGCCTTCTRGCA-3'
	IWB32069_G	5'-ATGTACTTTGCCTTCTRGCG-3'
	Common reverse	5'-AGGAACAAATTCCGAGGTGA-3'
IWB47487	IWB47487_A	5'-TGCTTGGTCACATTGACACA-3'
	IWB47487_G	5'-TGCTTGGTCACATTGACACG-3'
	Common reverse	5'-CACGTCCCTTTAGCTGGAGA-3'
IWB52095	IWB52095_A	5'-ATTCTTTCAGAAAGCATCTA-3'
	IWB52095_C	5'-ATTCTTTCAGAAAGCATCTC-3'
	Common reverse	5'-ATGCATCAGATCATGAATTACATAC-3'

To validate the usefulness of the KASP markers for MAS, these three KASP SNPs converted from array-based SNPs were evaluated in the TAM 112/TAM 111 population 124 RILs. We used CI of AR12 at booting and flowering stages, which displayed the same peak position as DS and IT separately, to separate the resistant and susceptible lines. For all three markers, the resistant allele was present in 94% and 90% of the resistant lines for AR12 at booting and flowering stages, respectively. Whereas the susceptible allele was present in 59% and 49% of the susceptible lines for AR12 at booting and flowering stages, respectively. There were still several lines with susceptible allele of this major QTL *QYr.tamu-2BL.1* based on linked markers showing resistance to stripe rust, indicating that the stripe rust resistance in TAM 111 should be pyramided with genes from other genetic resources to develop a high-level resistance effective through all growth stages. However, the markers effectively distinguished

resistant lines from susceptible ones and therefore could be applied in advanced breeding program to select the major QTL on chromosome 2BL in TAM 111 derived cultivars.

In addition, the three KASP markers for *QYr.tamu-2BL.1* were used to genotyped a set of 16 cultivars, elite lines, and synthetic derived lines in comparison with the resistant (TAM 111) and susceptible parents (TAM 112) (Table 7). TAM 111 contained the resistant allele with the 'B' genotype, whereas TAM 112 contained the susceptible allele with the 'A' genotype. For IWB47487, seven cultivars and lines (AMPSY003, AMPSY077, AMPSY515, Duster, KS11HW39-5, TX05A001822, and TX12A001078) showed the same haplotype as resistance parent TAM 111. Among these seven lines, two lines contained TAM 111 in their pedigree. For

Table 7. Lines and cultivars used for validation of major QTL on 2BL linked KASP markers.

Line or cultivar	Pedigree	IWB47487†	IWB29391†	IWB26631†	TAM 111 is in the pedigree
TAM 111	TAM 107//TX78V3630/Centurk 78/3/TX87V1233	B	B	B	-
TAM 112	TX98V9628=U1254-7-9-2-1/TXGH10440	A	A	A	-
AMPSY003	TAM 111*2/CIMMYT E951yn4152-5	B	B	B	yes
AMPSY077	TAM 111*2/CIMMYT E951yn4152-37	B	B	B	yes
AMPSY515	TAM 112*2/CIMMYT E951yn4152-50	B	B	B	no
AMPSY588	TAM 112*2/CIMMYT E951yn4152-46	A	-	A	no
CO960293	222668/TAM 107// CO850034	A	A	A	no
Duster	W0405/NE78488//W7469C/TX81V6187	B	B	A	no
Iba	OK93P656-RMH 3299/OK99621	-	B	A	no
Joe	KS04HW101-3(98HW423(JGR/93HW242)/ 98HW170(ARL/WGRC15))/KS04HW119-3 (TREGO*2/CO960293)	B	B	A	no
TAM113	TAM 200 "S" /TX78A3345-V34//U1254-1-8-1-1//TAM 202' (PI 561933)	A	A	A	no
TAM114	T107//TX78V3620/Ctk78/3/TX87V1233/4/ N87V106//TX86V1540/T200	A	A	A	yes
TAM204	TAM 112/TX01M5009(=Mason/Jagger/Pecos)	A	A	A	no
TX05A001822	2145/X940786-6-7	B	B	A	no
TX12A001044	RonL/TX04V072075 (=TX95D8907//TX92U2317/PECOS)	A	A	A	no
TX12A001078	TX04A001246 (=TX95V4339/TX94VT938-6)/TX04V076015 (=FLORIDA 304/JAGGER//PECOS/TX92U2317)	B	B	A	no
TX12M4068	AP04TW1318/KS980512-11-9//KS06O3A~49	-	-	A	no
TX13A001069	TX05A001506 (=KS94U215/TX95V4538)/TAM 111	A	A	A	yes

†B, resistance allele; A, susceptible allele; -, undetermined.

IWB29391, eight cultivars and lines (AMPSY003, AMPSY077, AMPSY515, Duster, Iba, KS11HW39-5, TX05A001822, and TX12A001078) displayed the same haplotype as resistance parent TAM 111. Similar results were obtained with IWB47487. Among the eight lines, two lines, AMPSY003 and AMPSY077, had TAM 111 in their pedigree. For IWB26631, three synthetic derived lines, AMPSY003, AMPSY077, and AMPSY515, contained the resistant allele as TAM 111 whereas TAM 111 was in the pedigree of AMPSY003 and AMPSY077.

2.4 Discussion

2.4.1 Efficiency of 90K array-based and GBS SNPs

SNPs have been widely used as markers in recent year due to their abundance in the genomes and their amenability for high-saturated genetic map construction and high-throughput detection. With the development of next-generation-sequencing, high-density genetic maps have been constructed for sorghum, wheat, rice, barley, and many other crops. Maps saturated with 90K array-based and GBS markers have proven very feasible and useful for fine mapping of QTL for different traits and candidate gene cloning in wheat (Poland et al., 2012; Saintenac et al., 2013; Spindel et al., 2013). The genetic map created previously (Basnet et al., 2014) by using DArT markers, which is a microarray hybridization-based technique (Jaccoud et al., 2001). One disadvantage of DArT genotyping is the limitation of the representation of the whole genome variation, making it difficult to be applied in many species and high-throughput screening. In addition, DArT genotyping requires special equipment which is unavailable in most research institutions. In contrast to DArT, SNPs have been successfully used in high-throughput screening for genetic analysis of many species. Therefore, the genetic map developed in this study with

90K and GBS SNPs has made feasible for whole-genome wide scan and KASP markers conversion.

2.4.2 Genetic basis of stripe rust resistance

The main objective of our study was to elucidate the genetic basis of the quantitative resistance to stripe rust in wheat 'TAM 111'. The stripe rust resistance of 'TAM 111' has been shown to be durable over a long period of cultivation in the U.S. High Plains, which remained effective against predominant races of the south central states. Therefore, it is of significant importance to incorporate this resistance into other breeding lines. For disease severity (DS), we identified 6 unique genomic regions on chromosomes 1A4, 2A1, 2BL, 4A3, 4D, and 7D3 which were relevant for the expression of stripe rust resistance under field conditions. The 'TAM 111' alleles improve the resistance at 5 out of 6 QTL regions. For infection type (IT), we found 4 genetic regions mapped onto the chromosomes 1A1, 2A1, 2BL, and 6B2 associated with stripe rust resistance, where 'TAM 111' contributing all the favorable alleles of these QTL. The number of the environment-specific minor QTL for quantitative stripe rust resistance identified in our study is higher than the ones identified by Basnet et al. (2014). In previously study, except the major QTL on chromosome 2BL, Basnet et al. (2014) detected minor QTL on chromosomes 1AS, 1AL, 2AS, 6B, and 7D. QTL including *QYr.tamu-1A1.1*, *QYr.tamu-1A4.1*, *QYr.tamu-2A1*, *QYr.tamu-6B2*, and *QYr.tamu-7D3* were also identified in this study, but we were not able to detect the QTL on the short arm of chromosome 1A. The two unique QTL on chromosome 1A were located on the long arm. Such discrepancy is common in QTL detection, especially for small effect QTL, which is often get masked by the genes with major effect. However, a high-density genetic map, as the one developed in the present study, serves as a

resource for gene-based marker saturation in mapping significant QTL or candidate genes associated with the traits.

The major QTL on the long arm of chromosome 2B, previously designated as *QYr.tamu-2BL* (Basnet et al., 2014) was the most important resistance loci identified in TAM 111. This QTL explained up to 29.3 and 49.2 % of the phenotypic variance for stripe rust DS and IT, respectively. The result indicates that *QYr.tamu-2BL.1* is a stable QTL with large effect on stripe rust resistance. In previously study, Basnet et al. (2014) mapped this QTL on the genetic position 45, 35, 23 and 10 cM from *Yr5*, *Yr44*, *Yr53*, *Yr43*, respectively, which are the *Yr* genes reported on the long arm of chromosome 2B. *Yr5* and *Yr7* are ones of the *Yr* genes widely applied by CIMMYT wheat breeding program during the 1970s and 1980s, and has been deployed in many breeding programs and commercial cultivars (Luo et al., 2009). Both genes are allelic or tightly linked based on phenotypic and genotypic data reported by Zhang et al. (2009). *Yr44*, first identified in cultivar Zak, is mapped about 42 cM away from *Yr5* by using 300 F2 plants from cross of Zak/*Yr5* (Sui et al. 2009). Naruoka et al. (2016) reported IWA6121 and IWA4096 were identified as flanking markers for *Yr5*. *Yr53* from durum wheat PI 480148 was resistance in all seeding tests with several predominant Pst races in the US, and SSR maker Xwmc441 flanked this resistance gene by 5.6 cM (Xu et al., 2013). *Yr43* is a single dominant gene conferring race-specific all-stage resistance to stripe rust. This gene from common wheat IDO377s were mapped at the similar chromosome region but linked to different markers (Cheng and Chen, 2010). IWA1040 was reported to be close to the regions of *Yr53* (5 – 11 cM) and *Yr43* (9 – 18 cM) by Muleta et al. (2017). However, the allelic relationships of these genes remain to be investigated. In previously study, most of the marker analysis for *Yr* genes was used with SSR or STS. The major QTL on chromosome 2BL was mapped at the marker interval of wPt6242 and

wPt6471and four SSR or STS markers of Xwmc441, Xgwm501, Yr5STS7/8, and Yr5STS9/10, previously mapped on 2BL were included in chromosome fragment 2B7 in this study (Figure 2). However, common markers for 90K array-based GBS SNPs are lacking to determine the genetic position to the annotated genes. We referend those 90K markers closely linked to the SSR/STS in Basnet et al. (2014) with the 90K-GBS markers identified in this study onto CSS physical position to study their relative locations. The flanking markers for those four SSR or STS

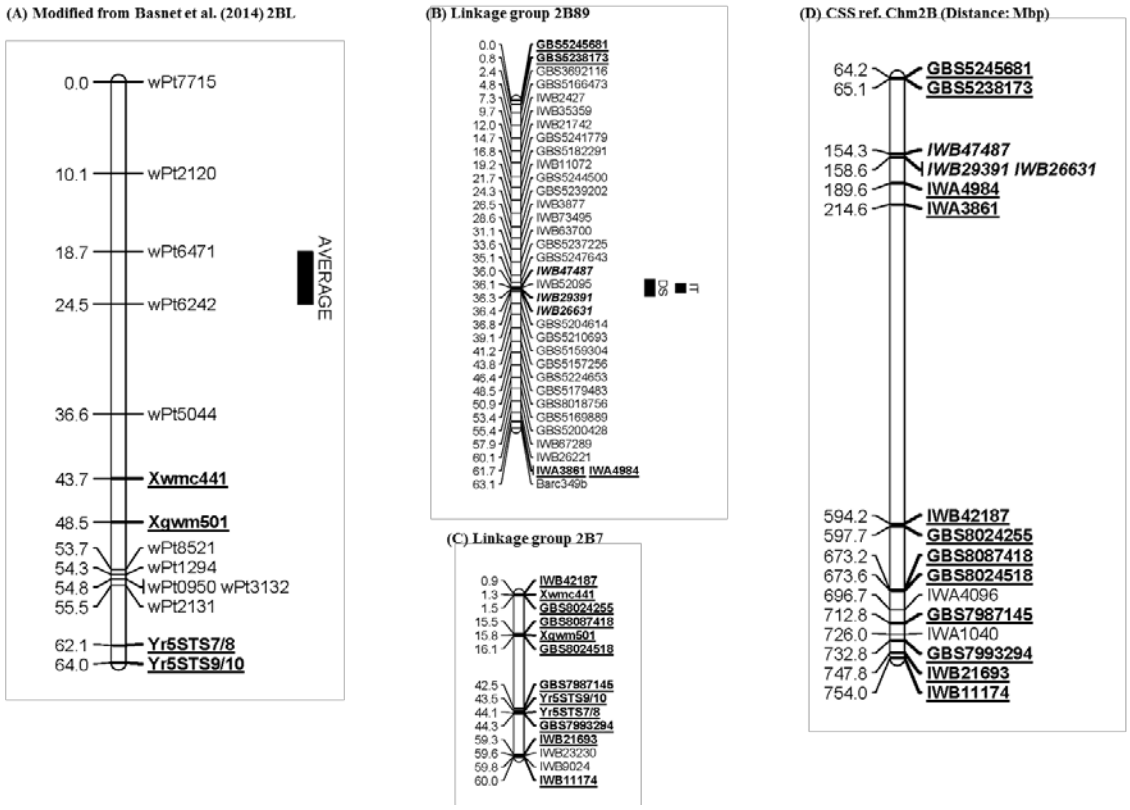

Figure 2. Linkage maps of SNPs associated with *QYr.tamu-2BL* on previous reported paper and in this study on chromosome 2B and their corresponding physical map locations on chromosome 2B of Chinese Spring. (A) Genetic map for 2BL with associated *QYr.tamu-2BL* for DS average by using DArT markers (Basnet et al., 2014), (B) Linkage group 2B89 with associated *QYr.tamu-2BL* for DS and IT by using 90K and GBS markers†, (C) Linkage group 2B7 in this study, (D) Fragment of wheat chromosome 2B reference map showing the physical location of the SNPs mapped on the high-resolution genetic map.
†The actual length in cM per chromosome fragment was divided by 5 in order to draw the whole fragment in MapChart and the linkage group was constructed by markers every 3 cM. The KASP SNPs were italic and bold.

common markers, the tail markers on chromosome 2B7, the lead and tail markers on chromosome 2B89, and the KASP replaced SNPs were referenced to Chinese Spring, and linkage analysis indicated that *QYr.tamu-2BL* was located at 154.3 Mbp physical position on Chinese Spring high resolution genetic map. This is also consistent with what Muleta et al. (2017) found through genome-wide association mapping that SNPs IWA3621, IWA2977, IWA4983, IWA4984, IWA5149, IWA6875, IWA6818 linked to Yr QTL in TAM 111, UC1110, Opata 85, Louise, and IDO444 clustered at 189 MB while the resistance genes, Yr43, Yr44, and Yr 53 clustered around 601 to 725 MB based on their associated SNPs, IWA1040 and IWA8266 (Figure 2D). SNPs IWA6121 and IWA4096 are around 696 to 714 MB regions (Naruoka et al., 2016). In addition, the saturated genetic map constructed by 90K and GBS SNPs in this study is accurate enough to identify the correct locations for genes or QTL, and will be a valuable platform for marker-assisted breeding and map-based cloning. However, the relationship among the KASP markers which were generated through the closely linked markers for *QYr.tamu-2BL* and annotated genes on chromosome 2BL needs for further confirmation.

QYr.tamu-1A4.1 and *QYr.tamu-1A1.1* peaked at the position at 45.9 cM and 379.3 cM on linkage group 1A4 and 1A1, respectively. These two QTL were identified on the long arm of 1A, and detected in five environments linked with the QTL for DS, where the positive allele came from female part ‘TAM 112’. Basnet et al. (2014) identified one QTL on the long arm of 1A (*QYr.tam-1AL*), which was detected in MTV11 and PULL11, and the favorable allele was derived from TAM 112. We assume that they are the same QTL, but we identified this QTL in two more environments in addition to MTV11 and PULL11. *QYr.tamu-1A1.1* was identified for resistance with IT, where ‘TAM 111’ contributing the allele to confer the stripe rust resistance.

So in this study, both parents contributed positive alleles for stripe rust resistance, allowing transgression breeding application. Although no formally named *Yr* genes have been reported on chromosome 1A, some researches have shown several minor stripe rust resistance QTL mapped onto the chromosome of 1A. One minor QTL associated with stripe rust was detected on the short arm of 1A chromosome by Prins et al (2011). Bulli et al. (2016) detected significant QTL on the long arm of chromosome 1A by using National Small Grain Collection (NSGC) diverse panel, and the marker associated with this QTL is IWA5505 and IWA3215. However, no common markers were found among these studies. Based on the CSS physical map, the markers closely linked to *QYr.tamu-1A4.1*, IWB72163 and IWB1256, were both positioned at 566.0 Mbp and 566.4 Mbp on CSS physical distance, whereas IWA5505 and IWA3215, identified in Bulli et al (2016), were placed at 556.9 Mbp and 593.3 Mbp, respectively. The closely enough distance among IWB72163, IWB1256, IWA 5505, and IWA3215 provided an evidence that the QTL mentioned in Bulli et al (2016) is the same one as *QYr.tamu-1A4.1* identified in present study.

QYr.tamu-2A1, detected on the short arm of chromosome 2A, has significant Genotype Environment Interaction (GEI) in AR12 and CAS10 for DS and in AR12 and ET12 for IT. The flanking markers for 2AS QTL are GBS5258582 and GBS5281750. Other studies have also reported stripe rust QTL on 2AS (Crossa et al., 2007; Mallard et al., 2005; Vazquez et al., 2012). Four major genes have been reported to be present in chromosome 2A are *Yr56*, *Yr17*, *Yr32*, and *Yr1*, (Bulli et al., 2016). *Yr56* has also been identified on the short arm of chromosome 2A. SNP markers IWA422, IWA2526, and IWA424 are closely linked *Yr56* gene(Bulli et al., 2016). However, none of these markers are in the same linkage fragment as our markers. We used CSS reference map to compare those markers physical places and determine whether they are the

same QTL or not. IWA422 was placed at 12.6 Mbp at an undetermined chromosome, whereas IWA2526, and IWA424 were positioned at 36.6 and 101.4 Mbp on CSS 2A chromosome physical map, respectively. Several flanking markers of *QYr.tamu-2A1* were also referenced to the CSS map. The closely-linked markers IWB9974 and GBS5258582, only 1 cM way from *QYr.tamu-2A1* detected in this study, positioned at the similar places as the IWA2526 reported by Bulli et al. (2016) for 22.2 Mbp and 21.6 Mbp. It is appropriate to conclude that they are the same QTL. A goatgrass (*Aegilops ventricosa* Tausch)-derived major gene, *Yr17* through 2NS-2AS translocation, has been reported and mapped on the 2AS chromosome arm. As *QYr.tam-2A1* was detected in the AR12 experiment where the RILs were inoculated with a *Yr17*-virulent *Pst* race, it is most likely that *QYr.tam-2A1* is different from, but closely linked to *Yr17*. Interestingly, *QYr.tamu-2A1* involves three out of six epistatic interactions, one of them with the major QTL *QYr.tamu-2BL.1*. This pair of QTL also showed significant epistatic effects by environment interaction, suggesting that pyramiding these genes with other genes can be used to achieve higher and more durable resistance to stripe rust.

GBS markers GBS7081733 and GBS7152618 associated with *QYr.tamu-4A3.1* for DS. This QTL was located onto the long arm of chromosome 4A. It was detected for significant GEI in almost all environments. In the previously study, Basnet et al. (2014) didn't report this QTL. However, we detected this QTL in the present study and viewed it as a major one since it was consistently detected in all environments. *Yr51* and *Yr60* were reported on the long arm of chromosome 4A. *Yr60* was identified as the seedling resistance gene and a QTL in cultivar 'Kariega' (Prins et al. 2011) was identified overlap with IWA6697 (Bulli et al., 2016), which was mapped at the similar position as previously reported IWA1034 (Maccaferri et al., 2015). However, after CSS referenced, the two GBS markers GBS7081733 and GBS7152618, closely

linked to the 4A QTL, identified in our study didn't share enough close physical location with the markers reported in other studies. Evidence is lacking to determine whether they were the same QTL or closely linked.

The markers GBS2273804 and IWB3253 were linked to the QTL mapped onto the short arm of chromosome 4D, *QYr.tamu-4D.1*. We consider *QYr.tamu-4D.1* as an environment-or race-specific QTL since it was only shown in MTV11 and PULL11, where more Pst races were presented in 2011 (Wan et al., 2016). Singh et al. (2000) mapped *Yr28* onto the chromosome 4DS, and reported that *Yr28* strongly influenced seedling resistance, it showed a strong effect in adult plants at only the warmer field sites.

The TAM 111-derived *QYr.tamu-6B2* was identified on 6BS in the ETR12 experiment. High temperature adult-plant resistance gene *Yr36* (Fu et al., 2009), major gene *Yr35* (Dadkhodaie et al., 2010), and other stripe rust resistance QTL (Crossa et al., 2007; Suenaga et al., 2003) have been mapped on the short arm of chromosome 6B. The stripe rust resistance gene *Yr36* is closely linked to the grain protein content (Gpc) locus, and the same markers used for tagging *Gpc-B1* can be used for *Yr36* (Uauy et al., 2005). Only several AFLP markers were reported to tag the *Gpc-B1* QTL on chromosome 6BS including Xmwg79-6B, Xabg458-6B, and Xglk582-6B. No common marker can be used to differentiate the relative locations for those markers with the GBS markers in our study. Similarly, *QYr.tamu-7D3* tagged by IWB17509 and IWB19321 conferred resistance in MTV10, MTV11, and PULL11 for DS. *Yr18* was reported on 7DS (Lagudah et al. 2009) and *Yr33* was mapped on 7DL (Zahravi et al. 2003). Because of different types of markers used in their studies and our study, we could not determine the relationships among the genes. Further tests of our mapping population with the markers

diagnostic for or linked to *Yr18* and *Yr33* should be used to answer the question whether *QYr.tamu-7D3* is the same or linked genes to the previously reported genes on chromosome 7B.

2.4.3 Application of SNPs associated with QYr.tamu-2BL in MAS

With the implementation of high-throughput genotyping platforms, the cost of marker analysis will be less important. Whole genome array-based assays, like 90K iSelect Infinium assay and GBS mainly focus on marker discovery for specific traits of high economic importance. Once closely linked SNPs marker have been identified, KASP allow the routine selection of favorable alleles in breeding population. The application of MAS provides an ideal approach for deployment of QTL of disease resistance in many breeding programs. IWB47487, IWB26631, and IWB29391 are the closest markers associated with QTL for stripe rust on the long arm of chromosome 2B in the population used in this study. All three KASP markers are found to be very effective in predicting stripe rust resistance allele from TAM 111. These markers can be used together to increase selection accuracy. In addition, SNPs or GBS markers associated with several minor QTL *QYr.tamu-1A4.1*, *QYr.tamu-1A1.1*, *QYr.tamu-2A1*, *QYr.tamu-4A3.1*, *QYr.tamu-4D.1*, *QYr.tamu-6B2* and *QYr.tamu-7D3*, can be used in pyramiding these stripe rust resistance QTL with other resistance genes to achieve an increased level of durable resistance.

2.5 References

Akbari, M., P. Wenzl, V. Caig, J. Carling, L. Xia, S. Yang, G. Uszynski, V. Mohler, A. Lehmensiek, H. Kuchel, M. Hayden, N. Howes, P. Sharp, P. Vaughan, B. Rathmell, E. Huttner, and A. Kilian. 2006. Diversity arrays technology (DArT) for high-throughput profiling of the hexaploid wheat genome. Theor. Appl. Genet. 113:1409-1420. doi:10.1007/s00122-006-0365-4

Basnet, B.R., A.M. Ibrahim, X. Chen, R.P. Singh, E.R. Mason, R.L. Bowden, S. Liu, D.B. Hays, R.N. Devkota, N.K. Subramanian, and J.C. Rudd. 2014. Molecular mapping of stripe rust resistance in hard red winter wheat TAM 111 adapted to the US high plains. Crop Sci. 54:1361-1373.

Boer, M.P., D. Wright, L. Feng, D.W. Podlich, M. Cooper, and F.A.v. Eeuwijk. 2007. Mixed-model quantitative trait loci (QTL) analysis for multiple-environment trial data using environmental covariables for QTL-by-environment interactions, with an example in maize. Genetics 177: 1801-1813.

Brondani, C., P. Hideo, N. Rangel, T.C.O. Borba, R.P.V. Brondani. 2003.Transferability of micro-satellite and ISSR markers in *Oryza* species. Hereditas 138:187-192.

Bulli, P., J. Zhang, S. Chao, X. Chen, and M. Pumphrey. 2016. Genetic architecture of resistance to stripe rust in a global winter wheat germplasm collection. G3: Genes| Genomes| Genetics 6: 2237-2253.

Chen, X.M. 2013. High-temperature adult-plant resistance, key for sustainable control of stripe rust. Am. J. Plant Sci. 4:608-627.

Cheng, P., and X.M. Chen. 2010. Molecular mapping of a gene for stripe rust resistance in spring wheat cultivar IDO377s. Theor. Appl. Genet. 121:195-204. doi:10.1007/s00122-010-1302-0

Crossa, J., J. Burgueno, S. Dreisigacker, M. Vargas, S.A. Herrera-Foessel, M. Lillemo, R.P. Singh, R. Trethowan, M. Warburton, J. Franco, M. Reynolds, J.H. Crouch, and R. Ortiz. 2007. Association analysis of historical bread wheat germplasm using additive genetic covariance of relatives and population structure. Genetics 177:1889-1913. doi:10.1534/genetics.107.078659

Dadkhodaie, N.A., H. Karaoglou, C.R. Wellings, and R.F. Park. 2010. Mapping genes *Lr53* and *Yr35* on the short arm of chromosome 6B of common wheat with microsatellite markers and studies of their association with *Lr36*. Theor. Appl. Genet. 122:479-487. doi:10.1007/s00122-010-1462-y

Elshire, R.J., J.C. Glaubitz, Q. Sun, J.A. Poland, K. Kawamoto, E.S. Buckler, and S.E. Mitchell. 2011. A robust, simple genotyping-by-sequencing (GBS) approach for high diversity species. PloS one 6:19379.

Fu, D., C. Uauy, A. Distelfeld, A. Blechl, L. Epstein, X. Chen, H. Sela, T. Fahima, and J. Dubcovsky. 2009. A kinase-START gene confers temperature-dependent resistance to wheat stripe rust. Science 323:1357-1360. doi:10.1126/science.1166289

Gregório, M., M.A. Pinhel, G.M. Florim, G. Sousa, M. Nakazone, D. Martins, S. Silva, A. Crestani, M.L. Santos, J.R. Ferraz Filho, and L.F. Lauletta. 2012. Relevance of Endothelial Nitric Oxide Sintase, Elastin and Endoglin Genetic Variants in Familial Intracranial Aneurysm (P01. 025). Neurology 78: 01-025.

Jaccoud, D., K. Peng, D. Feinstein, and A. Kilian. 2001. Diversity arrays: a solid state technology for sequence information independent genotyping. Nucleic acids research, 29: 25.

Johnson, R., M.S. Wolfe, and P.R. Scott. 1969. Annual Report 1968. Plant Breeding Institute, Cambridge, UK. p. 113–123.

Kalia, R.K., M.K. Rai, S. Kalia, R. Singh, and A.K. Dhawan. 2011. Microsatellite markers: an overview of the recent progress in plants. Euphytica 177:309-334.

Kosambi, D.D. 1943. The estimation of map distances from recombination values. Annals of Eugenics 12:172-175.

Lagudah, E.S. 2011. Molecular genetics of race non-specific rust resistance in wheat. Euphytica 179:81-91.

Lagudah, E.S, S.G. Krattinger, S. Herrera-Foessel, R.P. Singh, J. Huerta-Espino, Q. Spielmeyer, G. Brown-Guedira, L.L. Selter, and B. Beller. 2009. Gene-specific markers for the wheat gene Lr34/Yr18/Pm38 which confers resistance to multiple fungal disease. Theor Appl Genet 119:889-898

Iehisa, J.C.M., R. Ohno, T. Kimura, H. Enoki, S. Nishimura, Y. Okamoto, S. Nasuda, and S. Takumi. 2014. A high-density genetic map with array-based markers facilitates structural and quantitative trait locus analyses of the common wheat genome. DNA Res. 21:555-567.

Li, J, and L. Ji. 2005. Adjusting multiple testing in multilocus analyses using the eigenvalues of a correlation matrix. Heredity. 95:221-7. doi: 10.1038/sj.hdy.6800717.

Li, H., P. Vikram, R.P. Singh, A. Kilian, J. Carling, J. Song, J.A. Burgueno-Ferreira, S. Bhavani, J. Huerta-Espino, T. Payne, and D. Sehgal. 2015. A high density GBS map of bread wheat and its application for dissecting complex disease resistance traits. BMC genomics 16: 216.

Lin, M., S. Cai, S. Wang, S. Liu, G. Zhang, and G. Bai. 2015. Genotyping-by-sequencing (GBS) identified SNP tightly linked to QTL for pre-harvest sprouting resistance. Theor. Appl. Genet. 128:1385-1395.

Liu, S., J.C. Rudd, G. Bai, S.D. Haley, A.M.H. Ibrahim, Q. Xue, D.B. Hays, R.A. Graybosch, R.A. Devokota, P.S. Amand. 2014. Molecular markers linked to important genes in hard winter wheat. Crop Sci. 54:1304–1321. doi: 10.2135/cropsci2013.08.0564.

Liu, S., S. Ocheya, S. Dhakal, X. Gu, C.T. Tan, Y. Yang, J. Rudd, D. Hays, A. Ibrahim, Q. Xue, and S. Chao. 2016. Validation of chromosome locations of 90K array single nucleotide polymorphisms in US wheat. Crop Sci. 56:364-373. doi:10.2135/cropsci2015.03.0194

Luo, P., X. Hu, H. Zhang, and Z. Ren. 2009. Genes for resistance to stripe rust on chromosome 2B and their application in wheat breeding. Prog. Nat. Sci.19: 9-15.

Maccaferri, M., J. Zhang, P. Bulli, Z. Abate, S. Chao, D. Cantu, E. Bossolini, X. Chen, M. Pumphrey, and J. Dubcovsky. 2015. A genomewide association study of resistance to stripe rust (*Puccinia striiformis* f. sp. *tritici*) in a worldwide collection of hexaploid spring wheat (*Triticum aestivum* L.). G3 Genes Genom. Genet. 5: 449-465.

Macer, R. 1966. The formal and monosomic genetic analysis of stripe rust (*Puccinia striiformis*) resistance in wheat. Hereditas Suppl 2:127–142.

Mallard, S., D. Gaudet, A. Aldeia, C. Abelard, A.L. Besnard, P. Sourdille, and F. Dedryver. 2005. Genetic analysis of durable resistance to yellow rust in bread wheat. Theor. Appl. Genet. 110:1401–1409. doi:10.1007/s00122-005-1954-3

Miller, M.R., J.P. Dunham, A. Amores, W.A. Cresko, and E.A. Johnson. 2007. Rapid and cost-effective polymorphism identification and genotyping using restriction site associated DNA (RAD) markers. Genome research, 17: 240-248.

Muleta, T. K., P. Bulli, S. Rynearson, X. Chen, and M. Pumphrey. 2017. Loci associated with resistance to stripe rust (*Puccinia striiformis* f. sp. *tritici*) in a core collection of spring wheat (*Triticum aestivum*). Plos One 12: e0179087.

Peng, J.H., D. Sun, and E. Nevo. 2011. Domestication evolution, genetics and genomics in wheat. Mol. Breed. 28: 281.

Peterson, B.K., J.N. Weber, E.H. Kay, H.S. Fisher, and H.E. Hoekstra. 2012. Double digest RADseq: an inexpensive method for de novo SNP discovery and genotyping in model and non-model species. PloS one 7: 37135.

Bulli, P., J. Zhang, S. Chao, X. Chen, and M. Pumphrey. 2016. Genetic architecture of resistance to stripe rust in a global winter wheat germplasm collection. G3 Genes Genom. Genet. 6: 2237-2253.

Poland, J., J. Endelman, J. Dawson, J. Rutkoski, S. Wu, Y. Manes, S. Dreisigacker, J. Crossa, H. Sánchez-Villeda, M. Sorrells, and J.L. Jannink. 2012. Genomic selection in wheat breeding using genotyping-by-sequencing. The Plant Genome 5:103-113.

Prins, R., Z. A. Pretorius, C. M. Bender, and A. Lehmensiek. 2011. QTL mapping of stripe, leaf and stem rust resistance genes in a Kariega × Avocet S doubled haploid wheat population. Mol. Breed. 27: 259-270.

Saari, E.E. and R.D. Wilcoxson. 1974. Plant disease situation of high-yielding dwarf wheats in Asia and Africa. Annu. Rev. Phytopathol. *12*: 49-68.

Saintenac, C., D. Jiang, S. Wang, and E. Akhunov. 2013. Sequence-based mapping of the polyploid wheat genome. G3: Genes| Genomes| Genetics 3:1105-1114.

Singh, R.P., J.C. Nelson, and M.E. Sorrells. 2000. Mapping *Yr28* and other genes for resistance to stripe rust in wheat. Crop Sci. 40:1148-1155.

Sorrells, M.E., J.P. Gustafson, D. Somers, S. Chao, D. Benscher, G. Guedira-Brown, E. Huttner, A. Kilian, P.E. McGuire, K. Ross, and J. Tanaka. 2011. Reconstruction of the Synthetic W7984× Opata M85 wheat reference population. Genome 54:875-882.

Spindel, J., M. Wright, C. Chen, J. Cobb, J. Gage, S. Harrington, M. Lorieux, N. Ahmadi, and S. McCouch. 2013. Bridging the genotyping gap: using genotyping by sequencing (GBS) to

add high-density SNP markers and new value to traditional bi-parental mapping and breeding populations. Theor. Appl. Genet. 126:2699-2716.

Suenaga, K., R.P. Singh, J. Huerta-Espino, and H.M. William. 2003. Microsatellite markers for genes Lr34/Yr18 and other quantitative trait loci for leaf rust and stripe rust resistance in bread wheat. Phytopathology 93:881–890. doi:10.1094/PHYTO.2003.93.7.881

Sui, X.X., M.N. Wang, and X.M. Chen. 2009. Molecular mapping of a stripe rust resistance gene in spring wheat cultivar Zak. Phytopathology 99:1209–1215. doi:10.1094/PHYTO-99-10-1209

Tan, C.T., S. Assanga, G. Zhang, J.C. Rudd, S.D. Haley, Q. Xue, A. Ibrahim, G. Bai, X. Zhang, P. Byrne, and M.P. Fuentealba. 2017. Development and Validation of KASP Markers for Wheat Streak Mosaic Virus Resistance Gene. Crop Sci. 57:340-349.

Uauy, C., J.C. Brevis, X. Chen, I. Khan, L. Jackson, O. Chicaiza, A. Distelfeld, T. Fahima, and J., Dubcovsky. 2005. High-temperature adult-plant (HTAP) stripe rust resistance gene *Yr36* from *Triticum turgidum* ssp. *dicoccoides* is closely linked to the grain protein content locus *Gpc-B1*. Theor. Appl. Genet. 112:97. doi:10.1007/s00122-005-0109-x

Van Eeuwijk, F.A., M.C.A.M. Bink, K. Chenu, and S.C. Chapman. 2010. Detection and use of QTL for complex traits in multiple environments. Curr. Opin. Plant Biol. 13: 193-205. doi: 10.1016/j.pbi.2010.01.001.

Van Ooijen, J.W. 2006. JoinMap 4. Software for the calculation of genetic linkage maps in experimental populations. Kyazma BV: Wageningen, Netherlands.

Van Ooijen, J.W. 2009. MapQTL 6. Software for the mapping of quantitative trait loci in experimental populations of diploid species. Kyazma BV: Wageningen, Netherlands.

Vazquez, M.D., C. James Peterson, O. Riera-Lizarazu, X.M. Chen, A. Heesacker, K. Ammar, J. Crossa, and C. Mundt. 2012. Genetic analysis of adult plant, quantitative resistance to stripe rust in wheat cultivar ‘Stephens’ in multi-environment trials. Theor. Appl. Genet. 124:1–11. doi:10.1007/s00122-011-1681-x

Voorrips, R.E. 2002. MapChart: Software for the graphical presentation of linkage maps and QTLs. J. Hered. 93:77-78. doi:10.1093/jhered/93.1.77

Wan, A.M., Chen, X.M., and Yuen, J. 2016. Races of Puccinia striiformis f. sp. tritici in the United States in 2011 and 2012 and comparison with races in 2010. Plant Dis. 100:966-975.

Wang, S., D. Wong, K. Forrest, A. Allen, S. Chao, B.E. Huang, M. Maccaferri, S. Salvi, S.G. Milner, L. Cattivelli, and A.M. Mastrangelo. 2014. Characterization of polyploid wheat genomic diversity using a high-density 90 000 single nucleotide polymorphism array. Plant Biotechnol. J. 12: 787-796.

Wenzl, P., J. Carling, D. Kudrna, D. Jaccoud, E. Huttner, A. Kleinhofs, and A. Kilian. 2004. Diversity Arrays Technology (DArT) for whole-genome profiling of barley. Proc. Natl. Acad. Sci. U.S.A. 101: 9915-9920.

Xu, L.S., M.N. Wang, P. Cheng, Z.S. Kang, S.H. Hulbert, and X.M. Chen. 2013. Molecular mapping of *Yr53*, a new gene for stripe rust resistance in durum wheat accession PI 480148 and its transfer to common wheat. Theor. Appl. Genet. 126:523–533. doi:10.1007/s00122-012-1998-0

Yang J, Hu C, Hu H, Yu R, Xia Z, Ye X, Zhu J. 2008. QTLNetwork: mapping and visualizing genetic architecture of complex traits in experimental populations. Bioinformatics 24:721–723. doi: 10.1093/bioinformatics/btm494.

Zahravi, M., H.S. Bariana, M.R. Shariflou, P.V. Balakrishna, P.M. Banks, and M.R. Ghannadha. 2003. Bulk segregant analysis of stripe rust resistance in wheat (Triticum aestivum) using microsatellite markers. In: Pogna NE, Romano M, Pogna EA, Galterio G (eds) Proc 10th Intl Wheat Genet Symp, Instituto Sperimentale per Cerealcoltura, Rome, pp 861–863.

CHAPTER III

ANALYSIS OF QTL ASSOCIATED WITH YIELD AND YIELD COMPONENTS IN TAM111 AND TAM112 AND THEIR INTERACTIONS WITH ENVIRONMENTS

3.1 Introduction

Wheat (*Triticum aestivum* L.) is one of the most important cereal crops in the world providing needed caloric intake and protein requirements to world's population. The significance of wheat lays on the physical and chemical properties of its grains, which provides over 20% of the calories and protein requirements for human nutrition. About 40% of the world's population in more than 40 countries depends on wheat (Reddy et al., 2004). Grain yield (GY) is usually the trait of most importance to wheat breeders and subsequently grain producers. GY is a particularly polygenic and complex trait and is greatly influenced by various environmental conditions and environmental and genetic interactions throughout the processes of vegetative and reproductive growth and development (Wu et al. 2012). GY is usually broken down into three components, namely thousand kernel weight (TKW), kernels spike^{-1} (KPS), and spikes m^{-2} (SPM). Many genes or quantitative trait loci (QTL) influence GY and its components. Interactions between QTL and the environment also modify the expression of the QTL in different genetic backgrounds (Barton and Keightley, 2002). The condition that a QTL detected in one environment but not in others might indicate QTL-by-environment interaction (QEI), but assessing the contribution of such interactions to phenotypic variation by simply comparing QTL detected in multiple environments is difficult. Goldringer et al. (1997) first proposed the additive and epistatic genetic variances for agronomic traits in a population of doubled-haploid wheat and demonstrated that GY and its components showed either additive or additive plus epistatic

effects. Significant epistasis and QEI were identified subsequently for GY QTL (Kumar et al. 2007; Snape et al. 2007; Zhang et al. 2008; Reif et al. 2011; Patil et al. 2013). Thus, dissection of QTL effects and their interactions may facilitate better understanding of the genetic control of complex GY traits (Carlborg and Haley 2004).

Genetic linkage maps play a crucial role in QTL identification by providing not only measurements of the relative effects of alleles in a mapped chromosomal region but selectable DNA markers for breeders to manipulate traits through MAS (Torada et al. 2006). Several types of markers (SSR, EST, AFLP, BARC microsatellite, and DArT marker) were used in QTL mapping of wheat agronomic traits (Li et al. 2007; Cuthbert et al. 2008; Wang et al. 2009; Mir et al. 2012; McIntyre et al., 2010). More recently, single nucleotide polymorphisms (SNPs) were used to develop high-density genetic maps and QTL mapping in many crops. SNPs are the most common source of genetic variation among individuals of any species and the smallest unit of genetic variation, with virtually unlimited numbers (Deschamps and Campbell 2010). The availability of diverse SNP genotyping platforms facilitates genetic dissection, marker discovery, and genomic selection of complex crop traits (Collard and Mackill 2008; Jannink and Lorenz 2010). However, the extensive abundance of conserved repetitive element (~80%) nature of the hexaploid wheat genome has slowed progress in SNP discovery and detection (Wanjugi et al., 2009). A few SNP markers are ready to be used for studying complex agronomic traits. Cavanagh et al. (2013) developed 9K SNP assays and constructed the first high-density wheat consensus SNP map containing 7504 polymorphic loci. A genotyping-by-sequencing (GBS) protocol has recently emerged as a promising approach in wheat using restriction digestion to reduce the complexity of the genome (Poland et al. 2012). GBS takes advantage of NGS and keeps sequencing costs down by multiplexing samples using barcodes. These SNP assay and

maps provide a powerful resource for further mapping of wheat traits of interest and for genomic research and genome-wide association studies in wheat.

In this study, highly-saturated genetic map constructed with 90K SNP array and GBS was used to map QTL associated with grain yield, yield components, and other agronomic traits in 124 recombinant inbred lines (RILs) population developed from 'TAM 112'/'TAM 111' cross. Additionally, the QTL identified in multiple-environment analysis was used to determine the genotype-by-environment interaction (GEI). Genetic interaction between QTLs and epistatic-by-environments interaction was also considered for genetic effect on GY-related traits. Consistent and common QTL was identified from different software and the results from eight individual environments and three mega-environments analysis. Then closely linked makers' sequences were analyzed to reveal potential candidate genes functions.

3.2 Materials and methods

3.2.1 Plant Material and Phenotyping

The population of 124 F_7 RILs is derived from the cross of TAM112/TAM111. The pedigree of TAM 111 (Lazar et al., 2004) is 'TAM 107'//TX78V3630/ 'Centurk78'/3/TX87V1233 and the pedigree of TAM 112 (Rudd et al., 2014) is U1254-7-9-2-1/TXGH10440. Both parents, TAM 111 and TAM 112, are hard red winter wheat (HRWW) developed and released by Texas A&M AgriLife Research, and they are top-ranked cultivars in the U.S. Great Plains. TAM 112 has the excellent performance under drought stress conditions and possesses good milling and baking quality. TAM 111 is also a superior grain yield cultivar. The progenies were advanced to the F_5 generations using single-seed descent. The parents and $F_{5:6}$ to $F_{5:9}$ RILs were evaluated for yield traits in field experiments across eight environments

during four crop years ending in 2011, 2012, 2013, 2014 (A combination of location, year, and irrigation level was considered as an environment). All trials were planted in an alpha lattice design with an incomplete block size of five plots and each trial had two replications in every environment. Standard agronomic practices were carried out for each environment. The locations used in this study include Texas AgriLife Research stations in Bushland (35° 06' N, 102° 27' W) in 2011 and 2012 (BD11 and BD12), Chillicothe (34° 07' N, 99° 18' W) in 2012 and 2014 (CH12 and CH14), and two irrigation levels (75% and 100% ET requirement) in Etter (35° 59' N, 101° 59' W), TX in 2013 and 2014 (13EP4, 13EP5, 14EP4 and 14EP5).

Yield components were measured based on a half meter long inner row of biomass sample at maturity. The parameters included TKW; KPS; SPM; harvest index (HI); total dry biomass weight (BW); mean single head weight (MSHW); mean head grain weight (MHGW). The HI was determined as grain weight per sample divided by total weight of biomass plus grain. The GY of each entry was calculated from the yield of combine (YLD) after maturity with above 10% grain moisture plus hand harvest grain weight from the biomass sample (HHDG).

3.2.2 DNA extraction and genotyping

To obtain genotyping data, whole genomic DNA was extracted from leaf samples of parents and 124 RIL using the CTAB method with minor modification as described by Liu at al. (2013). The DNA was purified and assessed for quality and quantity at Texas A&M AgriLife Research wheat genetics laboratory in Amarillo, TX.

SNP genotyping was performed with Infinium iSelect assays containing 90K SNPs based on the manufacturer's protocol (Illumina Inc., San Diego, CA, USA). The assay was designed under International Wheat SNP Consortium protocols (Cavanagh et al. 2013). The fluorescence

signal was captured by Illumina scanner and analyzed using GenomeStudio software (www.illumina.com). The genotyping assay was conducted at the USDA Small Grains Genotyping Laboratory at Fargo, ND. Genotyping analysis module converts red and green signals for each SNP into A and B signals whose values reflect the relative abundance of arbitrarily assigned A and B alleles. The results for each SNP were displayed in Cartesian coordinates with normalized signal intensity on the y-axis and normalized theta values (deviation of the cluster from zero to one) on the x-axis. The x-axis reflects the genotype frequency for A and B locus with zero = AA genotype and one = BB genotype. The clusters were color coded with red color representing homozygous AA genotype, blue color for homozygous BB genotype and grey color for the heterozygotes (AB) (Liu et al., 2016; Assanga et al., 2017a, 2017b).

The 124 RILs and two parents were also processed following the double digest restriction-site associated DNA sequencing (ddRADSeq) method as developed by Peterson et al. (2012) with some noted modifications. The GBS libraries were constructed using 96-plex plate with single random blank well included for quality control. DNA was co-digested with the restriction enzymes *PstI* (CTGCAG) and *MspI* (CCGG) and barcoded adapters were ligated to individual samples. Detailed GBS protocols can reference in Peterson et al. (2012). Each library was sequenced on a 48 samples per lane with barcode index for Illumina HiSeq 2000 in Texas AgriLife Research Genomics & Bioinformatics Services at college station, TX (http://www.txgen.tamu.edu/).

3.2.3 Statistical analysis

Single environment analysis of variance was conducted to determine significant locations for pooling into combined environment analysis. Only single environment with heritability ≥ 0.2

were included into combined analysis. Combined analysis of variance for individual trait was determined the significance of genetic variance, phenotypic variance and genotype-by-environment interaction (GEI) components in each environment. Pearson's correlation coefficients among measured variables were calculated using the CORR procedure of SAS. Adjusted means (BLUE) and predicted means (BLUP) of individual environment and across all environment were computed using a restricted maximum likelihood (REML) approach based on META-R program with lme4 package in R software (Gregorio et al., 2015).

3.2.4 Linkage map construction and QTL identification

Principles regarding the linkage map construction were described in Liu et al. (2016). QTL mapping was performed using MapQTL (Van Ooijen 2009) with composite interval mapping Multiple QTL Mapping (MQM) analysis for eight individual environments and three mega-environments. LOD thresholds were used of 2.5 to select significant QTL. Single trait with multiple environments was implemented in GenStat based on a linear mixed model (LMM) framework (Van Eeuwijk et al., 2010). Under this GenStat framework, multi-environment QTL mapping was implemented in a stepwise process with simple interval mapping (SIM) followed by two or more successive rounds of composite interval mapping (CIM) using QTL identified in SIM as co-factor to control the genetic background (Bernardo, 2013). Significant QTL additive effects, epistasis effects between QTL by QTL interaction and epistatic by environment interaction were characterized by QTLNetwork2.0 (Yang et al., 2008).

3.2.5 Candidate gene analysis

The genetic consensus maps and physical maps of those tightly linked SNPs of consistent QTL through different models were compared across Chromosome Survey Sequence (CSS) of Chinese Spring, W7984 and NRgene Pseudo Molecular physical map of Chinese Spring. Best Contig or scaffold sequence hits determined in the IWGSC database were subjected to a BLASTN search against *Brachypodium*, rice (*O. sativa* ssp. *japonica*), and *Sorghum bicolor* (L.) genome databases (http://www.phytozome.org) to identify candidate genes annotation. A significant match was declared when a hit had at least 70% nucleotide identity with an e-value lower than e^{-20}.

3.3 Results

3.3.1 Linkage map

Details of the linkage groups can be found in Yang et al. (2017). Briefly, A set of 9928 markers from 80 chromosome fragments and covering all 21 chromosomes, including 19 SSR and STS, 5094 GBS, 4815 SNPs from 90K were used for QTL analyses. The cumulative maps have an average marker density of 1.5 cM. The 90K SNPs array mapped on A, B, and D genome have 43.2%, 42.5%, and 14.4% of total SNPs, respectively. In addition, the GBS markers mapped on A, B, and D genome have 36.2%, 49.1%, and 14.7% of total GBS marker.

3.3.2 Phenotypic summary

The combined ANOVA across environments indicated a significant level ($P < 0.001$) of genetic variance for all traits (Table 8). A high proportion of variation explained by GEI was common among all traits. Most of the traits displayed higher genotypic variation than GEI

component except grain yield, biomass weight, and yield from combine. These complex quantitative traits controlled by several genes are highly influenced by environmental conditions. Epistatic QTL, QEI, and epistasis-by-environment affecting those complex traits were further characterized.

Table 8. The combined ANOVA, heritability, and mean performance for all traits across environments.

Trait†	Units	Error Var	Gen Var‡	GenxEnv Var§	Env Var¶	Heritability	Trait Mean	LSD	CV
GY	kg / ha	45679.62	13148.57***	44641.99***	1019325.76***	0.66	2162.83	418.91	11.53
TKW	g	2.91	1.4345***	0.4482***	23.5042***	0.86	24.50	3.34	6.96
KPS	No. / head	9.52	1.9228***	1.2886***	2.025***	0.72	18.28	6.05	16.88
SPM	No. / m^2	14580.98	2196.4827***	141.7288***	15964.6193***	0.70	630.69	236.67	19.15
HI	%	18.86	1.75***	1.91**	32.66**	0.55	34.68	8.52	12.52
BW	g	22324.20	585.8131***	2148.1449*	37746.1607*	0.26	807.49	292.85	18.50
HHDG	kg / ha	3839.58	228.401***	513.899**	4426.3052**	0.43	2765.1	121.45	22.41
MSHW	mg / head	9669.99	3859.72***	1532.61***	22086.44***	0.83	725.39	192.74	13.56
MHGW	mg / head	6958.87	1984.36***	1012.86***	9485.05***	0.78	448.57	163.50	18.60
YLD	kg / ha	332.72	128.3603***	179.1955*	3468.0519*	0.75	1963.8	35.75	9.29
AG	1 - 9	0.1309	0.0481***	0.0316***	0.0001***	0.80	3.07	0.71	11.77

†Abbreviation of traits: GY grain yield, TKW thousand kernel weight, KPS kernels $spike^{-1}$, SPM spikes m^{-2}, HI harvest index, BW biomass weight, HHDG hand harvest dry grain, MSHW mean single head weight, MHGW mean head grain weight, YLD yield from combine and AG agronomic score.
‡Genotype.
§Genotype-by-environment interaction.
¶Environment
*, **, *** significant at 0.05, 0.01, and 0.001 probability levels, respectively.

The entry-mean heritability ranged from moderate to high. Three major yield components including thousand kernel weight, kernels $spike^{-1}$, spikes m^{-2} exhibited high heritability. Some other traits including mean single head weight, mean head grain weight, yield from combine, and agronomic score also showed high heritability (>0.6), while grain yield, harvest index, and hand

harvest dry grain displayed moderate heritability (0.4 to 0.6). Biomass weight expressed relatively low heritability (<0.4) (Table 8).

Positive phenotypic correlation coefficient was found between each of the three yield components and yield (Table 9). Across environments, grain yield showed positive genetic correlation with all the traits and most with significance level ($p < 0.01$). Among three yield components, kernels spike^{-1} displayed strongest positive correlation with grain yield. Biomass weight, hand harvest dry grain and yield from combine showed high correlation with grain yield as expected. The data suggests that improvement in grain yield may be achievable through indirect selection of these traits. Hence, mapping the QTL for yield and positively associated yield components could reveal consistent QTL across environments.

Table 9. Genetic correlation among grain yield and other traits measured in individual environments.

	Pearson Correlation Coefficients, N = 124									
Traits†	TKW	SPM	KPS	HI	BW	HHDG	MSHW	MHGW	YLD	AG
SPM	-0.44**									
KPS	0.09	-0.47**								
HI	0.38**	-0.06	0.48**							
BW	0.02	0.37**	0.39**	0.1						
HHDG	0.26**	0.26**	0.55**	0.67**	0.78**					
MSHW	0.51**	-0.64**	0.84**	0.38**	0.37**	0.48**				
MHGW	0.55**	-0.58**	0.87**	0.58**	0.35**	0.60**	0.95**			
YLD	0.18*	0.1	0.38**	0.48**	0.38**	0.54**	0.29**	0.38**		
AG	0.01	-0.12	0.16	-0.12	0.12	0.01	0.16	0.14	0.1	
GY	0.21**	0.23**	0.42**	0.33**	0.62**	0.63**	0.34**	0.38**	0.76**	0.21**

†Abbreviation of traits: GY grain yield, TKW thousand kernel weight, KPS kernels spike^{-1}, SPM spikes m^{-2}, HI harvest index, BW biomass weight, HHDG hand harvest dry grain, MSHW mean single head weight, MHGW mean head grain weight, YLD yield from combine and AG agronomic score.
*, ** significant at 0.05, and 0.01 probability levels, respectively.

3.3.3 Quantitative trait locus mapping for single environment

For validation the inference on QTL, mixed model account for the dependencies in the data due to blocking and spatial trends, which is crucial for multiple environment and multiple

traits. Genome-wide scan for single trait with multiple environments was performed using GenStat (Table 10). For grain yield, two significant QTL (*Qgy.tamu-1A4* and *Qgy.tamu-7D1.1*) were detected. *Qgy.tamu-1A4* peaked at the GBS marker 3979536_1al_394, accounted for 10.6 % of the phenotypic variance of grain yield. The GEI for this QTL was CH12 with significant additive effect of 0.06, and TAM 112 provided favorable allele to increase grain yield in that environment. *Qgy.tamu-7D1.1* was flanked by IWA1247 and IWB44453 at 56cM. TAM 111 allele increased grain yield at Etter in 2013 and 2014, while TAM 112 allele increased grain yield in BD11, CH12, and CH14. *Qgy.tamu-7D1.1* was detected in seven out of eight individual environments, indicating it is a consistent QTL. This QTL explained 3.7 - 10.5 % of the phenotypic variation of grain yield.

Two QTL were identified for thousand kernel weight, with one QTL found on chromosome fragment 2D1, and the other one was located on 4D (Table 10). *Qtkw.tamu-2D1.2* was tagged by *9861581_2dl_506* and explained 7 to 17.3 % of phenotypic variation of thousand kernel weight. This QTL was significant among almost all the environments. All the favorable alleles in these environments were contributed by TAM 111. The other QTL, *Qtkw.tamu-4D.1*, peaked at the position 52.7 cM with associated marker IWB61486 and explained 3.4 - 10.7 % of the phenotypic variation in four environments. TAM 111 contributed positive alleles in BD12 and CH14. TAM 112 provided positive alleles in 14EP4 and 14EP5.

Table 10. QTL for yield and yield components detected for the model of single trait with multiple environments using GenStat.

QTL†	QTL ID	Chrom	Associated markers	Position (cM)	Physical location (Mbp)	Trait‡	Env§	LOD¶	R^2 range (%)††	AE range‡‡	HVA§§
Qgy.tamu-1A4	3	1A4	3979536_1al_394	131.3	583.709	GY	CH12	2.83	10.6	0.06	P1
Qgy.tamu-7D1.1	52	7D1	IWA1247 - IWB44453	56	72.947	GY	BD11, CH12, 13EP4, 13EP5, CH14, 14EP4, 14EP5	8.7	3.7-10.5	0.02 - 0.07	P2, P2, P1, P1, P2, P1, P1
Qtkw.tamu-2D1.2	20	2D1	9861581_2dl_506	173.2	486.785	TKW	BD11, CH12, 13EP4, 13EP5, CH14, 14EP4, 14EP5	4.37	7-17.3	0.2 - 0.48	All P2
Qtkw.tamu-4D.1	28	4D	IWB61486	52.7	25.989	TKW	BD12, CH14, 14EP4, 14EP5	13.87	3.4-10.7	0.13 - 0.39	P2, P2, P1, P1
Qkps.tamu-1D2.3	8	1D2	IWB3939 - IWA3125	40.1	7.880	KPS	13EP4, 13EP5, 14EP4	4.09	5.3-7.4	0.1 - 0.26	All P1
Qkps.tamu-7D1.2	53	7D1	3938880_7ds_2029 - 3853219_7ds_2287	81.97	84.339	KPS	13EP4, 13EP5	3.92	9.7-10.4	0.11 - 0.31	All P1
Qhi.tamu-7D1.1	52	7D1	3950120_7ds_5316 - IWA1247	48.3	142.729	HI	CH12, CH14	6.92	4.7-19.6	0.01	All P2
Qmshw.tamu-1D2.4	9	1D2	1915633_1ds_1815 - IWB14343	103.98	11.402	MSHW	BD12, CH12, CH14	5.57	4.5-5	0.01	All P2
Qyld.tamu-1B7.2	5	1B3_1	3470420_1bs_1139	341	188.831	YLD	BD12, 13EP5	3.64	2.8-3.4	1.08 - 1.42	P2, P1
Qyld.tamu-5A5	32	5A2_1	IWB8369	133.7	580.803	YLD	13EP5	4.4	3.1	1.35	P2
Qyld.tamu-7D3	55	7D3	3392705_7dl_13504	103.9	597.125	YLD	BD12, 13EP4, 13EP5	3.85	8.1-11.1	2.13 - 3.93	All P2
Qag.tamu-5A3	33	5A3	2797074_5al_324	18.2	664.296	AG	14EP4	5.58	3.5-11.8	0.08	P2
Qag.tamu-7D1.1	52	7D1	IWA1247	54	72.947	AG	BD12, 14EP4, 14EP5	10.46	3.7-11.4	0.03 - 0.07	P2, P1, P1

†QTL name including trait, institute, and linkage group; the linkage group is unique for each numbered QTL if the peak positions were less than 30 cM; within each chromosome fragment, different numbered QTL will have various chromosome fragment parts starting from the fragment name, then adding ".1, .2, …"

‡Abbreviation of traits: GY grain yield, TKW thousand kernel weight, KPS kernels spike^{-1}, SPM spikes m^{-2}, HI harvest index, BW biomass weight, HHDG hand harvest dry grain, MSHW mean single head weight, MHGW mean head grain weight, YLD yield from combine and AG agronomic score.

§Abbreviation of environments: BD11 and BD12 Bushland, TX 2011 and 2012, CH12 and CH14 Chillicothe, TX 2012 and 2014, and 13EP4, 13EP5, 14EP4 and 14EP5 two irrigated levels (75% and 100%) Etter, TX 2013 and 2014.

¶peak -log(P) value.

††percentage of phenotypic variance explained by the QTL.

‡‡Additive effect range recorded for each QTL.

§§High value allele corresponding to each environment under environment column. P1 = TAM 112, P2= TAM 111.

For kernels spike^{-1}, two significant QTL (*Qkps.tamu-1D2.3* and *Qkps.tamu-7D1.2*) were mapped onto chromosome 1D2 and 7D1 (Table 10). The high value allele (HVA) for both QTL associated with KPS were contributed from TAM 112. *Qkps.tamu-1D2.3*, with interval IWB3939 and IWA3125, explained 5.3 - 7.4 % of phenotypic variation across three environments including 13EP4, 13EP5, and 14EP4. *Qkps.tamu-7D1.2* explained 9.7 - 10.4 % of phenotypic variance and mapped at the position 81.97 cM with closely linked markers 3938880_7ds_2029 and 3853219_7ds_2287.

A significant QTL associated with harvest index was detected on chromosome fragment 7D1. Its peak position was at 48.3 cM, with flanking markers of 3950120_7ds_5316 and IWA1247. *Qhi.tamu-7D1.1* was significant in two environments, which accounted for 4.7 - 19.6 % of phenotypic variation of harvest index. TAM 111 had HVA to increase HI. This QTL located at a similar genetic distance to the QTL *Qgy.tamu-7D1.1* for grain yield, since these two traits are highly correlated.

One significant QTL, *Qmshw.tamu-1D2.4*, was flanked by 1915633_1ds_1815 and IWB14343, associated with mean single head weight. The GEI effect was identified in three environments including BD12, CH12, and CH14, where HVA were all from TAM 111. This QTL had a constant additive effect in all the environments with R^2 ranging from 4.5 to 5.

Three QTL were identified for yield from combined environments, with two positive alleles on chromosome fragments 5A5 and 7D3 contributed by TAM 111 across environments. *Qyld.tamu-1B7.2* was detected by 3470420_1bs_1139 at the peak position 341 cM, explaining 2.8 – 3.4 % of the phenotypic variance of yield from combined environments. *Qyld.tamu-5A5* with closely linked marker IWB8369 was identified for GEI in 13EP5. This QTL explained 3.1 % of the phenotypic variation. *Qyld.tamu-7D3*, at the peak position 103.9 cM with

3392705_7dl_13504, showed the largest additive effect on yield from combined environments, accounting for 8.1-11.1 % of the phenotypic variation in three environments including BD12, 13EP4, and 13EP5.

For agronomic score, two significant QTL were identified onto chromosome 5A3 and 7D1. *Qag.tamu-5A3* with closely associated marker 2797074_5al_324 at 18.2 cM genetic position, accounted for 3.5 to 11.8 % phenotypic variation of agronomic score. TAM 111 provided the favorable allele to increase agronomic score in 14EP4. *Qag.tamu-7D1.1*, with flanking marker interval IWA1247 and IWB24584 peaked at 54 cM and explained 3.7 to 11.4 % of phenotypic variation across three environments including BD12, 14EP4, and 14EP5. In addition, this QTL was associated with grain yield and harvest index at the similar region. Closely linked markers IWA1247, IWB44453, and 3950120_7ds_5316 will be discussed later for candidate gene analysis.

3.3.4 Additive and epistatic QTLs by environments interaction

The main additive effect of QTL, epistatic QTL and their interaction with environment were analyzed using MCMC (Markov Chain Monte Carlo) algorithm from QTLNetwork-2.0. Five QTLs with additive effects were mapped to chromosome 1D2, 4D, 5B1, 7B1_2, and 7D1 for grain yield (Table 11). Except the QTL *Qgy.tamu-4D.2*, the other four QTL were identified with significant additive effects. Among the five QTL associated with grain yield, *Qgy.tamu-7D1.1* was repeatable in previous GenStat analysis, whereas the other four QTL were new from this analysis. *Qgy.tamu-1D2.5* peaked at 252.5 cM with closely linked markers 2268723_1dl_1658 and 2232936_1dl_5000 and this QTL was involved in two additive-by-environment interaction (AEI) with Ch12 and 14EP4. *Qgy.tamu-4D.2* didn't show significant

additive effect but display significant interactions with three environments including CH14, 14EP4, and 14EP5. *Qgy.tamu-5B1* had significant additive effect but not AEI. *Qgy.tamu-7B6.2* had negative additive effect, suggesting the HVA of this QTL contributed by TAM 112. The flanking markers were IWB6455 and 3166060_7bs_4109.

Table 11. Significant additive effects and additive by environment interactions of QTL for yield and yield components detected using QTLNetwork.

QTL[†]	QTL ID	Chrom	Trait[‡]	Marker interval	Peak (cM)	Range (cM)	Additive effect[§]	A × E[¶]
Qgy.tamu-1D2.5	10	1D2	GY	2268723_1dl_1658 - 2232936_1dl_5000	252.5	248.9-254.5	0.01	0.036(CH12), -0.0343(14EP4),
Qgy.tamu-4D.2	29	4D	GY	IWB15038 - IWB61488	51.5	47.5-57.7	ns	0.0274(CH14), -0.0426(14EP5), -0.0342(14EP4)
Qgy.tamu-5B1	34	5B1	GY	BARC349A - 10870815_5bl_383	128.5	121.7-134.5	0.01	ns
Qgy.tamu-7B6.2	48	7B1_2	GY	IWB6455 - 3166060_7bs_4109	239.1	236.3-242.1	-0.01	-0.0235(CH12), 0.0341(14EP4)
Qgy.tamu-7D1.1	52	7D1	GY	3950120_7ds_5316 - IWA1247	49.4	43.3-62.0	-0.01	0.0569(CH12), 0.025(CH14), -0.0605(14EP5), -0.0377(14EP4)
Qtkw.tamu-1D2.4	9	1D2	TKW	IWB14343 - IWB15488	120.9	115.9-124.7	0.23	ns
Qtkw.tamu-2D1.2	20	2D1	TKW	9821121_2dl_24264 - 9852937_2dl_2983	183.4	180.4-185.6	0.31	ns
Qtkw.tamu-4D.2	29	4D	TKW	14325597_4dl_1814 - 14410083_4dl_5128	71.4	67.4-74.0	-0.1	0.24(BD11), 0.15(CH14), -0.34(14EP5), -0.25(14EP4)
Qtkw.tamu-6A4	38	6A4	TKW	4396488_6as_6312 - IWA508	107.2	103.2-112.5	-0.18	ns
Qtkw.tamu-7D1.1	52	7D1	TKW	IWB35446 - 3950120_7ds_5316	44.3	39.3-49.4	0.23	0.20(BD11), -0.16(BD12)
Qkps.tamu-2A3.1	11	2A3	KPS	5309922_2as_1539 - 6348801_2al_2314	124.7	120.7-127.3	-0.17	-0.21(14EP5)
Qkps.tamu-4D.3	30	4D	KPS	2315419_4ds_1828 - 2278252_4ds_954	107.7	105.3-111.7	0.18	0.28(BD12)
Qkps.tamu-6B2.3	41	6B2	KPS	4261555_6bl_2981 - 4251919_6bl_279	345.7	325.8-352.1	-0.16	ns
Qkps.tamu-7D1.1	52	7D1	KPS	IWB35446 - 3950120_7ds_5316	45.3	40.3-51.4	ns	0.23(CH12), -0.20(14EP5)
Qspm.tamu-1A1.1	1	1A1	SPM	3869219_1al_592 - IWB45313	385.9	380.9-386.2	4.2	8.44(BD11), 4.66(CH12), -16.31(13EP4)
Qspm.tamu-3A3.1	21	3A3	SPM	4361944_3al_5464 - IWB6187	28.1	23.7-30.1	1.93	ns
Qspm.tamu-5D	37	5D	SPM	4594725_5dl_125 - IWB45668	25.2	22.5-29.2	ns	8.95(13EP4)
Qspm.tamu-7A4.2	46	7A4	SPM	4243810_7as_5611 - 4251058_7as_2777	99.1	95.5-104.1	3.23	4.06(BD12)
Qspm.tamu-7B2.1	49	7B2	SPM	IWB48219 - IWB1883	26.8	26.5-30.8	-2.95	-4.22(BD11), -11.09(13EP4)
Qhi.tamu-2B89	18	2B89	HI	5238173_2bs_15787 - IWB29874	5.1	2.0-17.0	0.01	ns

Table 11. Continued

QTL†	QTL ID	Chrom	Trait‡	Marker interval	Peak (cM)	Range (cM)	Additive effect§	A × E¶
Qhi.tamu-7D1.1	52	7D1	HI	3950120_7ds_5316 - IWA1247	49.4	41.3-59.0	0.01	0.01(CH12), -0.01(14EP5), -0.01(14EP4)
Qbw.tamu-6B2.4	42	6B2	BM	3219226_6dl_13102 - IWB6367	477	473.6-480.0	2.37	6.23(14EP4)
Qhhdg.tamu-2A3.2	12	2A3	HHDG	5223530_2as_3120 - 2952329_6bs_335	245.4	242.6-249.4	-1.81	2.01(CH14)
Qhhdg.tamu-4D.1	28	4D	HHDG	14467068_4dl_4639 - IWB15038	42.4	36.4-53.7	ns	3.45(BD12), 3.53(CH14),
Qhhdg.tamu-7B6.1	47	7B1_2	HHDG	3138767_7bs_7632 - IWB36813	102.6	97.2-112.5	ns	-3.54(CH12)
Qhhdg.tamu-7B2.2	50	7B2	HHDG	6741075_7bl_1993 - 6486793_7bl_3755	80.3	75.7-84.6	2.39	3.27(BD12)
Qmshw.tamu-2D1.2	20	2D1	MSHW	9852937_2dl_2983 - 9842271_2dl_198	186.6	181.4-189.8	0.01	0.01(14EP5)
Qmshw.tamu-3D1	24	3D1	MSHW	IWB7416 - IWB16687	199.3	195.2-201.3	0.01	0.01(14EP5)
Qmshw.tamu-4D.1	28	4D	MSHW	IWB61488 - 2280021_4ds_778	52.7	49.5-57.7	ns	0.01(BD12), 0.01(CH14), -0.01(14EP5), -0.01(14EP4)
Qmshw.tamu-6B2.3	41	6B2	MSHW	4261555_6bl_2981 - 4251919_6bl_279	346.7	340.0-352.1	-0.01	ns
Qmshw.tamu-7A4.1	45	7A4	MSHW	IWB53296 - IWB1406	38.1	38.0-53.1	-0.01	-0.01(14EP5)
Qmsgw.tamu-1D2.4	9	1D2	MSGW	IWB3662 - 1915633_1ds_1815	98.9	94.3-104.0	ns	0.01(CH12), -0.01(14EP5)
Qmsgw.tamu-2A3.3	13	2A3	MSGW	6385099_2al_945 - 6389752_2al_2895	290.4	276.2-298.5	ns	0.01(CH14), -0.01(14EP5)
Qmsgw.tamu-2D1.2	20	2D1	MSGW	9852937_2dl_2983 - 9842271_2dl_198	184.6	181.4-187.6	0.01	0.01(14EP5)
Qmsgw.tamu-4D.1	28	4D	MSGW	14467068_4dl_4639 - IWB15038	39.4	15.0-46.4	-0.01	-0.01(14EP5), -0.01(14EP4)
Qmsgw.tamu-4D.3	30	4D	MSGW	2315419_4ds_1828 - 2278252_4ds_954	108.7	103.3-114.3	0.01	0.01(BD11), -0.01(CH12)
Qmsgw.tamu-7A4.2	46	7A4	MSGW	IWB2238 - 6635261_7bl_1238	100.5	91.5-110.6	0.01	ns

†QTL name including trait, institute, and linkage group; the linkage group is unique for each numbered QTL if the peak positions were less than 30 cM; within each chromosome fragment, different numbered QTL will have various chromosome fragment parts starting from the fragment name, then adding ".1, .2, …"

‡Abbreviation of traits: GY grain yield, TKW thousand kernel weight, KPS kernels spike^{-1}, SPM spikes m^{-2}, HI harvest index, BW biomass weight, HHDG hand harvest dry grain, MSHW mean single head weight, MHGW mean head grain weight, YLD yield from combine and AG agronomic score.

§Negative sign indicates the favorable allele provided by TAM 112.

¶ Additive × Environment effect. Abbreviation of environments: BD11 and BD12 Bushland, TX 2011 and 2012, CH12 and CH14 Chillicothe, TX 2012 and 2014, and 13EP4, 13EP5, 14EP4 and 14EP5 two irrigated levels (75% and 100%) Etter, TX 2013 and 2014.

Five QTL associated with thousand kernel weight were placed onto the chromosome fragment 1D2, 2D1, 4D, 6A4, and 7D1 (Table 11). Among them, *Qtkw.tamu-2D1.2* and *Qtkw.tamu-4D.1* were repeatable in previous GenStat analysis, whereas the other three QTL were new. All of the five QTL had the significant additive effects. However, only two QTL *Qtkw.tamu-4D.1* and *Qtkw.tamu-7D1.1* had significant AEI. *Qtkw.tamu-4D.1* peaked at the

position 71.4 cM, whereas the QTL *Qgy.tamu-4D.1* associated with grain yield identified at 51.5 cM on chromosome 4D. This QTL had pleiotropic effect controlling grain yield and thousand kernel weight. Another QTL on chromosome 7D1 *Qtkw.tamu-7D1.1* peaked at the similar region for grain yield, harvest index, and agronomy score.

Four QTL were detected on chromosomes 2A3, 4D, 6B2, and 7D1 for kernels spike^{-1} (Table 11). Among them, *Qkps.tamu-7D1.1* was identified at the similar region around 45 cM with the major 7D1 QTL mentioned before. *Qsph.tamu-4D.3* had the highest additive effect with 0.18 and TAM 111 contributed this HVA for the QTL. The flanking markers of this 4D QTL were 2315419_4ds_1828 and 2278252_4ds_954. It was involved in one AEI with BD12.

Six QTL were mapped on the chromosome 1A1, 3A3, 5BD, 7A4, and 7B2 with association for spikes m^{-2} (Table 11). *Qhsm.tamu-1A.1* had the highest additive effect with 4.2 and TAM 111 provided the favorable allele for this QTL. The closely linked markers were 3869219_1al_592 and IWB45313 at 385.9 cM. *Qspm.tamu-3A3.1* was detected at 28.1 cM with associated markers 4361944_3al_5464 and IWB6187. The HVA of this QTL was provided by TAM 111. Flanking markers 4594725_5dl_125 and IWB45668 identified *Qspm.tamu-5D*. *Qspm.tamu-7A4.2* with closely linked markers 4243810_7as_5611 and 4251058_7as_2777 at 99.1 cM. *Qspm.tamu-7B2.1* was detected by IWB48219 and IWB1883 at 26.8 cM. This QTL was involved in AEI with BD11 and 13EP4.

There are two QTLs associated with harvest index and placed onto chromosome 2B89 and 7D1 (Table 11). *Qhi.tamu-7D1.1* was involved in three AEI with CH12, 14EP4 and 14EP5. Furthermore, this QTL repeatable in previously GenStat analysis. The other QTL *Qhi.tamu-2B89* with associated marker IWB29874 at 5.1 cM position.

One QTL *Qbw.tamu-6B2.4* was mapped with significant additive effect of 2.37 for biomass weight (Table 11). The flanking markers were 3219226_6dl_13102 and IWB6367 peaked at 477 cM. It has significant AEI with 14EP4. Four QTLs for hand harvest dry grain were positioned onto the chromosome 2A3, 4D, 7B1_2, and 7B2, respectively. Five, six, and one QTL were identified with either significant additive effect or additive by environment interaction for mean single head weight, mean head grain weight, and combine yield from combine, respectively (Table 11). For MSHW, QTL on chromosome 3D1, 4D, 6B2 and 7A4 were displayed, among which *Qshgw.tamu-4D* peaked at the similar region compared to the QTL on 4D for grain yield, thousand kernel weight, hand harvest dry grain, and mean head grain weight. For MHGW, QTL with additive effects were mapped onto chromosome 1D2, 2A3, 2D1, 4D, and 7A4, respectively. Among those, *Qmhgw.tamu-2D1.2* and *Qmhgw.tamu-4D.1* shared the similar regions with the QTLs associated with TKW and MSHW.

Four pairs of epistatic QTL were identified for grain yield. Pairs *Qgy.tamu-1A2* / *Qgy.tamu-1A4* and *Qgy.tamu-5B4* / *Qgy.tamu-7D3* showed a positive epistatic effect on grain yield with HVA from TAM 111 (Table 12), and had significant epistatic by environment interaction effect in 14EP5 and CH12 and 14EP4, respectively. However, the pair *Qgy.tamu-4B.1* / *Qgy.tamu-6D1* and *Qgy.tamu-4D.3* / *Qgy.tamu-7B1* showed negative epistatic effects and significant epistatic by environment interaction for the grain yield in 13EP5, 14EP5, and 14EP4. For kernels spike^{-1}, the major QTL on chromosome 7D1 associated with several traits at 45 cM position, had significant additive by additive (AA) effect with QTL on 2A3 *Qkps.tamu-2A3.1*. However, this pair of QTL was identified with negative AA effect, which decrease the kernels spike^{-1}, and was not detected involved in additive by additive by environment (AAE) interaction with any environments. Six pairs of QTL for spikes m^{-2} were identified in Table 12. Among

Table 12. Significant epstasis effects and epstasis by environment interactions of QTL for yield and yield components detected using QTLNetwork.

QTL1 ID	Chrom 1	Marker interval	Peak (cM)	QTL2[‡]	QTL2 ID	Chrom 2	Marker interval	Peak (cM)	A × A[§]	A × A × Env[¶]
new	1A2	IWB69322 - IWB9497	112.8	*Qgy.tamu -1A4*	*new*	1A4	GBS3918914 - GBS3979089	62.1	0.02	0.02(14EP5)
25	4B1234	4899312_4bs_1971 - 6353556_2al_10051	218.5	*Qgy.tamu -6D1*	*new*	6D1	IWB65463 - 4251907_7as_438	123.9	-0.03	0.03(13EP5), 0.04(E5), -0.04(14EP5), -0.08(14EP4)
30	4D	2318044_4ds_942 - 2285062_4ds_3434	120.4	*Qgy.tamu -7B1*	*new*	7B1	IWB41673 - 3094264_7bs_405	12.8	-0.01	- 0.03(14EP5), -0.03(14EP4)
new	5B4	131994_5bs_1129 - 409493_5bs_1235	130.2	*Qgy.tamu -7D3*	*55*	7D3	3335723_7dl_455 - 3356799_7dl_7319	118.9	0.02	-0.02(CH12), 0.04(14EP4)
11	2A3	5309922_2as_1539 - 6348801_2al_2314	124.7	*Qkps.tamu-7D1.1*	*52*	7D1	IWB35446 - 3950120_7ds_5316	45.3	-0.14	ns
1	1A1	3869219_1al_592 - IWB45313	385.9	*Qspm.tamu-7B2.1*	*49*	7B2	IWB48219 - IWB1883	26.8	3.11	ns
new	2B89	5186825_2bs_9170 - IWB39654	41	*Qspm.tamu-5B4*	*new*	5B4	2754177_5ds_18973 - 2249806_5bs_2889	141	-2.31	7.43(BD11), -4.70(BD12), - 14.74(13EP4)
new	3B1	10530958_3b_57 - 2334567_3b_298	111.9	*Qspm.tamu-6A1*	*new*	6A1	IWB11903 - IWB55508	84.6	2.28	5.86(BD11), -5.50(BD12), 4.24(13EP4), -4.13(CH14)
new	1A1	IWB34373 - IWB45313	133.2	*Qspm.tamu-6A1*	*new*	6A1	IWB11903 - IWB55508	84.6	-4.42	-6.40(BD12), -3.19(13EP4)
28	4D	14467068_4dl_4639 - IWB15038	41.4	*Qspm.tamu-7A1*	*new*	7A1	IWB9146 - 4561447_7al_2163	103.1	2.98	8.56(13EP4)
38	6A4	4396488_6as_6312 - IWA508	104.2	*Qspm.tamu-7D1*	*new*	7D1	IWB52359 - 3945987_7ds_6173	0	3.17	5.96(13EP4)
new	6A1	5833909_6al_1506 - 5833653_6al_7738	157.9	*Qhi.tamu-7A4.2*	*46*	7A4	4228882_7as_3132 - 4246367_7as_2898	78.2	ns	0.01(14EP5)
new	1A4	IWA7428 - 1510593_5as_1356	11.1	*Qbw.tamu -4D.3*	*30*	4D	14403569_4dl_1472 - 2315419_4ds_1828	103.3	2.22	14.47(BD12), -6.57(CH14)
16	2A4	6399682_2al_2436 - IWB71583	196	*Qbw.tamu -2D1.2*	*20*	2D1	5329935_2ds_3804 - 9861581_2dl_506	166.2	-4.2	- 11.60(14EP4)
new	5A2_1	IWB10117 - IWB54382	92.2	*Qbw.tamu -7A3*	*new*	7A3	4173707_7as_5352 - 4229423_7as_253	40.8	-4.74	5.41(CH12), -5.27(CH14)
20	2D1	9852937_2dl_2983 - 9842271_2dl_198	186.6	*Qmshw.tamu-3D1*	*24*	3D1	IWB7416 - IWB16687	199.3	0.01	0.01(14EP5)
20	2D1	9852937_2dl_2983 - 9842271_2dl_198	186.6	*Qmshw.tamu-7A4.1*	*45*	7A4	IWB53296 - IWB1406	38.1	-0.01	ns
new	3A1	IWB34603 - IWB52809	310	*Qmshw.tamu-3B1*	*new*	3B1	10680128_3b_818 - IWB34373	125	0.01	ns

Table 12. Continued

QTL1 ID	Chrom 1	Marker interval	Peak (cM)	QTL2‡	QTL2 ID	Chrom 2	Marker interval	Peak (cM)	A × A§	A × A × Env¶
new	5A2_1	IWB3651 - IWB54382	11.5	*Qmshw.tamu-6D3*	*new*	6D3	IWB31561 - IWB52782	81.3	ns	0.01(13EP4), -0.01(14EP5)
9	1D2	IWB3662 - IWB54789	98.9	*Qmsgw.tamu-2D1.2*	*20*	2D1	9852937_2dl_2983 - 9842271_2dl_198	184.6	0	ns
30	4D	2315419_4ds_1828 - 2279925_4ds_1008	108.7	*Qmsgw.tamu-7B2.2*	*50*	7B2	IWB2238 - 6635261_7bl_1238	100.5	0	ns
new	2B89	5184301_2bs_3322 - IWB54789	283.5	*Qmsgw.tamu-7A1*	*new*	7A1	IWB63338 - 4464015_7al_3158	45.8	0	-0.01(14EP5)
new	1A1	3898773_1al_2678 - 3905040_1al_7362	310.2	*Qyld.tamu-5B4*	*new*	5B4	2297010_5bs_12980 - IWB4335	179	-2.82	ns
new	3A1	3442213_3as_402 - IWB52809	22	*Qyld.tamu-7D1*	*new*	7D1	3860626_7ds_3312 - 3869530_7ds_1421	366.5	1.91	-1.88(BD12), 2.71(13EP4)

†Abbreviation of traits: GY grain yield, TKW thousand kernel weight, KPS kernels spike^{-1}, SPM spikes m^{-2}, HI harvest index, BW biomass weight, HHDG hand harvest dry grain, MSHW mean single head weight, MHGW mean head grain weight, and YLD yield from combine.
‡QTL selected for detection in at least two environments. QTL name including trait, institute, and linkage group; the linkage group is unique for each numbered QTL if the peak positions were less than 30 cM; within each chromosome fragment, different numbered QTL will have various chromosome fragment parts starting from the fragment name, then adding ".1, .2, …".
§ Additive × Additive effect. Negative sign indicates the recombination of the parental alleles increased the traits, while positive sign indicates parental allelic combination imparted enhanced the traits.
¶Additive × Additive × Environment effect. Abbreviation of environments: Texas AgriLife Research stations in Bushland, TX in 2011 and 2012 (BD11 and BD12), Chillicothe, TX in 2012 and 2014 (CH12 and CH14), and two irrigated levels (75% and 100%) in Etter, TX in 2013 and 2014 (13EP4, 13EP5, 14EP4 and 14EP5).

them, the epistatic interaction between *Qspm.tamu-2B89* and *Qspm.tamu-5B4*, and *Qspm.tamu-1A1* and *Qspm.tamu-6A1* showed negative AA effect, decreasing spikes m^{-2}. Four pairs of epistatic QTL, *Qmshw.tamu-2D1.2* / *Qmshw.tamu-3D1*, *Qmshw.tamu-2D1.2* / *Qmshw.tamu-7A4.1*, *Qmshw.tamu-3A1* / *Qmshw.tamu-3B1*, and *Qmshw.tamu-5A5* / *Qmshw.tamu-6D3* showed significant epistasis effect for mean single head weight. The QTL *Qmshw.tamu-2D1.2* showed significant for the association with TKW, MSHW and MHGW in GenStat analysis. In the epistatic studies, this QTL showed positive effect with *Qmshw.tamu-3D1*, and a negative effect with *Qmshw.tamu-7A4.1*. The QTL pair 5A5 / 6D3 didn't show significant AA effects but has significant AAE effects with 13EP4 and 14EP5. For mean head grain weight, the major QTL *Qmhgw.tamu-2D1.2* showed significant AA interaction with *Qmhgw.tamu-1D2.4*. For biomass

weight, *Qbw.tamu-2D1.2* displayed negative AA interaction with *Qbw.tamu-2A4*. There are other one, two, two, and two QTL pairs showed either AA effects or AAE effects for HI, BW, MHGW, and YLD, respectively.

3.3.5 Significant QTL additive effects and their interaction with mega-environments (MEs)

The grain yield data for eight individual environments was analyzed using GGE biplot. The graphic axes of such analysis are the first two principal components (PCs) of multivariate analysis and account for most of the data variance (Figure 3). The first and second PC explained 31.63 % and 20.37 % of grain yield data variations, respectively. The first ME constitute of Chillicothe, TX at 2012 and 2014, locating in Rolling Plains. The second ME is consisted of high plains Bushland (Dryland), TX at 2011 and 2012. The third ME has four environments also in high plains: Etter, TX at 2013 and 2014 with two irrigation levels.

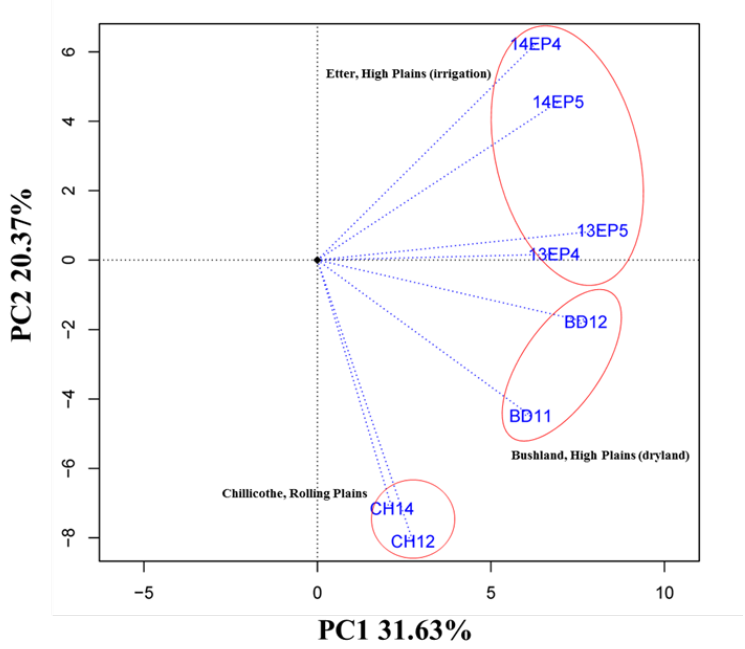

Figure 3. Three Mega-environments (MEs)† clustered by using principle component analysis (PCA) analysis.

†ME1: Chillicothe, TX, 2012 and 2014, Rolling Plains for dryland, ME2: Bushland, TX, 2011 and 2012, High Plains for dryland, and ME3: Etter, TX, 2013 and 2014, High Plains for two irrigation levels (75% and 100%), respectively.

After MapQTL analysis for mega-environments, several co-localized QTL associated with several traits were observed. Biomass weight, mean single head weight, and mean head grain weight were co-localized at the peak position of 93.4 cM on chromosome 1D1 with associated marker IWB27538 (Table 13). This QTL explained 9.4 %, 9.8 %, and 10 % of these three traits' phenotypic variance, respectively with all positive additive effect. Thousand kernel weight, mean single head weight, and mean head grain weight were co-localized on chromosome 2D1 at the position 185.6 cM with flanking marker 9852937_2dl_2983 and 9842271_2dl_198. This QTL explained these three traits 22.2 %, 13.7 %, and 13.9 % of phenotypic variation, respectively. The LOD range is 2.6 to 6.76. Spikes m^{-2}, mean single head weight, and mean head grain weight were co-localized on the chromosome 6B2 at the position of 211.6 cM with associated marker 1833621_6bs_423. The corresponding R^2 is 14.4 %, 14.9 %, and 12.1 %. The

LOD score ranged from 3.47 to 4.35. *Qmt.tamu-7D*, at the position 47.4 cM with flanking markers 3950120_7ds_5316 and IWA1247, was associated with grain yield, thousand kernel weight, harvest index, hand harvest dry grain and mean single head weight. The phenotypic variance explained by this QTL ranged from 12.1 % to 15.8 %. There are several other QTL regions mapped onto the chromosome 3A3 with flanking marker IWB23583, 4B1234 with associated marker 4955526_4bs_3828, 4D with 2326187_4ds_1762, and 6B2 with flanking marker 3013109_6bs_15 with two traits linked to them.

Table 13. Significant additive effects QTL detected for association with multiple traits across three ME using MapQTL.

QTL†	QTL ID	Chrom	Position (cM)	Associated marker	LOD‡	Associated traits§	Additive effect¶	R^2 range (%)††
Qmt.tamu-1D1.2	*7*	1D1	93.4	IWB27538	2.65 - 2.84	BW, MSHW, MSGW	3.64, 0.02, 0.01	9.4, 9.8, 10
Qmt.tamu-2D1.2	*20*	2D1	185.6	9852937_2dl_2983, 9842271_2dl_198	2.6 - 6.76	TKW, MSHW, MSGW	0.62, 0.02, 0.02	22.2, 13.7, 13.9
Qmt.tamu-3A3.2	*22*	3A3	136.3	IWB23583	2.54 - 3.78	HHDG, MSGW	1.94, 0.01	9, 13.1
Qmt.tamu-3A7	*23*	3A7	24.4	4440800_3al_1066	2.69 - 3.05	KPS, MSHW	-0.42, -0.02	10.7, 9.5
Qmt.tamu-4B.1	*25*	4B1234	169.8	4955526_4bs_3828	3.91 - 4.19	HHDG, MSGW	4.69, 0.02	13.5, 14.4
Qmt.tamu-4D.3	*30*	4D	108.1	2326187_4ds_1762	3.07 - 3.78	KPS, MSGW	0.4, 0.01	13.1, 10.8
Qmt.tamu-6B2.1	*39*	6B2	5.6	3013109_6bs_15	4.02 - 4.08	KPS, SPM	-0.22, 15.09	13.9, 14.1
Qmt.tamu-6B2.2	*40*	6B2	211.6	1833621_6bs_423	3.47 - 4.35	SPM, MSHW, MSGW	15.21, -0.01, -0.01	14.4, 14.9, 12.1
Qmt.tamu-7D1.1	*52*	7D1	47.4	3950120_7ds_5316, IWA1247	2.66 - 4.64	GY, TKW, HI, HHDG, MSHW	0.04, 0.24, 0.01, 1.34, 0.01	12.3, 9.4, 15.8, 12.1, 12

†QTL selected for detection with associated with at least two traits.QTL name including trait, institute, and linkage group; the linkage group is unique for each numbered QTL if the peak positions were less than 30 cM; within each chromosome fragment, different numbered QTL will have various chromosome fragment parts starting from the fragment name, then adding ".1, .2, …"
‡peak -log(P) value.
§ Abbreviation of traits: GY grain yield, TKW thousand kernel weight, KPS kernels spike^{-1}, SPM spikes m^{-2}, HI harvest index, BW biomass weight, HHDG hand harvest dry grain, MSHW mean single head weight, MHGW mean head grain weight, and AG agronomic score.
¶ Negative sign indicates the favorable allele provided by TAM 112.
††percentage of phenotypic variance explained by the QTL.

The main additive effect of QTL and QTL by environment interactions were estimated across three MEs from QTLNetwork analysis (Table 14). Three QTL including *Qgy.tamu-2A3.2*,

Table 14. Significant additive effects and additive by environment interactions of QTL detected by ME analysis using QTLNetwork.

QTL[†]	QTL ID	Chrom	Trait[‡]	Marker interval	Peak (cM)	Range (cM)	Additive effect[§]	Additive × Environment (A × E)[¶]
Qgy.tamu-2A3.2	*12*	2A3	GY	6405584_2al_3432 - IWB73597	220.9	213.3-224.9	-0.01	0.02(ME1), -0.03(ME3)
Qgy.tamu-4D.1	*28*	4D	GY	6405413_2al_883 - IWB15038	40.4	29.6-46.4	ns	0.04(ME1), -0.04(ME3)
Qgy.tamu-7D1.1	*52*	7D1	GY	3950120_7ds_5316 - IWA1247	53.4	47.4-60.0	ns	0.03(ME1), -0.04(ME3)
Qtkw.tamu-1D2.4	9	1D2	TKW	IWB14343 - IWB15488	120.9	115.9-126.7	0.34	ns
Qtkw.tamu-2A3.4	*14*	2A3	TKW	6434336_2al_861 - 6337268_2al_1661	350.1	340.3-356.4	0.13	ns
Qtkw.tamu-2D1.2	*20*	2D1	TKW	9861581_2dl_506 - 9821121_2dl_24264	174.2	168.2-177.2	0.32	ns
Qtkw.tamu-6A4	*38*	6A4	TKW	IWA508 - 4396488_6as_6312	108.5	105.2-110.5	-0.09	ns
Qtkw.tamu-7D1.1	*52*	7D1	TKW	IWB35446 - 3950120_7ds_5316	44.3	39.3-50.4	0.29	0.15(ME3)
Qkps.tamu-4B.1	*25*	4B1234	KPS	4945007_4bs_3055 - 4912707_4bs_1739	138.7	136.0-140.7	0.29	-0.17(ME3)
Qspm.tamu-2A4	*16*	2A4	SPM	6405413_2al_1076 - 6371486_2al_2589	185.4	178.4-193.1	-5.64	ns
Qspm.tamu-2D1.1	*19*	2D1	SPM	IWB17135 - 5349085_2ds_35	139	131.3-143.1	-3.38	ns
Qspm.tamu-4B.2	*26*	4B1234	SPM	4945007_4bs_3055 - IWA4490	277.3	272.0-281.9	4.93	4.17(ME3)
Qspm.tamu-7A4.2	*46*	7A4	SPM	4243810_7as_5611 - 4251058_7as_2777	99.1	95.5-103.1	5.28	3.79(ME3)
Qhi.tamu-2B89	*18*	2B89	HI	5242109_2bs_1102 - IWA2571	13	9.1-16.0	0	ns
Qhi.tamu-7D1.1	*52*	7D1	HI	3950120_7ds_5316 - IWA1247	50.4	43.3-61.0	0	0.01(ME1)
Qbw.tamu-1D1.1	*6*	1D1	BW	IWB644 - IWB64147	45	37.1-51.0	1.28	1.5(ME3)
Qbw.tamu-5B1.1	*35*	5B1	BW	4496119_5dl_15631 - BARC349A	119.7	108.7-127.7	1.8	ns
Qbw.tamu-6D1	*43*	6D1	BW	3233494_6dl_408 - 2124199_6ds_877	88.6	83.9-94.9	-1.35	ns
Qhhdg.tamu-2A3.2	*12*	2A3	HHDG	6434336_2al_571 - IWB73597	220.9	213.3-226.6	-1.19	1.12(ME2), -2.1(ME3)
Qhhdg.tamu-4B.1	*25*	4B1234	HHDG	6975707_4bl_1435 - 4883837_4bs_489	169.2	163.0-173.5	1.92	-1.13(ME1), -1.44(ME2), 2.65(ME3)
Qhhdg.tamu-4D.1	*28*	4D	HHDG	IWB8475 - 14467522_4dl_2408	22	9.0-25.0	ns	1.2(ME2), -2.25(ME3)
Qhhdg.tamu-5B1.2	*36*	5B1	HHDG	10795839_5bl_11118 - 10783103_5bl_2731	164.5	149.2-172.0	1.36	ns
Qmshw.tamu-2D1.2	*20*	2D1	MSHW	9852937_2dl_2983 - 9842271_2dl_198	184.6	181.4-188.6	0.02	ns
Qmsgw.tamu-2D1.2	*20*	2D1	MSGW	9861581_2dl_506 - 9842271_2dl_198	186.6	182.4-189.8	0.01	ns

†QTL name including trait, institute, and linkage group; the linkage group is unique for each numbered QTL if the peak positions were less than 30 cM; within each chromosome fragment, different numbered QTL will have various chromosome fragment parts starting from the fragment name, then adding ".1, .2, …"

‡Abbreviation of traits: GY grain yield, TKW thousand kernel weight, KPS kernels spike^{-1}, SPM spikes m^{-2}, HI harvest index, BW biomass weight, HHDG hand harvest dry grain, MSHW mean single head weight, MHGW mean head grain weight, and AG agronomic score.

§Negative sign indicates the favorable allele provided by TAM 112.

¶Abbreviation of environments: ME1: Chillicothe, TX, 2012 and 2014, Rolling Plains for dryland, ME2: Bushland, TX, 2011 and 2012, High Plains for dryland, and ME3: Etter, TX, 2013 and 2014, High Plains for two irrigation levels (75% and 100%), respectively.

Qgy.tamu-4D.1 and *Qgy.tamu-7D1.1* were identified to be associated with grain yield, and all of them have a significant interaction with ME1 and ME3. Only 2A3 QTL has favorable effects derived from TAM 112. For three major yield components, five, four, and one QTL were detected with thousand kernel weight, kernels spike^{-1}, and spikes m^{-2}, respectively. Among five QTL associated with thousand kernel weight, four have favorable alleles to increase kernel weight from TAM 111. *Qtkw.tamu-7D1.1* has a significant AEI with ME3. One QTL *Qkps.tamu-4B.1* was identified for kernels spike^{-1}, with the TAM 111 allele providing favorable allele. Among four QTL associated with spikes m^{-2}, the positive alleles of *Qspm.tamu-2A4* and *Qspm.tamu-2D1.1* were contributed by TAM 112 and positive alleles of *Qspm.tamu-4B.2* and *Qspm.tamu-7A4.2* were contributed by TAM 111, with a significant AEI with ME3. Two QTL *Qhi.tamu-2B89* and *Qhi.tamu-7D1.1* associated with harvest index. Three QTL located on 1D1, 5B1, and 6D1 and four QTL mapped on 2A3, 4B1234, 4D, and 5B1 were associated with biomass weight and hand harvest dry grain, respectively. The major QTL on 2D1 peaked at the position 185 cM was identified for both mean single head weight and mean head grain weight, with TAM 111 providing the positive allele.

3.3.6 Epistasis and interaction effects between epistasis and environments based on two-locus analyses

Two pairs of epistatic QTL including *Qtkw.tamu-6A4* / *Qtkw.tamu-7B6* and *Qtkw.tamu-6D1* / *Qtkw.tamu-7B6* were detected for thousand kernel weight (Table 15). Neither of them has significant epistasis by environment interaction effects. One QTL pair *Qbw.tamu-5A5* / *Qbw.tamu*-7D3, One QTL pair *Qhhdg.tamu-2B7* / *Qhhdg.tamu-7B4*, One QTL pair *Qmshw.tamu-6A1* / *Qmshw.tamu*-7B6, and One QTL pair *Qmhgw.tamu-5A5* / *Qmhgw.tamu-7D*

were identified to have a significant epistasis effect for biomass weight, hand harvest dry grain, mean single head weight, and mean head grain weight, respectively. These QTL pairs have a negative effect to decrease the yield performance.

Table 15. Epistatic QTL and their interaction with ME analysis using QTLNetwork.

Trait†	QTL1‡	QTL1 ID	Chrom 1	Marker interval	Peak (cM)	QTL2‡	QTL2 ID	Chrom 2	Marker interval	Peak (cM)	A × A§	A × A × Env¶
TKW	*Qtkw.tamu-6A4*	*new*	6A4	4421295_6as_10854 - 4423958_6as_1441	28.3	*Qtkw.tamu-7B6*	*new*	7B1_2	3092894_7bs_377 - 712093_7bs_27	43	-0.13	ns
TKW	*Qtkw.tamu-6D1*	*43*	6D1	2114048_6ds_695 - 2079278_6ds_1420	101.2	*Qtkw.tamu-7B6*	*new*	7B1_2	3118037_7bs_210 - 6380245_2al_4697	287.9	0.11	ns
BW	*Qbw.tamu-5A5*	*new*	5A2_1	IWB35862 - 2779962_5al_63	213.8	*Qbw.tamu-7D3*	*new*	7D3	3391666_7dl_513 - 3326863_7dl_3589	53.1	-1.63	1.34(ME1)
HHDG	*Qhhdg.tamu-4D.1*	*28*	4D	IWB8475 - 14467522_4dl_2408	22	*Qhhdg.tamu-5B1.2*	*36*	5B1	4496119_5dl_15631 - 10783103_5bl_2731	164.5	ns	-1.64(ME3)
HHDG	*Qhhdg.tamu-1B7*	*new*	1B3_1	3893913_1bl_480 - 3753254_1bl_4281	82.7	*Qhhdg.tamu-3D2*	*new*	3D2	IWB52937 - IWB17170	103.4	ns	-1.48(ME2), 2.47(ME3)
HHDG	*Qhhdg.tamu-2B7*	*new*	2B7	IWB4155 - IWA3937	228.9	*Qhhdg.tamu-7B4*	*new*	7B4	6716171_7bl_4749 - IWB31227	74.4	-1.3	1.07(ME1), -1.76(ME3)
MSHW	*Qmshw.tamu-6A1*	*new*	6A1	5830720_6al_4110 - 5832580_6al_2835	142.2	*Qmshw.tamu-7B6*	*new*	7B1_2	3120801_7bs_207 - 3139504_7bs_2211	182.2	-0.01	ns
MSGW	*Qmsgw.tamu-5A5*	*new*	5A2_1	IWB66780 - IWA4805	179.3	*Qmsgw.tamu-7D*	*51*	7D2	IWA6878 - IWB3214	104.2	-0.01	-0.01(ME3)

†Abbreviation of traits: TKW thousand kernel weight, BW biomass weight, HHDG hand harvest dry grain, MSHW mean single head weight, and MHGW mean head grain weight.

‡QTL selected for detection in at least two environments. QTL name including trait, institute, and linkage group; the linkage group is unique for each numbered QTL if the peak positions were less than 30 cM; within each chromosome fragment, different numbered QTL will have various chromosome fragment parts starting from the fragment name, then adding ".1, .2, …"

§Additive × Additive effect. Negative sign indicates the recombination of the parental alleles increased the traits, while positive sign indicates parental allelic combination imparted enhanced the traits.

¶Additive × Additive × environment effect. Abbreviation of environments: ME1: Chillicothe, TX, 2012 and 2014, Rolling Plains for dryland, ME2: Bushland, TX, 2011 and 2012, High Plains for dryland, and ME3: Etter, TX, 2013 and 2014, High Plains for two irrigation levels (75% and 100%), respectively.

3.3.7 Common QTLs from eight individual environments and three ME analysis

After analyzing and comparing using GenStat with single trait multiple environments, MapQTL for single environment, and QTLNetwork for main additive effect, four unique and consistent QTL identified on the chromosomes 1D2, 2D1, 4D and 7D1 (Table 16). The QTL region on chromosome 1D2 at 102 to 124 cM associated with TKW, MSHW, and MHGW. The QTL region on chromosome 2D1 at 173 to 191 cM associated with TKW, HHDG, MSHW, and MHGW. The QTL on chromosome 4D at 35 to 53 cM associated with GY, KPS, HHDG, and MSHW. The QTL on chromosome 7D1 at 38 to 53 cM position was identified for GY, TKW, KPS, HI, HHDG, MSHW, and AG.

Table 16. Comparisons of QTL identified from three models of GenStat, QTLNetwork, and MapQTL, and for yield and major yield components.

Trait†	GenStat single trait multi-env	QTLNetwork single trait multi-env‡	MapQTL single trait single env§	GenStat single trait three mega-env	QTLNetwork single trait three mega-env¶	MapQTL single trait three mega-env#
GY	2	5 (1)	2	0	3	1(0, 1, 0)
TKW	2	5 (1)	6(1, 2, 1)	2	5 (1)	2 (1, 1, 1)
KPS	2	4 (0)	3	0	1	3
SPM	0	6 (0)	0	0	4	3
HI	1	2 (1)	1	3	2 (2)	1 (1, 1, 1)
Total number of QTL	7	22	12	5	15	10
Total unique QTL	6	18	12	10	13	6

†Abbreviation of traits: GY grain yield, TKW thousand kernel weight, KPS kernels spike^{-1}, SPM spikes m^{-2}, and HI harvest index.
‡Number of QTL inside the parentheses are the common ones when compared with the QTL from single trait with multiple environments model in GenStat.
§Among the three numbers inside the parentheses, the first number is the consistent QTL when compared with the results from single trait with multiple environments model in GenStat. The second number represents the consistent QTL when compared with results from single trait with multiple environments model in QTLNetwork. The third number refers to the consistent QTL between the first two numbers.
¶Inside the parentheses were the consistent QTL based on the comparisons of QTLNetwork and GenStat for three mega-environments.
#Inside the parentheses, the first number is the consistent QTL based on the comparisons of MapQTL and multi-environments model of GenStat for three mage-environments; the second number is the consistent QTL compared with MapQTL and QTLNetwork. The third number refers to the consistent QTL between the first two numbers.

3.3.8 Candidate gene associated with yield and yield components

Based on the four consistent QTL region identified, the sequence of tightly linked markers located in the regions were used to locate them onto the consensus maps of Chinese spring and W7984, their corresponding contigs, as well as their physical positions of pseudomolecule IWGSC RefSeqv1.0. Comparative analyses were conducted in wheat and brachypodium, rice and sorghum. The predicted gene functions based on the top BLAST hits of protein sequences based on the linked SNP sequences were summarized. Sequence of IWA1247, closely linked with the 7D1 QTL was found that it is 99% identical to *Aegilops tauschii* sequence ID AF091802.1, encoding wheat starch synthase I gene. *Aegilops tauschii* is the D genome donor of common wheat (AABBDD). And 99% identical to wheat (*Triticum aestivum*) mRNA for starch synthase I-1 (*wSsI-1* gene). This protein is involved in the pathway starch biosynthesis, which is part of Glycan biosynthesis. Sequence of IWB44453 was identified to be Barley (*Hordeum vulgare*) mRNA for predicted protein, and identical to gene ID XM_006651055.2 for *Oryza brachyantha* (wild rice), which is a distant relative of cultivated rice (*O. satia Japonica* and *O. sativa Indica*) and distributed in west and central Africa. This gene encoded ubiquitin carboxyl-terminal hydrolase 3-like, involved in protein biosynthesis and degradation. Several other types of genes were also listed, such as Rab5-interacting protein (*Rab5ip*), acetyl-CoA carboxylase (*Acc-1*) gene, ethylene response factor 1 (*ERF1*) gene, receptor protein kinase TMK1-like, ubiquitin-like modifier-activating enzyme.

3.4 Discussion

3.4.1 Saturated genetic map with SNP array and GBS markers

Molecular markers are widely used in plant genetic research and breeding. Single Nucleotide Polymorphisms (SNPs) are currently the most widely-used marker due to their large existing numbers in all populations of individuals. GBS has broad application in generation of high-density genetic maps at a low cost (Poland et al., 2012). The application of high-saturated genetic maps created with SNP-GBS in sorghum, rice, wheat, and barley have clearly been demonstrated in fine-mapping of QTLs for different agronomic traits and identification of candidate genes for map-based cloning (Poland et al., 2012; Saintenac et al., 2012; Liu et al., 2014; Spindel et al., 2013). One disadvantage of GBS is the presence of large proportion of missing data in the dataset because of low coverage sequencing. Therefore, it is necessary to use imputation methods to predict genotypes of missing values. Another widely-applicable method to increase the efficiency of the GBS data is removing SNPs with > 20 % missing data. In this study, imputation was firstly conducted to reduce missing value and only those markers with less than 20 % missing value were used for QTL mapping analysis.

A total 1451 markers were formed D genome. The 90K SNP array markers mapped on D genome were 692 with 14.4% of total array SNP marker, whereas the GBS markers mapped on D genome were 749 with 14.7% of total GBS marker. Mapping resolution of *Aegilops tauschii* (the D-genome donor of bread wheat) library has been significant enriched with SNP-GBS, and more QTLs associated with yield and yield components have been identified in the D genome. The short arm of 7D QTLs shows major effects in several traits, including grain yield and other yield component. This QTL has candidate gene of starch synthase I, which has been encoded in

Aegilops tauschii. It is a promising candidate for map-based cloning of the yield gene, and the SNP identified in this study laid a solid foundation for several other kinds of work.

3.4.2 Evaluation of yield and yield component in individual and mega-environments

Grain yield is a complicated trait, and many components contribute to grain yield, including three major yield components, thousand kernel weight, kernels spike^{-1}, spikes m^{-2}. Environment conditions also interfere with grain yield. Therefore, multi-year and multi-location experiments with suitable field design are crucial to provide increased accuracy for grain yield and yield components estimation and genetic effects analysis. In this study, we used alpha lattice layout with five plots as a block to conduct experiments in four growing seasons and four locations. Grain yield, other yield-related traits have been analyzed for combined ANOVA and heritability test, and only those variables with genetic variance showed a significance level and heritability has more than 0.4 reserved for QTL mapping analysis. QTL mapping revealed the association between the loci which contains the genes and the quantitative traits. Significant level of genetic variance and relative high heritability are crucial for meaning of QTL studies. The Pearson's correlation was conducted among all traits, and most of the correlations are significant with variable ranging from negative values to positive value. Significant genetic correlations were further supported by co-localized QTLs linked to yield, yield components and agronomic traits to indicate the presence of pleiotropy in genomic regions modulating the quantitative traits (Mackay et al. 2009). In addition, positive genetic correlation points to a possible linkage that exists in coupling phase or presence of positive pleiotropic effects. On the other hand, the negative genetic correlation suggests a possible repulsion linkage or presence of antagonistic pleiotropic effects (Mackay et al. 2009).

Besides individual environment QTL analysis from genome-wide scan, mega-environments were also conducted. Based on the PCA clusters, three mega-environments (ME) were grouped with their different geographic distribution. ME has been initially defined by CIMMYT as similar biotic and abiotic stress, cropping system requirements, and environments conditions by a volume of production (Rajaram et al., 1994). As a quantitative trait, grain yield is highly affected by environments and needs to be conducted several environments analysis to estimate its genetic basis. Most of the grain yield QTL are identified using the individual environment data and even the average grain yield data across all environments. To maximize the genetic effects explaining the phenotypic variation across different environments and minimize the genotype-by-environment effects, ME analysis was introduced into this study. We have determined whether the QTL is a common and consistent one resulted not only in individual environment but in ME. This analysis will increase the accuracy to predict a potential major QTL and better interpret the candidate genes associated with it.

3.4.3 Co-localized QTLs for grain yield and yield components

Comparative analysis was conducted using MapQTL, GenStat, and QTLNetwork, and four common QTLs were identified all in D genome. Co-localized QTL for grain yield and and yield components have been reported in previous studies (McCartney et al., 2005; Quarrie et al., 2006). In this study, four co-localized QTL region on chromosome 1D2, 2D1, 4D and 7D were identified with more than two traits. Identifying co-localized QTL controlling different traits will lead to markers for more effective MAS of correlated traits.

One QTL associated with TKW, MSHW, and MHGW was mapped onto 1D2 chromosome and positioned in the interval 102 to 123 cM. The linked SNPs in this region were

1915633_1ds_1815, IWB14343, and IWB15488. Wu et al. (2015) and Zhang et al. (2014) reported QTLs on 1D for grain yield and seed weight, but common markers among those QTL are lacking to determine if they are the same QTL. Another pleiotropic region for TKW, MSHW, and MHGW were detected on chromosome 2D1, which was identified at the position 184.6 cM distance. The closely associated marker for this 2D1 QTL was 9852937_2dl_2983. For thousand kernel weight, we found this QTL on chromosome 2D1 (*Qtkw.tamu-2D1.2*) that accounted for 7 – 13.7 % of the phenotypic variance for individual environment analysis (Table 10) and explained 8.8 – 20.3 % of the phenotypic variations for three mega-environments analysis (Table 17). Zou et al. (2017) reported that the QTL mapped onto chromosome 2D was associated with both grain yield, flowering time and grain protein content, and the flanking markers for this 2D QTL was IWB62960 and IWA4789. Since both 90K markers were not included in this study, we referencd to the CSS physical map and genetic map. IWB62960 and IWA4789 were located at 460 Mbp and 481 Mbp on the 2D pseudo_physical position, whereas the closely linked GBS marker in this study for 2D1 QTL, 9852937_2dl_2983, was located at 531 Mpb on the same database. In addition, IWB62960 and IWA4789 at CSS genetic map 79.9 and 76.5 cM, whereas 9852937_2dl_2983 was detected at 73.8 cM. Thus, it is confident to conclude both QTL identified in different studies were the same one. Furthermore, the photoperiod sensitivity gene (*Ppd-D1*) on chromosome 2D has been widely applied in many breeding programs for early maturing wheat cultivars to better adapt to their environments (Quarrie et al. 2005; Wu et al., 2012). Perez-Lara et al. (2016) reported A QTL associated with grain yield mapped on chromosome 2D and this QTL adjacent to well-known photoperiod response *Ppd-D1*. The closely linked marker was IWA760. However, IWA was located at 34 Mbp in 2D

pseudo_physical map, which is too genetically far away to suggest any association between *Qtkw.tamu-2D1.2* and *Ppd-D1*.

Table 17. QTL for yield and yield components detected for the model of single trait with multiple environments for ME analysis using GenStat.

QTL†	QTL ID	Chrom	Associated markers	Position (cM)	Trait‡	Env§	LOD¶	R2 range (%)††	AE range‡‡	HVA§§
Qtkw.tamu-7D1.2	53	7D1	3938880_7ds_2029	75.1	TKW	ME2, ME3, ME4	7.4	0.4 - 13.3	0.05 - 0.46	All P2
Qtkw.tamu-2D1.2	20	2D1	9852937_2dl_2983	181.5	TKW	ME2, ME3, ME4	6.4	8.8 - 20.3	0.21 - 0.56	All P2
Qhi.tamu-1B7.1	4	1B3_1	IWB8611	267.4	HI	ME2, ME3, ME4	4.77	3.5 - 8.2	0.03	All P2
Qhi.tamu-2B89	18	2B89	5242109_2bs_1102	13	HI	ME2, ME3, ME4	5.89	4.4 - 10.2	0.03	All P1
Qhi.tamu-7D1.1	52	7D1	IWA1247	48.3	HI	ME2, ME3, ME4	5.39	0.3 - 19.2	0.003 - 0.005	All P2
Qmshw.tamu-1D2.4	9	1D2	IWB42815	97.7	MSHW	ME2, ME3, ME4	6.17	2.0 - 5.8	0.008 - 0.01	P2, P2, P1
Qmshw.tamu-2D1.2	20	2D1	9852937_2dl_2983 - 9842271_2dl_198	186	MSHW	ME2, ME3, ME4	3.06	1.7 - 7	0.008	All P2

†QTL name including trait, institute, and linkage group; the linkage group is unique for each numbered QTL if the peak positions were less than 30 cM; within each chromosome fragment, different numbered QTL will have various chromosome fragment parts starting from the fragment name, then adding ".1, .2, …".
‡Abbreviation of traits: TKW thousand kernel weight, HI harvest index, and MSHW mean single head weight.
§Abbreviation of environments: ME1: Chillicothe, TX, 2012 and 2014, Rolling Plains for dryland, ME2: Bushland, TX, 2011 and 2012, High Plains for dryland, and ME3: Etter, TX, 2013 and 2014, High Plains for two irrigation levels (75% and 100%), respectively.
¶peak -log(P) value.
††percentage of phenotypic variance explained by the QTL.
‡‡Additive effect range recorded for each QTL.
§§High value allele corresponding to each environment under environment column. . P1 = TAM 112, P2 = TAM 111.

One major QTL detected on chromosome 4D and associated with GY, TKW, HHDG, MSHW, and MHGW. This QTL was positioned at 35 to 54 cM and the closely linked makers in this region were 14467068_4dl_v2_4639, IWB15038, IWA752, IWB61488, IWB61486, and IWB30733. In hexaploid wheat, dwarfing has been achieved mainly through the introducing of semi-dwarfing gene *Rht-B1b* on chromosomes 4B and *Rht-D1b* on chromosomes 4D, which have been introduced in many cultivars grown worldwide (Ellis et al., 2002; Pearce et al., 2011). The concept that improvements in wheat grain yield ascribed to 'semi-dwarfing' since 1960s and one of the major factors of the 'Green Revolution' (Borlaug, 1968). Perez-Lara et al. (2016)

reported that IWA752 was closely linked to *Rht-D1b* that accounted for 38 % of the phenotypic variance of plant height across five environments, which was equivalent to a reduction in plant height by 13 cm. In addition, IWA752 was one of the closely associated markers of 4D QTL and mapped at 47.48 cM, indicating this 4D QTL identified in this study may closely related to *Rht-D1b*.

One QTL detected on short arm of chromosome 7D peaked at 54 cM with associated markers IWA1247, IWB44453, 3950120_7ds_5316, and IWB35446 has displayed pleiotropic effect on GY, TKW, KPS, HI, and AG. In addition, this QTL explained 19.6 % of phenotypic variance of harvest index, 10.5 % and 10.4 % of phenotypic variance of GY and SPH, respectively. The QTL on 7D chromosome has been reported for significance on GY (Atkinson et al., 2015). The closely linked marker is IWA7039. However, we didn't detect this marker in our 90K marker dataset to determine whether it is a same one. And after referencing the CSS physical map, distance between those markers with IWA7039 was too far to suggest any association between these two studies. Identifying co-localized QTL controlling different traits will lead to markers for more effective MAS of correlated traits. The bioinformatics analysis of SNP marker IWA1247 closely linked to the 7D1 QTL for GY and many other yield components corresponded to the candidate gene wheat starch synthase I gene, encoded in *Aegilops tauschii*, the wheat D-genome progenitor. The protein encoded by wheat starch synthase I gene is involved in the pathway starch biosynthesis, which is part of Glycan biosynthesis. It is of the utmost importance products in the grain filling stage of wheat growth and strongly influences grain yield and wheat quality. Since the draft genome of *Aegilops tauschii* were recently released (Jia et al., 2013). The accurate and detailed genetic maps constructed in this study can provide new insights into D genomes and directly support map-based gene cloning of candidate gene.

3.4.4 Epistatic effects on major QTL

Respect to unbiased estimation of genetic effects of the interested traits, it is necessary to estimate the importance of main effect versus epistatic effects (Kearsey et al., 1968). Epistasis refers to the phenotypic effects of interactions between alleles of different loci. In this study, epistatic effect between two QTLs should be much more environment-sensitive. The major QTL on chromosome 7D1 showed negative epistatic interaction with the 2A3 QTL for kernels spike^{-1}, but this pair of QTL didn't show epistatic by environment interaction. Another major QTL on 4D displayed epistatic interaction with 7A1 QTL for spikes m^{-2}, and this pair of QTL showed interaction with 13EP4. 2D1 QTL for SHDW exhibited epistatic effects with 3D1 and 7A4. In the quantitative genetics of epistasis, although the analytical methods can provide estimates for effects, it is nonetheless impossible to evaluate the importance of the epistatic interaction in determining the performance of the traits. And only a small proportion of QTL pairs could be detected in multiple environments. Statistical estimation of the epistatic effects regarding the genetic effects on the performance of plants remains to be the subject of future studies.

3.4.5 Application of QTL in MAS and map-based cloning

Because grain yield and yield components are easily affected by environmental factors and phenotyping these traits is time-consuming and labor-intensive, marker-assisted selection offers a desirable approach to more accurate and repeatable measurement across environments in our breeding programs. 3950120_7ds_5316 and IWA1247 are the closest markers associated with QTL on chromosome 7D1 in the population in this study. IWA725, IWB15038 and IWB61488 are the flanking markers of the QTL mapped onto chromosome 4D.

9852937_2dl_2983 associated with the QTL on 2D1 in several traits, and IWB14343 closely linked to 1D2 QTL. These markers are promising for MAS. In addition, closely linked SNP array and GBS markers for the common and consistent QTL can be valuable in pyramiding multiple yield-related effects to achieve an increased level of accuracy of MAS. Due to the high-density genetic map used in this study, it is more likely that these QTL represent actual candidate genes for some specific trait, such as starch synthesis gene. Thus, this will be potential candidates for fine mapping and gene discovery.

3.5 References

Amrine, J. W., and T.A. Stasny. 1994. Catalog of the Eriophyoidea (Acarina: Prostigmata) of the world. 798 pp. Indira Publishing House, West Bloomfield, Michigan, USA.

Assanga, S., G. Zhang, C.T. Tan, J.C. Rudd, A. Ibrahim, Q. Xue et al. 2017. Saturated genetic mapping of wheat streak mosaic virus resistance gene *Wsm2* in wheat. Crop Sci. 57:332-9.

Assanga, S., M. Fuentealba, G. Zhang, C.T. Tan, S. Dhakal, J.C. Rudd et al. 2017. Mapping of quantitative trait loci for grain yield and its components in a US popular winter wheat TAM 111 using 90K SNPs. PLoS ONE 12:e0189669

Atkinson, J.A., L.U. Wingen, M. Griffiths, M.P. Pound, O. Gaju, M.J. Foulkes, J. Le Gouis, S. Griffiths, M.J. Bennett, J. King, and D.M. Wells. 2015. Phenotyping pipeline reveals major seedling root growth QTL in hexaploid wheat. J. Exp. Bot. erv006.

Barton, N. H., and P. D. Keightley. 2002. Understanding quantitative genetic variation. Nature Rev. Genet.1:11-21.

Berzonsky, W. A., H.J. Ding, S.D. Haley, M.O. Harris, R.J. Lamb, R.I.H. McKenzie, H.W. Ohm, F.L. Patterson, F. Peairs, D.R. Porter, and R.H. Ratcliffe. 2003. Breeding wheat for resistance to insects. Plant Breed. Rev. 22:221-296.

Borlaug, N.E. 1968. Wheat breeding and its impact on world food supply. In: K.W. Findlay & K.W. Shepherd (Eds.), Proceedings of the Third International Wheat Genetics Symposium, Australian Academy of Science, Canberra, Australia, pp.1–35.

Carlborg, Ö., and C. S. Haley. 2004. Epistasis: too often neglected in complex trait studies? Nature Rev. Genet. 8:618-625.

Cavanagh, C. R., S. Chao, S. Wang, B.E. Huang, S. Stephen, S. Kiani, K. Forrest, C. Saintenac, G.L. Brown-Guedira, A. Akhunova, and D. See. 2013. Genome-wide comparative diversity uncovers multiple targets of selection for improvement in hexaploid wheat landraces and cultivars. Proc. Nat. Acad. Sci. 20:8057-8062.

Collard, B. CY, and D. J. Mackill. 2008. Marker-assisted selection: an approach for precision plant breeding in the twenty-first century. Phil. Trans. R. Soc. 1491:557-572.

Cox, T. S., W.W. Bockus, B.S. Gill, R.G. Sears, T.L. Harvey, S. Leath, and G.L. Brown-Guedira.1999. Registration of KS96WGRC40 hard red winter wheat germplasm resistant to wheat curl mite, Stagnospora leaf blotch, and Septoria leaf blotch. Crop Sci. 2: 597-598.

Cui, Fa, C. Zhao, A. Ding, J. Li, L. Wang, X. Li, Y. Bao, J. Li, and H. Wang. 2014. Construction of an integrative linkage map and QTL mapping of grain yield-related traits using three related wheat RIL populations. Theor. Appl. Genet. 127: 659-675.

Cuthbert, J. L., D.J. Somers, A.L. Brûlé-Babel, P.D. Brown, and G.H. Crow. 2008. Molecular mapping of quantitative trait loci for yield and yield components in spring wheat (*Triticum aestivum* L.). Theor. Appl. Genet. 117:595-608.

Deschamps, S., and M.A. Campbell. 2010. Utilization of next-generation sequencing platforms in plant genomics and genetic variant discovery. Mol. Breed. 25: 553-570.

Dubcovsky, J., A.J. Lukaszewski, M. Echaide, E.F. Antonelli, and D.R. Porter. 1998. Molecular characterization of two *Triticum speltoides* interstitial translocations carrying leaf rust and greenbug resistance genes. Crop Sci. 38:1655-1660.

Edwards, J. T., R.M. Hunger, E.L. Smith, G.W. Horn, M-S. Chen, L. Yan, G. Bai, R.L. Bowden, A.R. Klatt, P. Rayas-Duarte, and R.D. Osburn. 2012. 'Duster' Wheat: A Durable, Dual-

Purpose Cultivar Adapted to the Southern Great Plains of the USA. J. Plant Regist. 6:37-48.

Ellis M.H., W. Spielmeyer, K.R. Gale, G.J. Rebetzke, R.A. Richards. 2002. Perfect markers for the *Rht-B1b* and *Rht-D1b* dwarfing genes in wheat. Theor Appl Genet. 105:1038-42.

Elshire, R. J., J.C. Glaubitz, Q. Sun, J.A. Poland, K. Kawamoto, E.S. Buckler, and S.E. Mitchell. 2011. A robust, simple genotyping-by-sequencing (GBS) approach for high diversity species. PLoS ONE 6:19379.

Goldringer, I., P. Brabant, and A. Gallais. 1997. Estimation of additive and epistatic genetic variances for agronomic traits in a population of doubled-haploid lines of wheat. Heredity 79.

Harvey, T.L., D.L. Seifers, and T.J. Martin. 2001. Host range differences between two strains of wheat curl mites (*Acari: Eriophyidae*). J. Agr. and Urban Entomol. 18:35-41.

Hawkesford, M.J., J.L. Araus, R. Park, D. Calderini, D. Miralles, T. Shen, J. Zhang, and M.A. Parry. 2013. Prospects of doubling global wheat yields. Food and Energy Secur. 2: 34-48.

Jannink, J.L., A.J. Lorenz, and H. Iwata. 2010. Genomic selection in plant breeding: from theory to practice. Brief. Funct. Genomics. 9:166-177.

Jia, J., S. Zhao, X. Kong, Y. Li, G. Zhao, W. He, R. Appels, M. Pfeifer, Y. Tao, X. Zhang, and R. Jing. 2013. Aegilops tauschii draft genome sequence reveals a gene repertoire for wheat adaptation. Nature, 496:91-95.

Joppa, L.R., R.G. Timian, and N.D. Williams. 1980. Inheritance of resistance to greenbug toxicity in an amphiploid of *Triticum turgidum/T. tauschii*. Crop. Sci. 20: 343-344.

Kearsey, M.J. and J.L. Jinks. 1968. A general method of detecting additive, dominance and epistatic variation for metrical traits. Heredity 23:403-409.

Kosambi, D. D. 1943. The estimation of map distances from recombination values. Ann. Hum. Genet. 12:172-175.

Kosina, P., M. Reynolds, J. Dixon, and A. Joshi. 2007. Stakeholder perception of wheat production constraints, capacity building needs, and research partnerships in developing countries. Euphytica 157: 475-483.

Kumar, N., P.L. Kulwal, H.S. Balyan, and P.K. Gupta. 2007. QTL mapping for yield and yield contributing traits in two mapping populations of bread wheat. Mol. Breed. 19:163-177.

Lazar, M.D., W.D. Worrall, G.L. Peterson, A.K. Fritz, D. Marshall, L.R. Nelson, and L.W. Rooney. 2004. Registration of 'TAM 111' wheat. Crop. Sci. 44:355-357.

Lazar, M.D., W.D. Worrall, G.L. Peterson, K.B. Porter, L.W. Rooney, N.A. Tuleen, D.S. Marshall, M.E. McDaniel, and L.R. Nelson. 1997. Registration of 'TAM 110'wheat. Crop Sci. 37:1978-1979.

Li, S, J. Jia, X. Wei, X. Zhang, L. Li, H. Chen, Y. Fan. 2007. A intervarietal genetic map and QTL analysis for yield traits in wheat. Mol. Breed. 20:167-178.

Li, W. L., J.D. Faris, J.M. Chittoor, J.E. Leach, S.H. Hulbert, D.J. Liu, P.D. Chen, and B.S. Gill. 1999. Genomic mapping of defense response genes in wheat. Theor. Appl. Genet. 98:226-233.

Liu, H., M. Bayer, A. Druka, J.R. Russell, C.A. Hackett, J. Poland, L. Ramsay, P.E. Hedley, and R. Waugh. 2014. An evaluation of genotyping by sequencing (GBS) to map the Breviaristatum-e (ari-e) locus in cultivated barley. BMC genomics 15:104.

Liu, S., J.C. Rudd, G. Bai, S.D. Haley, A M. Ibrahim, Q. Xue, D.B. Hays, R.A. Graybosch, R. N. Devkota, and P.S. Amand. 2014. Molecular markers linked to important genes in hard winter wheat. Crop Sci. 54:1304-1321.

Liu, S., S. Ocheya, S. Dhakal, X. Gu, C.-T. Tan, Y. Yang et al. 2016. Validation of chromosome locations of 90K array single nucleotide polymorphisms in US wheat. Crop Sci. 56:364–373. doi:10.2135/cropsci2015.03.0194

Lobell, D.B., W. Schlenker, and J. Costa-Roberts. 2011. Climate trends and global crop production since 1980. Science 333:616–620.

Mackay TFC, E.A. Stone, J.F. Ayroles. 2009. The genetics of quantitative traits: challenges and prospects. Nature Rev. Genet. 10:565-577

Malik, R., G.L. Brown-Guedira, C.M. Smith, T.L. Harvey, and B.S. Gill. 2003. Genetic Mapping of Wheat Curl Mite Resistance Genes and in Common Wheat. Crop Sci. 43:644-650.

Martin, T.J., T.L. Harvey, and J.H. Hatchett. 1982. Registration of Greenbug and Hessian Fly Resistant Wheat Germplasm (Reg. Nos. GP 197 and GP 198). Crop Sci. 22:1089-1089.

Maxmen, A. 2013. Crop pests: under attack. Nature 501:15-17.

McCartney, C.A., D.J. Somers, D.J. Humphreys, and O. Lukow. 2005. Mapping quantitative trait loci controlling agronomic traits in the spring wheat cross RL 4452 ×AC 'Domain'. Genome 48:870-883. doi:10.1139/g05-055

McKinney, H.H. 1937. Mosaic diseases of wheat and related cereals. US Dept. Agriculture Circular 442.

Mir, R.R., N. Kumar, V. Jaiswal, N. Girdharwal, M. Prasad, H.S. Balyan, and P.K. Gupta. 2012. Genetic dissection of grain weight in bread wheat through quantitative trait locus interval and association mapping. Mol. Breed. 29:963-972.

Murugan, M., P.S. Cardona, P. Duraimurugan, A.E. Whitefield, D. Schneweis, S. Starkey, and C.M. Smith. 2011. Wheat curl mite resistance: Interaction of mite feeding with wheat streak mosaic virus infection. J. Econ. Entomol. 104:1406-1414.

Nelson, J.C., M.E. Sorrells, A.E. Van Deynze, Y.H. Lu, M. Atkinson, M. Bernard, P. Leroy, J.D. Faris, and J.A. Anderson. 1995. Molecular mapping of wheat: major genes and rearrangements in homologous groups 4, 5, and 7. Genetics 141:721-731.

Oldfield, G.N. 1970Mite transmission of plant viruses. 1970. Annu. Rev. Entomol. 15: 343-380.

Patil, R. M., S. A. Tamhankar, M. D. Oak, A. L. Raut, B. K. Honrao, V. S. Rao, and S. C. Misra. Mapping of QTL for agronomic traits and kernel characters in durum wheat (*Triticum durum* Desf.). 2013. Euphytica 190:117-129.

Parry, M. A. J. Food and energy security: exploring the challenges of attaining secure and sustainable supplies of food and energy. 2012. Food Energy Secur. 1:1–2.

Parry, M. A. J., and M. J. Hawkesford. 2010. Genetic approaches to reduce greenhouse gas emissions: increasing carbon capture and decreasing environmental impact. M. P. Reynolds, ed. Climate change and crop production. CABI International, Wallingford, U.K. 139-150.

Pearce S., R. Saville, S.P. Vaughan, P.M. Chandler, E.P. Wilhelm, C.A. Sparks, N. Al-Kaff, A. Korolev, M.I. Boulton, A.L. Phillips, and P. Hedden. 2011. Molecular characterization of *Rht-1* dwarfing genes in hexaploid wheat. Plant Physiol. 157:1820–31.

Perez-Lara, E., K. Semagn, H. Chen, M. Iqbal, A. N'Diaye, A. Kamran, A. Navabi, C. Pozniak, and D. Spaner. 2016. QTLs associated with agronomic traits in the Cutler× AC Barrie spring wheat mapping population using single nucleotide polymorphic markers. PloS ONE 11:160623.

Poland, J.A., P.J. Brown, M.E. Sorrells, and J.L. Jannink. 2012. Development of high-density genetic maps for barley and wheat using a novel two-enzyme genotyping-by-sequencing approach. PLoS ONE 7:32253.

Poland, J.A., and T.W. Rife. 2012. Genotyping-by-sequencing for plant breeding and genetics. Plant Genome 5: 92-102.

Porter, D.R., J.A. Webster, and B. Friebe. 1994. Inheritance of greenbug biotype G resistance in wheat. Crop Sci. 34:625-628.

Porter, D.R., J.D. Burd, K.A. Shufran, J.A. Webster, and G.L. Teetes. 1997. Greenbug (*Homoptera: Aphididae*) biotypes: selected by resistant cultivars or preadapted opportunists? J. Econ. Entomol. 90:1055-1065.

Quarrie, S.A., A. Steed, C. Calestani, A. Semikhodskii, C. Lebreton, C. Chinoy, N. Steele, D. Pljevljakusić, E. Waterman, J. Weyen, and J. Schondelmaier. 2005. A high-density genetic map of hexaploid wheat (*Triticum aestivum* L.) from the cross Chinese Spring× SQ1 and its use to compare QTLs for grain yield across a range of environments. Theor. Appl. Genet. 110:865-880.

Quarrie, S.A., S. Pekic Quarrie, R. Radosevic, D. Rancic, A. Kaminska, J.D. Barnes, M., Ceoloni, C. Leverington, and D. Dodig. 2006. Dissecting a wheat QTL for yield present in a range of environments: from the QTL to candidate genes. J. Exp. Bot. 57:2627-2637.

Rajaram, S., M. van Ginkel, and R.A. Fischer. 1994. CIMMYT's wheat breeding mega-environments (ME). In Proc. Intl. Wheat Genet. Symp. 1101-1106.

Ray, D.K., N.D. Mueller, P.C. West, and J.A. Foley. 2013. Yield trends are insufficient to double global crop production by 2050. PloS ONE 8:66428.

Rebetzke, G.J., D.G. Bonnett, and M.H. Ellis. 2012. Combining gibberellic acid-sensitive and insensitive dwarfing genes in breeding of higher-yielding, sesqui-dwarf wheats. Field Crops Res. 127:17-25.

Reddy, S.K., Y. Weng, J.C. Rudd, A. Akhunova, and S. Liu. 2013. Transcriptomics of induced defense responses to greenbug aphid feeding in near isogenic wheat lines. Plant Sci. 212:26-36.

Reddy, S.K., S. Liu, J.C. Rudd, Q. Xue, P. Payton, S.A. Finlayson, J. Mahan, A. Akhunova, S.V. Holalu, and N. Lu. 2014. Physiology and transcriptomics of water-deficit stress responses in wheat cultivars TAM 111 and TAM 112. J. Plant Physiol. 171:1289-1298.

Reif, J.C., H.P. Maurer, V. Korzun, E. Ebmeyer, T. Miedaner, and T. Würschum. 2011. Mapping QTLs with main and epistatic effects underlying grain yield and heading time in soft winter wheat. Theor. Appl. Genet. 123:283-292.

Rudd, J.C., R.N. Devkota, J.A. Baker, G.L. Peterson, M.D. Lazar, B. Bean, D. Worrall. 2014. 'TAM 112' Wheat, Resistant to Greenbug and Wheat Curl Mite and Adapted to the Dryland Production System in the Southern High Plains. J. Plant Regis. 8:291-297.

Saintenac, C., D. Jiang, S. Wang, and E. Akhunov. 2013. Sequence-based mapping of the polyploid wheat genome. G3: Genes| Genomes| Genetics 3:1105-1114.

Sánchez-Sánchez, H., M. Henry, E. Cárdenas-Soriano, and H.F. Alvizo-Villasana. 2001. Identification of Wheat streak mosaic virus and its vector *Aceria tosichella* in Mexico. Plant Dis. 85:13-17.

Sebesta, E.E., E.A. Wood, D.R. Porter, J.A. Webster, and E.L. Smith. 1995. Registration of amigo wheat germplasms resistant to greenbug. Crop Sci. 35:293-293.

Semagn, K., R. Babu, S. Hearne, and M. Olsen. 2014. Single nucleotide polymorphism genotyping using Kompetitive Allele Specific PCR (KASP): overview of the technology and its application in crop improvement. Mol. Breed. 33:1-14.

Singh, R.P., J.C. Nelson, and M.E. Sorrells. 2000. Mapping and Other Genes for Resistance to Stripe Rust in Wheat. Crop Sci. 40:1148-1155.

Slykhuis, J.T. 1976. Virus and virus-like diseases of cereal crops. Annu. Rev. Phytopathol. 14: 189-210.

Snape, J.W., M.J. Foulkes, J. Simmonds, M. Leverington, L.J. Fish, Y. Wang, and M. Ciavarrella. 2007. Dissecting gene × environmental effects on wheat yields via QTL and physiological analysis. Euphytica 154:401-408.

Sourdille, P., M.R. Perretant, G. Charmet, P. Leroy, M.F. Gautier, P. Joudrier, J.C. Nelson, M.E. Sorrells, and M. Bernard. 1996. Linkage between RFLP markers and genes affecting kernel hardness in wheat. Theor. Appl. Genet. 93:580-586.

Spindel, J., M. Wright, C. Chen, J. Cobb, J. Gage, S. Harrington, M. Lorieux, N. Ahmadi, and S. McCouch. 2013. Bridging the genotyping gap: using genotyping by sequencing (GBS) to add high-density SNP markers and new value to traditional bi-parental mapping and breeding populations. Theor. Appl. Genet. 126:2699-2716.

Tan, C.T., Development of Kaspar SNP Markers for Host Plant Resistance to Biotic Stress in Wheat. 2015. In Plant and Animal Genome XXIII Conference. Plant and Animal Genome.

Thomas, J.B., R.L. Conner. 1986. Resistance to colonization by the wheat curl mite in *Aegilops squarrosa* and its inheritance after transfer to common wheat. Crop Sci. 26:527-530.

Torada, A., M. Koike, K. Mochida, and Y. Ogihara. 2006. SSR-based linkage map with new markers using an intraspecific population of common wheat. Theor. Appl. Genet. 112: 1042-1051.

Tosic, M. 1971. Virus diseases of wheat in Serbia. I. Isolation and determination of the Wheat streak mosaic virus and Brome mosaic virus. Phytopathol Z.

Tyler, J.M., J.A. Webster, and O.G. Merkle. 1987. Designations for genes in wheat germplasm conferring greenbug resistance. Crop Sci. 27:526-527.

Van Ooijen, J.W. 2006. JoinMap® 4, Software for the calculation of genetic linkage maps in experimental populations. Kyazma BV, Wageningen 33:10-1371.

Wang, B., W. Guo, X. Zhu, Y. Wu, N. Huang,and T. Zhang. 2007. QTL mapping of yield and yield components for elite hybrid derived-RILs in upland cotton. J. Genet. Genomics 34:35-45.

Wang, R.X., L. Hai, X.Y. Zhang, G.X. You, C.S. Yan, and S.H. Xiao. 2009. QTL mapping for grain filling rate and yield-related traits in RILs of the Chinese winter wheat population Heshangmai× Yu8679. Theor. Appl. Genet. 118:313-325.

Webster, J.A., and P. Kenkel. 1995. Benefits of managing small-grain pests with plant resistance. In Wiseman BR, Webster J A. Proc Symp Economic Environmental and Social Benefits of Resistancein Field Crops, edited by B. R. Wiseman, and J. A. Webster, vol. 15. 13Dec.

Weng, Y., W. Li, R.N. Devkota, and J.C. Rudd. 2005. Microsatellite markers associated with two *Aegilops tauschii*-derived greenbug resistance loci in wheat. Theor. Appl. Genet. 110: 462-469.

Weng, Y., and M.D. Lazar. 2002. Amplified fragment length polymorphism-and simple sequence repeat-based molecular tagging and mapping of greenbug resistance gene *Gb3* in wheat. Plant Breed. 121:218-223.

Whelan, E.D.P., and G.E. Hart. 1988. A spontaneous translocation that transfers wheat curl mite resistance from decaploid *Agropyron elongatum* to common wheat. Genome 30: 289-292.

Whelan, E.D.P., and J.B. Thomas. 1989. Chromosomal location in common wheat of a gene (*Cmc1*) from *Aegilops squarrosa* that conditions resistance to colonization by the wheat curl mite. Genome 32:1033-1036.

Wilhelm, E.P., A.S. Turner, and D.A. Laurie. 2009. Photoperiod insensitive *Ppd-A1*a mutations in tetraploid wheat (*Triticum durum* Desf.). Theor. Appl. Genet. 118:285-294.

Wu, Q.H., Y.X. Chen, S.H. Zhou, L. Fu, J.J. Chen, Y. Xiao, D. Zhang, S.H. Ouyang, X.J. Zhao, Y. Cui, and D.Y. Zhang. 2015. High-density genetic linkage map construction and QTL

mapping of grain shape and size in the wheat population Yanda1817× Beinong6. PloS ONE 10:0118144.

Wu, X., X. Chang, and R. Jing. 2012. Genetic insight into yield-associated traits of wheat grown in multiple rain-fed environments. PloS ONE:31249.

Yoshida, T., H. Nishida, J. Zhu, R. Nitcher, A. Distelfeld, Y. Akashi, K. Kato, and J. Dubcovsky.2010. *Vrn-D4* is a vernalization gene located on the centromeric region of chromosome 5D in hexaploid wheat. Theor. Appl. Genet. 120:543-552.

Zhang, K., J. Tian, L. Zhao, and S. Wang. 2008. Mapping QTLs with epistatic effects and QTL× environment interactions for plant height using a doubled haploid population in cultivated wheat. J. Genet. Genomics 35:119-127.

Zhang, X., Z. Deng, Y. Wang, J. Li, and J. Tian. 2014. Unconditional and conditional QTL analysis of kernel weight related traits in wheat (*Triticum aestivum* L.) in multiple genetic backgrounds. Genetica 142:371-379.

Zou, J., K. Semagn, M. Iqbal, H. Chen, M. Asif, A. N'Diaye, A. Navabi, E. Perez-Lara, C. Pozniak, R.C. Yang, and H. Randhawa. 2017. QTLs associated with agronomic traits in the Attila× CDC Go spring wheat population evaluated under conventional management. PloS ONE 12:0171528.

CHAPTER IV

GENOME-WIDE ASSOCIATION MAPPING FOR YIELD COMPONENTS IN SYNTHETIC DERIVED WHEAT LINES

4.1 Introduction

Wheat is among the most important food crops in the world. Grain yield is the most important trait in wheat improvement, which is governed by numerous genes with interaction with each other and is highly influenced by environment conditions. Traditional breeding methods have achieved tremendous success in the last century in pushing the annual genetic gain to up to 1 % in grain yield, but today's wheat breeders should make further efforts to cope with 2 % yearly increase of world population (Sehgal et al., 2017). Furthermore, through natural and human selection and domestication, we have lost access to around 70% of the genetic diversity. A narrow genetic background and continuous pressure from climate change pose an immense challenge to wheat breeding worldwide.

Synthetic hexaploid wheat (SHW), developed by interspecific hybridization between durum or emmer wheat (*Triticum turgidum* L.), the donor of A and B genomes and accessions of wild goat grass (*Aegilops tauschii* L.), the donor of D genome, is an excellent combination of large genetic variations (Mujeen et al., 1996). Using SHW in breeding is one of the approaches to address the challenge of raising the genetic wheat yield potential (Ogbonnaya et al., 2007). Since 1980s, the International Maize and Wheat Improvement Center (CIMMYT) has developed about 1200 winter and spring SHW lines (Van et al., 2007). However, these SHW usually show poor overall agronomic performance. Generally, these SHW lines needs to be backcrossed with elite cultivar or breeding lines to develop synthetic derived wheat (SDW) lines. Studies reported

that SDW lines increased grain yield through backcrossing to 20 CIMMYT spring bread wheat cultivars (Jafarzadeh et al., 2016).

In addition, the rapid development of new sequencing technologies has provided the opportunity to enhance our understanding of genetic basis of yield improvement for SDW (Varshney et al., 2014). The advances in high-throughput genotyping systems by whole genome sequencing has revolutionized to the plant genomic studies. Genotyping-by-sequencing (GBS), which simultaneously performs SNP discovery and genotyping, has taken marker technologies to a next level, offering breeders with a cost-effective way to characterize their breeding lines (Poland et al., 2012). This is particularly beneficial to wheat since marker number and density have often been the limiting factors. Therefore, a growing number of breeding lines are being genotyped, making it amendable for genome wide association study (GWAS).

As an excellent complement to QTL mapping, GWAS has become a leading method for dissecting the genetic architecture of complex trait and genome-wide scan for identification and selection of chromosome regions harboring novel and superior QTL alleles. Associated mapping identifies QTL based on the historic recombination in a diverse panel based on the linkage disequilibrium (LD) between SNPs and QTL, detecting statistical associations between genetic and phenotypic variations throughout the genome (Walsh, 1998; Zhu et al., 2008). A high density of genetic marker covering the genome is essential to detect the density of recombination break-points for QTL position in the population. GBS on an association panel lines is an ideal application to address this case.

In this study, we performed GWAS on a population of SDW lines from the cross of selected CIMMYT SHW lines to Texas A&M AgriLife Research hard red winter wheat (HRWW) varieties: TAM 111 and TAM 112 to map QTL for yield, yield components and other

agronomic traits. TAM 111 and TAM 112 are the two most widely grown cultivars in the Texas High Plains and they are almost always among the top yielding cultivars. GWAS results evaluated the SDW performance and are leveraged for marker-assisted selection (MAS). Highly significant markers identified from this study could be fit as fixed effect to allow more accurate prediction of breeding values for these SDW.

4.2 Materials and methods

4.2.1 ***Plant materials and phenotyping***

The 419 SDW lines used in this study were developed by backcrossing of 23 selected CIMMYT (International Center for Maize and Wheat Improvement) SHW from Elite-I and Elite-II sets to Texas A&M AgriLife Research hard red winter wheat varieties, TAM 111 and TAM 112. Elite I set is comprised of 95 primary synthetics with better morphological characteristics and abiotic and biotic stress tolerance (Mujeeb-Kazi et al., 2000). Similarly, Elite II set consists of 33 selected primary synthetics that had better resistance to biotic stresses such as leaf rust, stripe rust, stem rust and other common wheat diseases (Mujeeb-Kazi et al., 2001). Data collected from BC1F5:9 is used in this study.

Field trials comprising 419 SDW lines were planted across eight environments during three crop years ending in 2015, 2016, and 2017. Each location-by-year combination was considered as one environment. All trials were planted in incomplete block design (alpha lattice design) with two replications in each environment. The location used in this study: Texas at Texas AgriLife Research stations in Chillicothe (34° 15' N, 99° 30' W) dryland location in 2017 (CH17), Bushland (35° 06' N, 102° 27' W) dryland and irrigated land, Dumas (35° 51' N, 101° 58' W), Clovis (34° 24' N, 103° 12' W), NM irrigated arear in 2016 and 2017 (BI17, BD17,

BD16, BI16, DMS17, DMS16, CVI17, and CVI16 respectively), McGregor (31° 25' N, 97° 25' W) irrigated locations in 2016 (MCG16), and two irrigated levels (50% and 75%) in Etter (35° 59' N, 101° 59' W), TX in 2015 (15EP3 and 15EP4). All trials had two replications. Standard agronomic practices were carried out for each environment.

A half meter row sample from a uniformly filled and representative inner row was harvested from each plot and used for the measurement of biomass and yield components. The traits for 419 SDW lines include three major yield components, yield and test weight. Three major yield components data including thousand kernel weight (TKW) (g), kernel spike^{-1} (KPS), and spike m^{-2} (SPM) were calculated from the plot sample. Harvest index (HI) (%) and several other traits were collected from plot sample. The thousand kernel weight was determined by counting and weighing three sets of 100 kernels for each plot and multiplying the average weight by 10. The spikes m^{-2} were computed by dividing the number of heads by the sample plot area. The kernels spike^{-1} were calculated based on TKW, kernel spike^{-1}, and grain weight from plot sample. The harvest index was calculated as grain weight per sample divided by total weight of dry biomass after three days drying at 60 ℃. All trials were harvested using a combine harvester and the yield was calculated in metric kilograms per hectare. Three agronomic traits including height (HEIGHT, cm), heading date (HEADING), and test weight (TW) were also summarized in this study. Test weight, in kg/m^3, was measured using Seedburo equipment (www.seedburo.com, Des Plaines, IL, USA).

Subset of 419 SDW for three-hundred genotypes, called AMPSY population, was selected for the following yield component recording: single stem weight (SSWT, g/culm), single head dry weight with glume (SHDW, g/culm), biomass per culm (BMPC, g/culm), stem

weight (STWT, g/m2), head dry weight (HDWT, g / m2), hand harvest yield (HHY, g/m2), and dry biomass (BM, g/m2).

4.2.2 ***DNA isolation and genotyping by double digested RAD-seq (DDRAD-seq)***

Leaf tissue was collected at the two-leaf stage from each of the 419 lines from plants grown in ag-genomic lab in soil and crop science in college station, TX. Genomic DNA was isolated using a modified a modified cetyltrimethyl ammonium bromide (CTAB) method (Zhang et al., 2010). Extracted DNA was checked for quality and quantity by gel analyses. The GWAS panel was genotyped with GBS at Texas A&M AgriLife Research Genomic and Bioinformatics Service Center in College Station, TX. GBS libraries were prepared as developed by Peterson et al. (2012) with some noted modifications. Two different kinds of restriction enzymes (PstI and MseI) were used to digest the genomic DNA into small fragments. Y-adaptors were ligated to the ends of DNA fragments, which ensured that only the fragments with the adaptor combinations can be amplified in PCR and sequenced later. Barcodes were built into the adaptors for multiplexing different samples, which can reduce the sequencing cost and time. In this experiment, we used combinatorial barcodes; one being an in-line barcode and the other an Illumina index. GBS libraries were sequenced on the Illumina Hiseq 2500 for the production of raw paired-end reads.

The GBS analysis was conducted using various bioinformatics tools. A custom Perl pipeline was developed to analyze the genotypic data. The analysis procedure and parameter settings were conducted according to the description in Wang et al. (2014) with slight modification. Firstly, the raw reads were trimmed and quality-filtered via QC toolkit v2.3 (Patel and Jain 2012). The reads with more than 80% of the bases having a Phred score $\geqslant$15 were used

for further analysis. A three-step iterative mapping strategy was used for the ungapped alignment of the quality-filtered reads to the CSS assemblies using Bowtie2. A more stringent mapping strategy was used on the reads that had not been mapped. A gapped mapping process preceded for the identification of insertion/deletion (indel) polymorphisms. The aligned reads with low mapping quality (MAQ < 5) were removed from the analysis. Variant calling was performed using Genome Analysis Toolkit (GATK). The SNPs with the allele separation of 1:1 in the progenies were filtered for further analysis. Imputation was done to reduce the missing values. Genotype of each line was converted from two letters: A = A : A, C = C : C, G = G : G, T = T : T, R = A : G, Y = C : T, S = C : G, W = A : T, K = G : T, M = A : C. Therefore, A, C, G, and T are homozygotes and the others are heterozygotes. N is for missing. SNPs with less than 5 % minor allele frequency (MAF) are filtered. GBS with more than 20 % missing values or heterozygotes more than 10 % were also excluded from the dataset along with all monomorphic GBSs. A total set of 76K GBS were retained and used to perform GWAS. Imputation was also done according to three different populations including a bi-parental mapping population: TAM 112 / TAM 111, 23 parental primary synthetic lines, and 419 SDW lines. Same filtering criteria were implemented. 164 K GBS dataset was developed to be used as supplemental information to find more novel significant QTL.

4.2.3 ***Statistical analysis and genome-wide association analysis***

Best linear unbiased predications (BLUPs) were calculated for each line using 'lme4' package in R 3.2.2 (Bates et al., 2014) with year and location as random effects in the model. Only single environment with trait heritability $\geqslant$ 0.2 were included into the following GWAS analysis. Combined analysis of variance (ANOVA) for individual trait was determined for the

significance of genetic variance, phenotypic variance and genotype-by-environment interaction (GEI) components in each environment. Pearson's correlation coefficients among measured variables were calculated using the CORR procedure of SAS. Genome-wide association analysis was conducted using the mix linear model (MLM) with a Q matrix as fixed effects and a kinship matrix as random effects. Q is the population structure matrix determined from principal component analysis, while K is the kinship matrix determined from the correlation between lines based on the marker information. Association analysis of GBS data was conducted using the genome association and prediction integrated tool (GAPIT) implemented in R (Lipka et al., 2012). $p < 0.0001$ was set to claim significant associations between SNPs and the traits. Linkage disequilibrium (LD) values were calculated from SNP datasets. Only SNP alleles with a MAF > 0.05 were used in calculations. LD values were plotted against the genetic distance (cM) to estimate LD decay and average distribution of r^2 values between SNP marker pairs in the full set of SDW lines.

4.3 Results

4.3.1 ***Phenotypic performance in yield components***

419 synthetic derived lines were recorded for yield, three major yield components including thousand kernel weights, kernels spike^{-1}, and spikes m^{-2}. Several other yield components and two agronomic traits including plant height and heading date were also included in the phenotypic analysis. Combined ANOVA analysis showed highly significant genotypic difference ($P < 0.001$) for most of the traits (Table 18). The average for the yield in this synthetic population was 4612.07 kg/ha. The trait means for thousand kernel weight, kernels spike^{-1}, and spikes m^{-2} were 29.72 g, 23.76 kernels spike^{-1}, and 884.12 spikes m^{-2}, respectively. Harvest

index's average was 16.77 %. The population had 112 days to heading and the mean plant height was 91 cm. The heritability for most traits ranged from moderate (0.4 – 0.6) to high (> 0.6) except for biomass with the heritability less than 0.1. High heritability was identified for yield, thousand kernels weight, kernels spike^{-1}, spikes m^{-2}, harvest index, single stem weight, single head dry weight, single head biomass with glum, height, and heading date. Hand harvest yield, stem weight, head dry weight showed moderate heritability.

Table 18. The combined ANOVA, heritability, and mean performance for all traits across environments.

Trait†	Units	Error Var	Gen Var‡	GenxEnv Var§	Env Var¶	H	Trait Mean	Min	Max	CV
YIELD	kg/ha	173823.80	120363.77	149126.05	1400629.30	0.77	4612.07	3382.21	5292.05	10.14
TKW	g	4.28	2.83	1.05	0.52	0.73	29.72	25.74	35.15	6.16
KPS	kernel/spike	4.99	4.44	1.51	2.94	0.77	23.76	15.98	29.65	14.62
SPM	spike/ m^2	32997.86	6844.91	1018.54	48465.76	0.70	884.12	731.96	1105.00	20.55
HI	%	3.58	1.46	2.86	322.86	0.65	16.77	13.31	18.96	11.28
BM	g/m^2	134053.74	3425.56	0.00	313670.68	0.06	1754.47	1684.00	1832.00	20.87
HHY	g/m^2	2061980.52	399048.87	90763.61	4161800.19	0.52	7049.83	5665.68	7734.38	23.86
STWT	g/m^2	36095.50	2597.18	0.00	118963.47	0.46	844.58	767.52	943.27	22.50
HDWT	g/m^2	39121.12	2674.23	1499.01	74974.77	0.43	858.57	763.35	932.60	23.04
SSWT	g/culm	0.01	0.01	0.01	0.10	0.78	0.78	0.64	0.99	11.95
SHDW	g/culm	0.01	0.01	0.01	0.06	0.70	0.79	0.66	0.95	11.83
BMPC	g/culm	0.03	0.02	0.02	0.28	0.79	1.66	1.40	1.97	9.75
HEIGHT	cm	23.33	21.26	4.16	98.14	0.89	91.01	82.51	105.51	5.31
TW	kg/m^3	1.27	1.26	12.78	11.42	0.22	58.90	51.34	59.57	2.91
HEADING		0.78	2.62	0.49	2.06	0.95	112.11	108.65	115.76	0.79

†Abbreviation of traits: Yield (YLD), thousand kernel weight (TKW), kernels spike^{-1} (KPS), spikes m-2 (SPM), harvest index (HI), hand harvest dry grain (HHY), head dry weight (HDWT), single stem weight (SSWT), single seed dry weight with glume (SHDW), biomass er culm (BMPC), height (HEIGHT), test weight (TW), heading date (HEADING).
‡Genotype
§Genotype-by-environment interaction
¶Environment
*, **, *** significant at 0.05, 0.01, and 0.001 probability levels, respectively.

4.3.2 ***Correlations between traits***

Pearson's coefficients of correlation between yield and other traits were analyzed based on the data across all environments (Table 19). Thousand kernel weight, kernels spike^{-1}, spikes m^{-2}, harvest index, hand harvest yield, head dry weight, single head dry weight, and test weight showed positive correlation with yield, whereas single stem weight, single head biomass with glum, height, and heading date showed negative correlation with yield. Hand harvest yield exhibited the highest positive correlation with yield (r = 0.64). Height showed a highest negative correlation with yield (r = -0.54). Most of the traits showed highly significant level of correlation except single head biomass with glum and heading date. Among all the traits, the highest positive correlation was identified between single head biomass with glum and single stem weight (r = 0.88). The largest negative correlation was observed between spikes m^{-2} and single head biomass with glum (r = -0.80). These highly significant correlations with yield and other traits indicating that improvement in yield can be achieved through indirect selection of these traits.

Table 19. Genetic correlation among yield and other traits measured in individual environments.

Trait†	YIELD	TKW	KPS	SPM	HI	HHY	HDWT	SSWT	SHDW	BMPC	HEIGHT	TW
TKW	0.28***											
KPS	0.41***	-0.17ns										
SPM	0.23***	-0.41***	-0.37***									
HI	0.71***	-0.05ns	0.48***	0.24***								
HHY	0.64***	-0.09ns	0.46***	0.42***	0.75***							
HDWT	0.45***	-0.08ns	0.31***	0.30***	0.48***	0.77***						
SSWT	-0.40***	0.40***	0.27***	-0.74***	-0.53***	-0.35***	-0.26***					
SHDW	0.27***	0.28***	0.79***	-0.57***	0.36***	0.36***	0.29***	0.46***				
BMPC	-0.12ns	0.42***	0.59***	-0.80***	-0.17ns	-0.05ns	-0.04ns	0.88***	0.79***			
HEIGHT	-0.54***	0.24***	0.01ns	-0.37***	-0.56***	-0.38***	-0.36***	0.68***	0.07ns	0.47***		
TW	0.23***	-0.06ns	0.07ns	0.16ns	0.20ns	0.22ns	0.16ns	-0.14ns	0.04ns	-0.09ns	-0.19ns	
HEADING	-0.10ns	-0.04ns	0.24***	-0.24***	-0.29***	-0.17ns	-0.22ns	0.38***	0.11ns	0.33***	0.51***	-0.13ns

†Abbreviation of traits: Yield (YLD), thousand kernel weight (TKW), kernels spike^{-1} (KPS), spikes per m2 (SPM), harvest index (HI), hand harvest dry grain (HHY), head dry weight (HDWT), single stem weight (SSWT), single seed dry weight with glume (SHDW), biomass er culm (BMPC), height (HEIGHT), test weight (TW), heading date (HEADING).
*, **, *** significant at 0.05, 0.01, and 0.001 probability levels, respectively.

4.3.3 ***Genome-wide association studies on yield components***

The major QTL for each yield component trait was defined as significant from at least two environments. Based on the CSS CSS pseudo physical map, QTL within 50 Mbp was viewed as the same one. After comparing with the annotated chromosome location, the QTL with the consistent chromosome information was included. QTL for individual traits are described below.

4.3.3.1 Yield

GWAS studies showed one QTL associated with yield, which were located on the chromosome 5A (Table 20). The 5A QTL explained 3.5 % to 4.7 % of the total phenotypic variance across BD16, DMS16 and 15EP5 (Figure 4). LOD significance range for this QTL within 50 cM was 4.38 to 4.95, with associated markers 2764622_5al_2022 and 2789287_5al_3539. The corresponding locations on physical map were 692 to 698 Mbp.

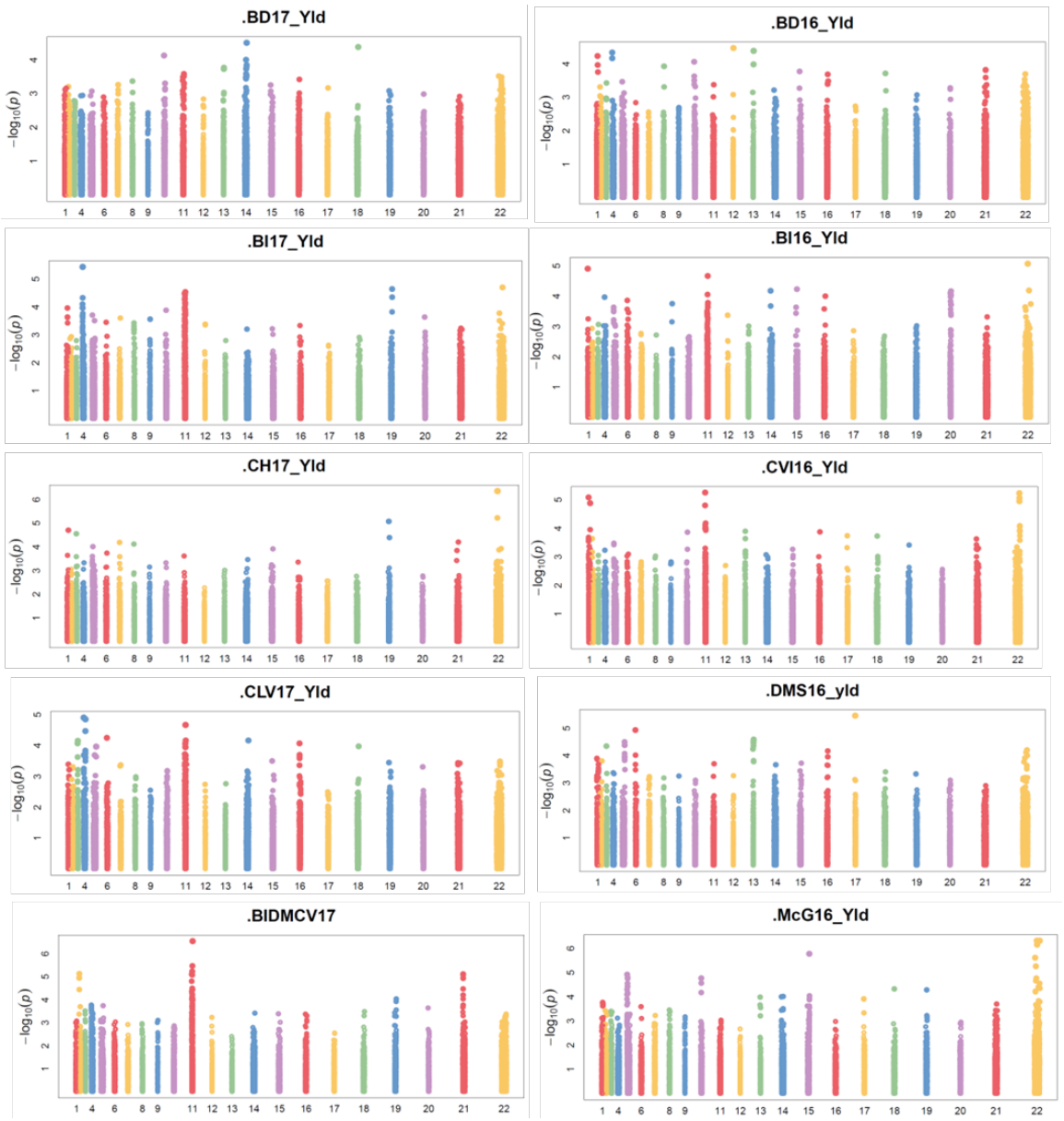

Figure 4. Manhattan plot for significant SNP associated with yield in different environments.

Table 20. QTL identified associated with yield and yield components from GWAS.

Trait[†]	Chrom	PseudoM_ physicalPosition (Mbp)	Significant Markers	QTL ID	LOD[‡]	R^2 (%)	Env[§]	A[‡‡]	B[‡‡]	C[‡‡]	D[‡‡]
YLD	chr5A	692 - 698	2764622_5al_2022	167	4.38 - 4.97	3.54 - 4.76	BD16, DMS16, 15EP5	n	y	n	n
TKW	chr2D	533	9844879_2dl_961	75	4.16 - 5.73	3.54 - 4.88	15EP3, 15EP4	n	y	n	n
TKW	chr4A	640 - 689	7083588_4al_2078	130	4.31 - 5.97	4.04 - 6.98	15EP3, 15EP4, 15EP5	y	n	n	n

Table 20. Continued

Trait[†]	Chrom	PseudoM_ physicalPosition (Mbp)	Significant Markers	QTL ID	LOD[‡]	R^2 (%)	Env[§]	A[‡‡]	B[‡‡]	C[‡‡]	D[‡‡]
TKW	chr4B	371- 398	7093954_4al_4480	140	4.88 - 5.11	3.88 - 4.49	CVI16, 15EP4	y	y	n	n
TKW	chr5B	599 - 645	10838006_5bl_4440	179	4.19 - 4.47	3.59 - 3.86	BI16, 15EP5	n	y	n	n
KPS	chr4A	661 - 698	7107364_4al_2064	131	4.40 - 5.31	3.60 - 4.05	BD16, CVI16, 15EP5	n	y	n	n
KPS	chr5B	529 - 573	10892498_5bl_5380	178	4.59 - 4.69	3.52 - 3.73	BD16, BI16	n	y	n	n
KPS	chr5D	432 - 434	4540821_5dl_3705	190	4.49 - 4.54	3.58 - 3.96	15EP3, 15EP4	n	y	n	n
KPS	chr6A	31 - 53	4352999_6as_23761	193	4.37 - 4.78	3.52 - 3.91	BD16, 15EP4	n	y	n	n
SPM	chr1A.1	365 - 372	3974579_1al_10315	7	4.07 - 4.81	3.73 - 4.06	15EP4, 15EP5	n	y	n	n
SPM	chr1A.2	589 - 593	3976442_1al_9784	11	4.27 - 4.57	3.82 - 3.94	15EP4, 15EP5	n	y	n	n
SPM	chr1B	366 - 410	3797631_1bl_11031	19	4.32 - 4.44	3.66 - 3.72	BD16, 15EP3	n	y	n	n
SPM	chr2A	2 - 18	5300435_2as_1323	35	4.09 - 4.41	3.52 - 3.75	15EP4, 15EP5	n	y	n	n
SPM	chr6B	20 - 31	2977047_6bs_5685	205	4.09 - 4.72	3.74 - 4.05	15EP3, 15EP5	n	y	n	n
HI	chr1A.1	23	3313347_1as_4300	1	4.08 - 4.59	3.54 - 3.61	BD16, 15EP3	n	y	n	n
HI	chr1A.2	291	3114055_1al_688	6	5.23 - 5.70	4.19 - 4.63	15EP3, 15EP4	n	y	n	n
HI	chr2A	3 - 51	5284462_2as_8447	35	4.42 - 4.75	3.60 - 5.07	15EP3, 15EP4, 15EP5	n	y	n	n
HI	chr2B	30 - 34	5200367_2bs_9023	50	4.12 - 4.70	3.58 - 3.71	BD16, 15EP3	n	y	n	n
HI	chr4A.1	523 - 567	7140204_4al_9649	128	4.22 - 4.89	4.38 - 4.78	BD16, 15EP5	n	y	n	n
HI	chr4A.2	643 - 658	3726482_4al_1648	130	4.58 - 4.69	3.70 - 5.26	15EP3, 15EP5	n	y	n	n
HI	chr4B	93	3114055_1al_647	134	5.36 - 5.81	4.50 - 4.74	15EP3, 15EP4	n	y	n	n
HT	chr2B	50 - 51	5177974_2bs_2193	51	4.62 - 4.78	3.58 - 3.78	15EP3, 15EP4	n	y	n	n
HT	chr4B	37 - 63	4954173_4bs_3367	134	4.17 - 7.83	4.18 - 6.32	BD16, 15EP4, 15EP5	y	y	n	n
TW	chr2D	109 - 127	5375012_2ds_3028	67	4.11 - 4.67	3.73 - 13.76	BD16, CVI16, DMS16	n	y	n	n
TW	chr3D	479 - 516	6942710_3dl_3473	116	4.20 - 4.88	3.69 - 4.11	BD16, BI16, MCG16	n	y	n	n
TW	chr4A	683 - 727	2713402_4al_14112	131	4.29 - 5.75	3.57 - 4.70	BD16, CVI16, MCG16	n	y	n	n
TW	chr5B	10 - 38	647748_5bs_7309	168	4.09 - 4.87	3.58 - 4.30	BD16, BI16, MCG16	y	n	n	n
TW	chr6B.1	31 - 64	2975664_6bs_1889	205	4.21 - 5.62	3.59 - 5.17	BD16, BI16, MCG16	y	y	n	n
TW	chr6B.2	668 - 716	1347737_6bl_1404	217	4.13 - 5.13	3.62 - 4.57	BD16, BI16, CVI16	y	y	n	n
TW	chr7D	575 - 618	3390938_7dl_5843	267	4.0 - 5.07	3.51 - 4.59	BD16, BI16, CVI16	y	y	n	n
HEADING	chr2D	613 - 640	4402942_6as_1927	77	4.04 - 4.29	3.86 - 4.41	BD16, BI16	**y**	n	n	n
HEADING	chr6D	462	3294879_6dl_3022	227	4.09 - 4.23	3.91 - 4.32	BD16, BI16	y	n	n	n
SSWT	chr4B.1	55 - 95	4954173_4bs_3367	134	4.09 - 4.65	4.34 - 5.12	CVI16, 15EP4	y	y	n	n

Table 20. Continued

Trait†	Chrom	PseudoM_ physicalPosition (Mbp)	Significant Markers	QTL ID	LOD‡	R^2 (%)	Env§	A‡‡	B‡‡	C‡‡	D‡‡
SSWT	chr4B.3	241 - 267	4961132_4bs_5511	138	4.12 - 4.68	4.28 - 5.03	BD16, 15EP3	y	n	n	n
SSWT	chr5B	700 - 702	10859743_5bl_761	181	4.33 - 4.86	4.54 - 5.08	CVI16, 15EP3	y	n	n	n
SSWT	chr6A	531 - 560	5815326_6al_7897	203	4.02 - 4.07	4.27 - 5.01	BD16, 15EP4	y	n	n	n
SSWT	chr7A	711 - 730	4551774_7al_1331	241	4.06 - 4.56	4.71 - 5.08	CVI16, 15EP4, 15EP5	y	n	n	n
SHDW	chr1D	461 - 469	2247049_1dl_2152	34	4.18 - 4.85	4.44 - 6.25	BD16, 15EP4	y	n	n	n
SHDW	chr3A	670 - 684	4428100_3al_2570	90	4.48 - 6.08	5.70 - 6.87	BD16, 15EP4	y	n	n	n
SHDW	chr4B	88 - 95	9891568_2dl_3242	134	4.09 - 5.81	5.12 - 6.52	CVI16, BD16, 15EP4	y	n	n	n
SHDW	chr5A	581 - 619	2793355_5al_1266	165	4.22 - 4.36	4.60 - 4.75	CVI16, 15EP3	y	n	n	n
SHDW	chr7A	711 - 730	4542941_7al_9623	240	4.06 - 4.30	4.53 - 5.08	15EP4, 15EP5	y	n	n	n
BMPC	chr1B	430 - 431	3809577_1bl_580	20	4.02 - 4.06	4.15 - 4.19	BD16, CVI16	y	n	n	n
BMPC	chr2D	414 - 445	9906847_2dl_5221	73	4.20 - 4.28	4.37 - 4.44	CVI16, BI16	y	n	n	n
BMPC	chr4B	225 - 241	4900567_4bs_4951	137	4.09 - 4.14	4.19 - 4.35	BD16, BI16, 15EP3	y	n	n	n
BMPC	chr5B	700 - 702	10859743_5bl_761	181	4.27 - 4.34	4.53 - 4.57	CVI16, 15EP3	y	n	n	n
BMPC	chr5D	184	2713457_5ds_206	185	4.27 - 5.42	4.45 - 5.88	BD16, CVI16	y	n	n	n
BMPC	chr6D	429 - 433	3310863_6dl_7650	226	4.09 - 4.56	4.26 - 4.71	BI16, 15EP3	y	n	n	n

†Abbreviation of traits: Yield (YLD), thousand kernel weight (TKW), kernels spike^{-1} (KPS), spikes per m2 (SPM), harvest index (HI), hand harvest dry grain (HHY), head dry weight (HDWT), single stem weight (SSWT), single seed dry weight with glume (SHDW), biomass er culm (BMPC), height (HEIGHT), test weight (TW), heading date (HEADING).
‡-log(p-value).
§Abbreviation of environments: Chillicothe, TX in 2017 (CH17), Bushland, TX dryland and irrigated land in 2017 and 2016 (BI17, BD17, BD16, and BI16), Dumas, TX irrigated area in 2017 and 2016 (DMS17 and DMS16), Clovis, NM irrigated area in 2016 and 2017 (CVI17 and CVI16), McGregor, TX irrigated locations in 2016 (MCG16), and three irrigated levels (50%, 75%, and 100%) in Etter, TX in 2015 (15EP3, 15EP4, and 15EP5).
‡‡Identified in A, B, C, or D. A = 76KSDL298, B = 76KSDL419, C = 164KSDL298, D = 164KSDL419.

4.3.3.2 Thousand kernel weight (TKW)

GWAS studies identified four QTL on chromosome 2D, 4A, 4B, and 5B for thousand kernel weight (Table 20). The QTL on chromosome 2D, with associated markers 9844879_2dl_961, explained 4.16 % to 5.73 % of the phenotypic variance across 15EP3 and 15EP4 for thousand kernel weight (Figure 5). This QTL was referenced at around 533 Mbp on physical map. Several GBS markers were associated with the QTL on chromosome 4A, including 7159067_4al_2315, 7177265_4al_2107, 7093954_4al_4495, 7083588_4al_2078,

7169829_4al_8539 and 7094829_4al_320. The corresponding physical location region was 640 to 689 Mbp. GBS7083588 were identified with the highest significant LOD score for 7.84. The 4A QTL explained 4.04 % to 6.98 % of the phenotypic variance through 15EP3, 15EP4 and 15EP5 environments. Two GBS markers including 7093954_4al_4480 and 3812861_1bl_8436, was associated with the QTL located on chromosome 4B, referenced on 371 to 398 Mbp on physical map. The corresponding R^2 of 4B QTL was from 3.88 % to 4.49 % across 15EP4 and CVI16 environments. The QTL mapped onto chromosome 5B explained 3.59 % to 3.86 % of the phenotypic variance of 15EP5 and BI16. The closely linked markers are 10891904_5bl_186 and 10838006_5bl_4440. The 5B QTL was referenced to physical map region for 599 to 645 Mbp.

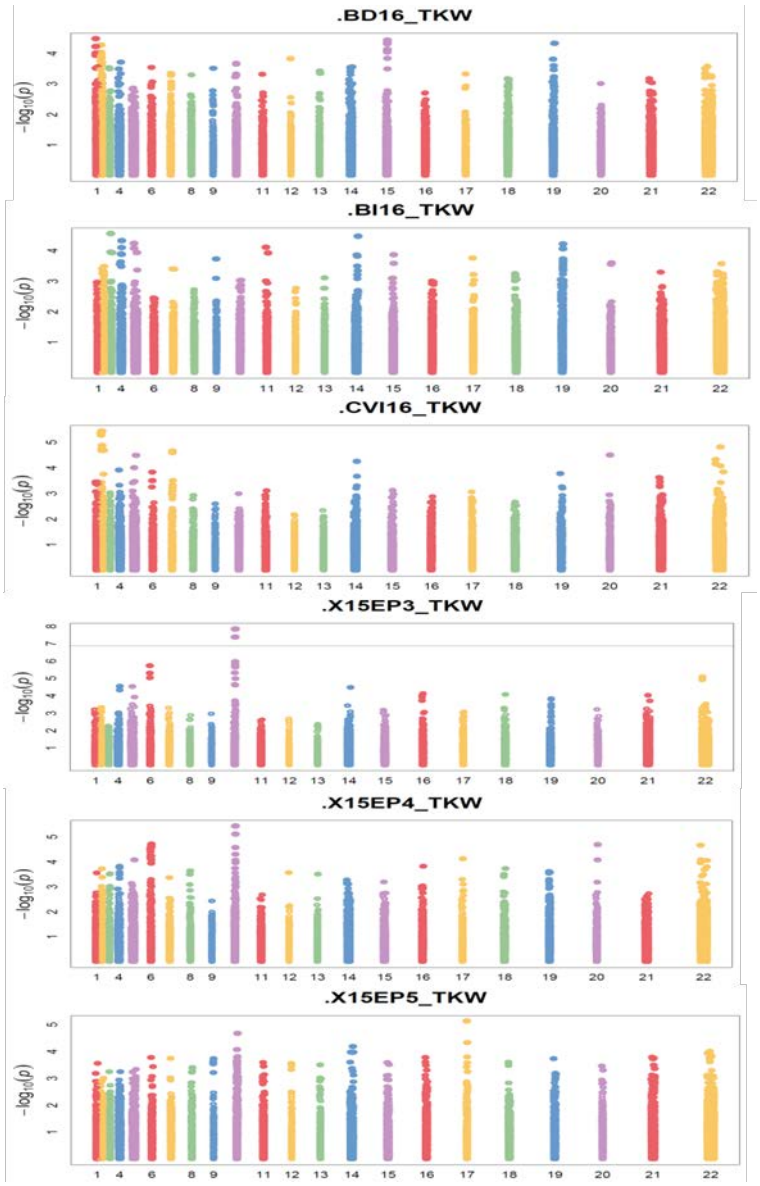

Figure 5. Manhattan plot for significant SNP associated with thousand kernel weight in different environments.

4.3.3.3 Kernel number spike^{-1} (KPS)

Four QTL across four different chromosomes including 4A, 5B, 5D, and 6A were identified for significant for kernel number spike^{-1} (Table 20). The QTL on chromosome 4A was identified with closely linked GBS marker: 7133803_4al_3568, 7133034_4al_5389, and

7107364_4al_2064, explaining 3.60 % to 4.05 % of the phenotypic variation across 15EP5, BD16, and CVI16 (Figure 6). The corresponding locations of the 4A QTL on physical map were 661 to 698 Mbp. The QTL on chromosome 5B had associated marker 10919729_5bl_10018 and 10892498_5bl_5380. The corresponding R^2 was 3.52 % to 3.73 % for BD16 and BI16 environments. The 5B QTL was referenced to 529 to 573 Mbp on 5B physical map. The QTL on chromosome 5D, with closely linked markers 4592332_5dl_226 and 4540821_5dl_3705 explained 3.58 % to 3.96 % of the phenotypic variation for 15EP3and 15EP4 environments. The corresponding locations of the 5D QTL on physical map were 432 to 434 Mbp. Two closely associated markers 4352999_6as_23761 and 4408386_6as_11880 were linked to the QTL on chromosome 6A, and the corresponding R^2 of this QTL was 3.52 % to 3.91 % for 15EP4 and BD16. The 6A QTL was referenced to 31 to 53 Mpb on physical map.

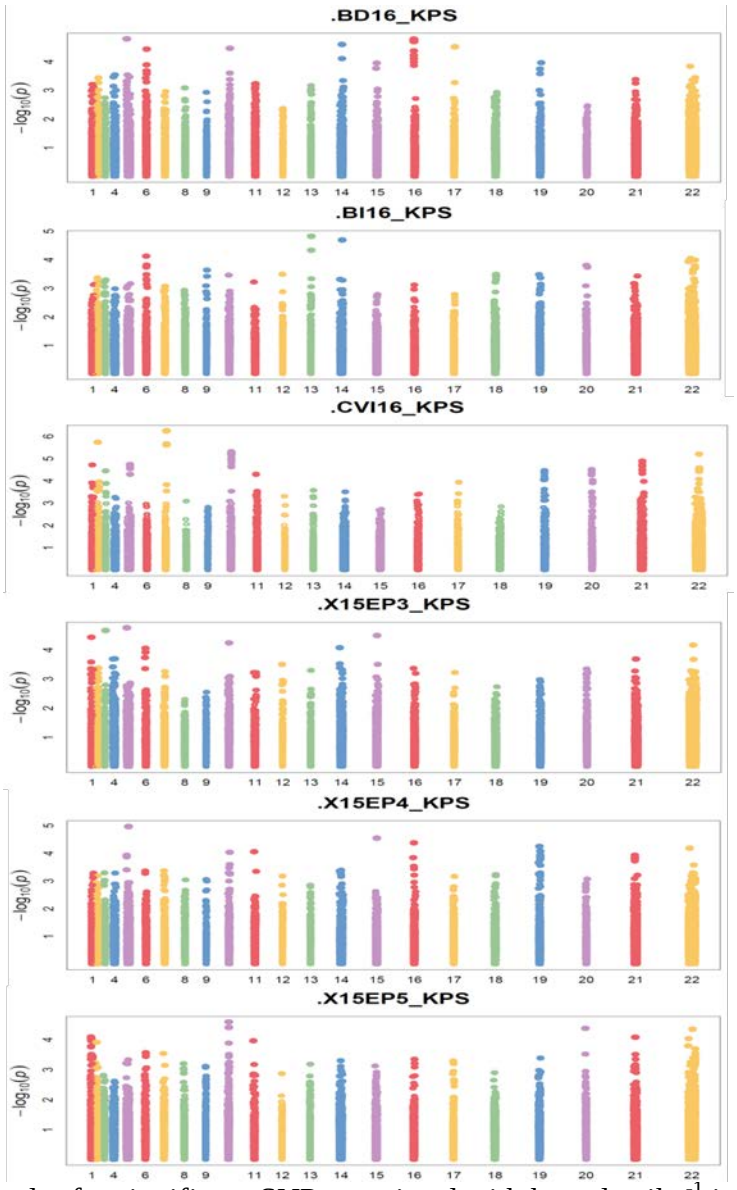

Figure 6. Manhattan plot for significant SNP associated with kernel spike^{-1} in different environments.

4.3.3.4 Spike number m^{-2} (SPM)

Five significant QTLs across four different chromosomes including 1A, 1B, 2A, and 6B were found with association for spikes m^{-2} (Table 20). Two QTLs identified on chromosome 1A. The first QTL on chromosome 1A, with closely linked marker 3930811_1al_6955 and

3974579_1al_10315 accounted for 3.73 % to 4.06 % of the phenotypic variance for 15EP4 and 15EP5 environments (Figure 7). The first 1A QTL was referenced to physical map at 365 to 372 Mbp regions. For the second QTL located on chromosome 1A, two GBS markers including 3976442_1al_9784 and 3959084_1al_9049, were closely associated with it. The corresponding physical location was 589 to 593 Mbp on chromosome 1A. This QTL explained 3.82 % to 3.94 % across 15EP4 and 15EP5 environments. The QTL on chromosome 1B accounted for 3.66 % to 3.72 % of the phenotypic variations across 15EP3 and BD16. The associated markers of the 1B QTL were 3872634_1bl_556 and 3797631_1bl_11031. The corresponding physical location on chromosome 1B was 366 to 410 Mbp. Three markers closely associated with the QTL on chromosome 2A, which was detected by 5300435_2as_1323, 5291609_2as_6803, and 5195481_2as_1609. The corresponding R^2 rang was from 3.52 % to 3.75 % for 15EP4 and 15EP5. The 2A QTL was referenced onto the physical map at 2 to 18 Mbp.

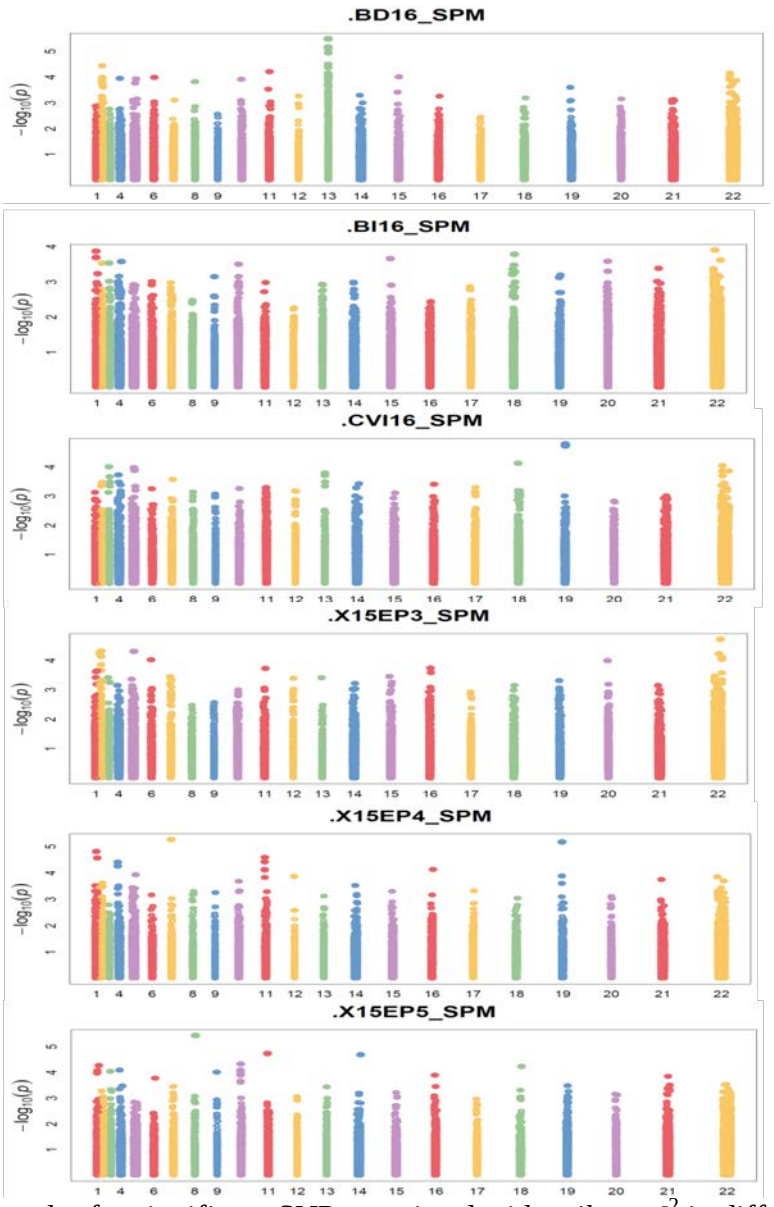

Figure 7. Manhattan plot for significant SNP associated with spikes m^{-2} in different environments.

4.3.3.5 Harvest index (HI)

Seven significant QTLs across five different chromosomes including 1A, 2A, 2B, 4A, and 4B were identified for association with harvest index (Table 20). Two significant QTLs identified on chromosome 1A, with the first one referenced on 23 Mbp and the other one on 291

Mbp on physical map. The first QTL 1A.1, with closely linked marker 3313347_1as_4300, accounted for 3.54 % to 3.61 % of the phenotypic variance for 15EP3 and BD16 (Figure 8). The second QTL 1A.2, detected by marker 3114055_1al_688, explained 4.19 % to 4.63 % of the phenotypic variation across 15EP3 and 15EP4 environments. Three GBS markers including 5291609_2as_6803, 5284462_2as_8447, and 5216900_2as_7249, were closely associated with the QTL located onto chromosome 2A. The corresponding R^2 of this QTL was 3.60 % to 5.07 % across 15EP3, 15EP4, and 15EP5 environments. The 2A QTL was referenced to 3 to 51 Mbp on physical map. The QTL on chromosome 2B accounted for 3.58 % to 3.71 % of the phenotypic variations of 15EP3 and BD16 environments. The associated markers were 5245089_2bs_3337 and 5200367_2bs_9023. The corresponding physical location on chromosome 2B was 30 to 34 Mbp. Two QTLs was located onto chromosome 4A, with the first one referenced on 523 to 567 Mbp and the other one on 643 to 658 Mbp of physical map. The 4A.1 QTL corresponded to the 7083958_4al_2283 and 7140204_4al_9649, and accounted for 4.38 % to 4.78 % of the phenotypic variance across 15EP5 and BD16 environments. The 4A.2 QTL corresponded to the markers 3726482_4al_16482 and 7063576_4al_6305. The phenotypic variance explained by this QTL was 3.70 % to 5.26 % for 15EP3 and 15EP4. The QTL on chromosome 4B was identified by 3114055_1al_647. The 4B QTL explained 4.50 % to 4.74 % of the phenotypic variance across 15EP3 and 15EP4 environments. The 4B QTL was referenced at 93 Mbp on the physical map.

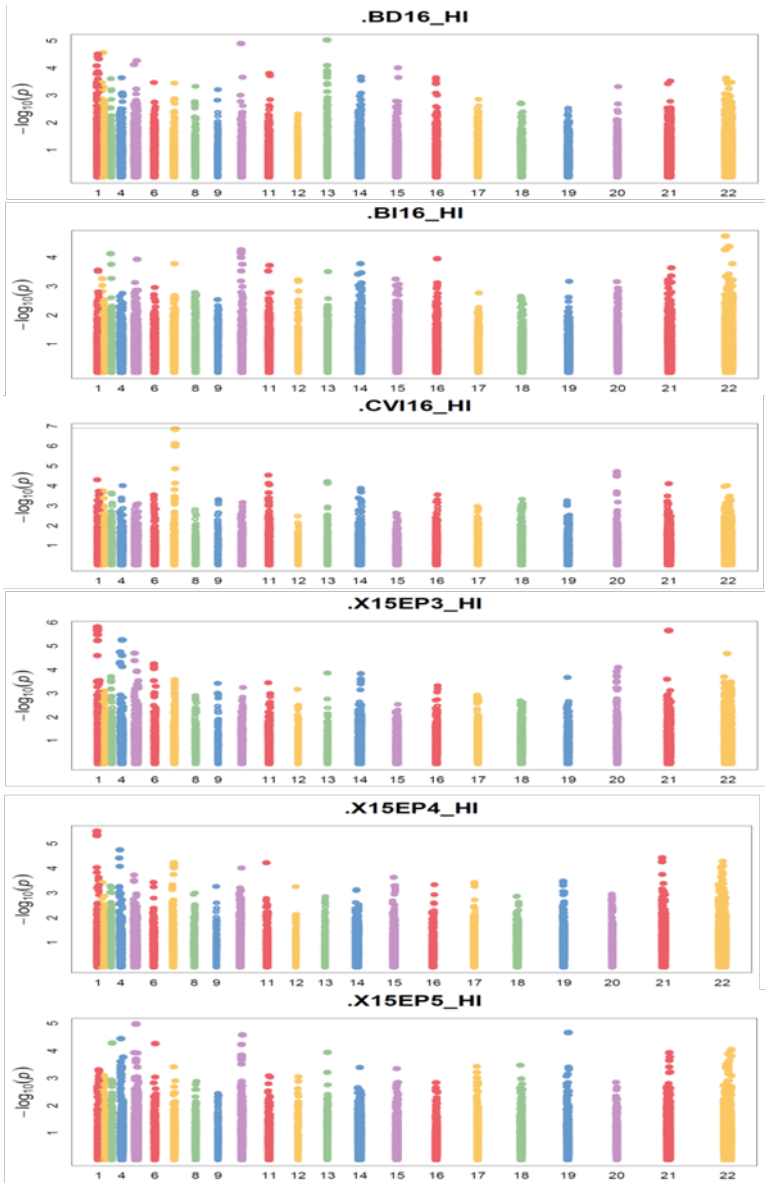

Figure 8. Manhattan plot for significant SNP associated with harvest index in different environments.

4.3.3.6 Height and test weight (HT and TW)

Two agronomic traits of height and test weight data were also included in the GWAS analysis. Totally, two QTL was identified for height and seven QTL was detected for test weight. QTL were detected for association with height onto the chromosomes 2B and 4B. The QTL on

chromosome 2B, with associated markers 5230746_2bs_22095 and 5177974_2bs_2193, explained 3.58 % to 3.78 % of the phenotypic variance across 15EP3 and 15EP4 environments. The corresponding physical location for the 2B QTL was 50 to 51 Mbp. The more significant QTL for height was identified on chromosome 4B. The markers 4910409_4bs_1741, 4954173_4bs_3367, and 4922257_4bs_9541 were closely linked to the 4B QTL, which was detected across three environments: 15EP4, 15EP5, and BD16 environments, and accounted for up to 6.32 % of the phenotypic variations. The 4B QTL for height was referenced onto the physical location at 37 to 63 Mbp regions.

For test weight, there are seven QTL located onto six different chromosomes including 2D, 3D, 4A, 5B, 6B, and 7D. For QTL identified on chromosome 2D, the closely associated markers were 5375012_2ds_3028, 5366987_2ds_8073, and 5388296_2ds_293.The corresponding R^2 for the 2D QTL was 3.73 % to 13.76 % for BD16, CVI16, and DMS16 environments. The physical location of this QTL was mapped at 109 to 127 Mbp. For the QTL on chromosome 3D, it explained 3.69 % - 4.11 % of phenotypic variances across BD16, BI16, and MCG16 environments. The associated markers of the 3D QTL were 6922682_3dl_1367, 6899730_3dl_977 and 6942710_3dl_3473. The corresponding physical location for this QTL was 479 to 516 Mbp. There are other two QTL identified on chromosome 4A and 5B, accounting for 3.57 % to 4.70 % and 3.58 % to 4.30 % of the phenotypic variations for BD16, CVI16, MCG16 environments, and BD16, BI16, MCG16 environments, respectively. The associated markers of 4A QTL were 7166605_4al_4959, 2713402_4al_14112, and 7177050_4al_7133. The closely linked markers for 5B QTL were 2276491_5bs_10745, 2234929_5bs_3053, 647748_5bs_7309, and 2269440_5bs_8454. The corresponding physical locations for QTL on 4A and 5B were 683 - 727 Mbp and 10 - 38Mbp, respectively. Two QTL was located onto

chromosome 6B, with the first one referenced on 31 to 64 Mbp and the other one on 668 to 716 Mbp of physical map. The 6B.1 QTL corresponded to the 2975664_6bs_1889, 3039630_6bs_1396, and 3043078_6bs_4791, and accounted for 3.62 % to 5.17 % of the phenotypic variance across BD16, BI16, and MCG16 environments. Five markers were identified with association for the 6B.2 QTL including 4398610_6bl_2285, 4357423_6bl_1536, 1347737_6bl_1404, 3860494_6bl_562, and 4316933_6bl_305. The phenotypic variance explained by this QTL was 3.62 % to 4.57 % for BD16, BI16, and CVI16 environments. The other QTL detected for test weight was located on chromosome 7D, and the closely associated markers were 3390938_7dl_5843, 3391820_7dl_3567, and 3352992_7dl_8035. The 7D QTL accounted for 3.51 % - 4.59 % of the phenotypic variance across BD16, BI16, and CVI16 environments. The corresponding physical location on chromosome 7D was 575 to 618 Mbp.

4.3.3.7 Heading date (HEADING)

For trait heading date, there are two significant QTL located onto the chromosome 2D and 6D (Table 20). The QTL identified on chromosome 2D, explained 3.86 % to 4.41 % of the phenotypic variance across BD16 and BI16 environments. The closely associated markers were 9894730_2dl_2064 and 4402942_6as_1927. The corresponding physical locations for 2D QTL were 613 to 640 Mbp. For the 6D QTL, the corresponding R^2 range was 3.91 % to 4.32 % for BD16 and BI16 environments. The closely linked markers are 3294879_6dl_3022 and 117920_6dl_2982. The 6D QTL was referenced onto the physical map at 462 Mbp.

4.3.3.8 Single stem weight (SSWT)

Six significant QTL across four different chromosomes including 4B, 5B, 6A, and 7A was identified for association with single stem weight (Table 20). Three QTL was identified on the chromosome 4B. The first QTL 4B.1 explained 4.34 % to 5.12% of the phenotypic variance across CVI16 and 15EP4 environments. Five closely associated markers were detected this QTL including 4954173_4bs_3367, 4952601_4bs_8944, and 4933209_4bs_13900. The corresponding location of 4B.1 QTL regarding of physical map was 55 to 95 Mbp. The second QTL located on the chromosome 4B 4B.2 was detected for significance across CVI16 and BD16 environments, with association markers 1720369_4bs_12403 and 4893378_4bs_1179. The 4B.2 QTL accounted for 4.20 % - 4.46 % of the phenotypic variations across these environments. The corresponding location of 4B.2 QTL according to physical map was 128 to 133 Mbp. The third QTL detected onto the chromosome 4B 4B.3 explained 4.28 % to 5.03 % of phenotypic variance across 15EP3 and BD16 environments. The closely linked markers for this 4B.3 QTL were 4774970_4bs_1267 and 4961132_4bs_5511. The corresponding location of 4B.3 QTL referenced to physical map was 241 to 267 Mbp. The QTL, displayed on the chromosome 5B, accounted for 4.54 % - 5.08 % of the phenotypic variations for 15EP3 and CVI16 environments. The closely linked markers were 10859743_5bl_761 and 10876715_5bl_16862. The 5B QTL was referenced onto physical map 700 to 702 Mbp. Two markers 4862369_4bs_1113 and 5815326_6al_7897 identified the QTL on chromosome 6A, and the corresponding R^2 of this QTL was 4.27 % to 5.01% across 15EP4 and BD16. The 6A QTL was mapped to physical map at 531 - 560 Mbp. For the 7A QTL, it accounted for 4.71% - 5.08 % of the phenotypic variations across 15EP4, 15EP5, and CVI16 environments. The associated markers are 4542941_7al_9623,

4551774_7al_1331, and 4558951_7al_3513. This QTL was referenced to physical genome at 711 to 730 Mbp.

4.3.3.9 Single head dry weight (SHDW)

Five QTL were detected for significance with single head dry weight, which were located onto the chromosomes 1D, 3A, 4B, 5A, and 7A. The QTL on chromosome 1D, with associated markers 2277284_1dl_9230 and 2247049_1dl_2152, explained 4.44 % to 6.25 % of the phenotypic variance across 15EP4 and BD16 environments. The corresponding location of 1D QTL referenced to physical genome was 461 to 469 Mbp. The markers 4348688_3al_419 and 4428100_3al_2570 identified the QTL on chromosome 3A, and the corresponding R^2 of the 3A QTL was 5.70 % to 6.87 % for 15EP4 and BD16. The 3A QTL was referenced onto physical map 670 to 684 Mbp. The QTL onto the chromosome 4B was detected across three environments: 15EP4, BD16, and CVI16, and accounted for 5.12 % to 6.52 % of the phenotypic variations for these environments. The closely associated markers were 9891568_2dl_3242 and 4933209_4bs_13900. The corresponding location of 4B QTL according to physical map was 88 to 95 Mbp. For the QTL on chromosome 5A, it explained 4.60 % - 4.75 % of phenotypic variances across 15EP3 and CVI16. The associated markers of the 5A QTL were 2793355_5al_1266 and 8091615_2bl_9287. The corresponding location of 5A QTL regarding of physical map was 581 to 619 Mbp. There is another QTL on chromosome 7A, accounting for 4.53 % to 5.08 % of the phenotypic variations for 15EP4 and 15EP5. The associated markers of 7A QTL were 4542941_7al_9623 and 4558951_7al_3513. The corresponding location of 7A QTL regarding of physical map was 711 to 730 Mbp.

4.3.3.10 Biomass per culm (BMPC)

Six significant QTL was identified biomass per culm on chromosome 1B, 2D, 4B, 5B, 5D, and 6D. The 1B QTL, with associated markers 3864416_1bl_1043 and 3809577_1bl_580, explained 4.15 % - 4.19 % of the phenotypic variance across BD16 and CVI16 environments. This QTL was referenced to physical genome at 430 to 431Mbp.The 2D QTL accounted for 4.37 % to 4.44 % of the phenotypic variations for BI6 and CVI16 environments. The closely associated markers were 3189801_2dl_724, 9908083_2dl_2996, and 9906847_2dl_5221. The 2D QTL was referenced onto physical map 414 to 445 Mbp. Two markers 4900567_4bs_4951 and 4774970_4bs_1267 detected the QTL on chromosome 4B, and the corresponding R^2 of this QTL was 4.19 to 4.35 % across 15EP3, BD16, and BI16. The corresponding location of 4B QTL regarding of physical map was 225 to 241 Mbp. The 5B QTL, with closely linked markers 10859743_5bl_761 and 10876715_5bl_16862, accounted for 4.53 % - 4.57 % of the phenotypic variations for 15EP3 and CVI16. The 5B QTL was referenced onto the physical map at 700 to 702 Mbp. The marker 2713457_5ds_206 discovered the QTL on chromosome 5D, which accounted for 4.45 % - 5.88 % of the phenotypic variations for BD16 and CVI16 environments. The 5D QTL was mapped to physical map at 184 Mbp. The QTL was identified on chromosome 6D with associated markers including 3296966_6dl_7394 and 3310863_6dl_7650. The corresponding R^2 for the 6D QTL was 4.26 % - 4.71 % across 15EP3 and BI16 environments. The corresponding location of 6D QTL referenced to physical map was 429 to 433 Mbp.

4.3.4 ***Common QTL associated with yield, yield components, and agronomic traits***

Common QTL for yield, yield components, and other agronomic traits were identified on the chromosome 2A, 2B, 4A, 4B, 5B, 6B, and 7A, indicating the pleiotropic effects (Table 21). The QTL, identified on the chromosome 2A, associated with spikes m^{-2} and harvest index. The marker to detect 2A QTL was mapped to the reference genome at 2 to 51 Mbp. For the QTL on chromosome 2B, peaked at the 30 to 51 Mbp on physical map, it has

Table 21. Common QTL identified associated with yield and yield components from GWAS.

Common QTL ID	Trait†	Chrom	PseudoM_ physicalPosition (Mbp)	Significant Markers	QTL ID	LOD‡	R2 (%)	Env§
1	HI	chr2A	3 - 51	5284462_2as_8447	35	4.42 - 4.75	3.60 - 5.07	15EP3, 15EP4, 15EP5
1	SPM	chr2A	2 - 18	5300435_2as_1323	35	4.09 - 4.41	3.52 - 3.75	15EP4, 15EP5
2	HI	chr2B	30 - 34	5200367_2bs_9023	50	4.12 - 4.70	3.58 - 3.71	BD16, 15EP3
2	HT	chr2B	50 - 51	5177974_2bs_2193	51	4.62 - 4.78	3.58 - 3.78	15EP3, 15EP4
3	TKW	chr4A	640 - 689	7083588_4al_2078	130	4.31 - 5.97	4.04 - 6.98	15EP3, 15EP4, 15EP5
3	KPS	chr4A	661 - 698	7107364_4al_2064	131	4.40 - 5.31	3.60 - 4.05	BD16, CVI16, 15EP5
3	TW	chr4A	683 - 727	2713402_4al_14112	131	4.29 - 5.75	3.57 - 4.70	BD16, CVI16, MCG16
4	HI	chr4B	93	3114055_1al_647	134	5.36 - 5.81	4.50 - 4.74	15EP3, 15EP4
4	HT	chr4B	37 - 63	4954173_4bs_3367	134	4.17 - 7.83	4.18 - 6.32	BD16, 15EP4, 15EP5
4	SHDW	chr4B	88 - 95	9891568_2dl_3242	134	4.09 - 5.81	5.12 - 6.52	CVI16, BD16, 15EP4
4	SSWT	chr4B.1	55 - 95	4954173_4bs_3367	134	4.09 - 4.65	4.34 - 5.12	CVI16, 15EP4
5	BMPC	chr5B	700 - 702	10859743_5bl_761	181	4.27 - 4.34	4.53 - 4.57	CVI16, 15EP3
5	SSWT	chr5B	700 - 702	10859743_5bl_761	181	4.33 - 4.86	4.54 - 5.08	CVI16, 15EP3
6	SPM	chr6B	20 - 31	2977047_6bs_5685	205	4.09 - 4.72	3.74 - 4.05	15EP3, 15EP5
6	TW	chr6B.1	31 - 64	2975664_6bs_1889	205	4.21 - 5.62	3.59 - 5.17	BD16, BI16, MCG16
7	SHDW	chr7A	711 - 730	4542941_7al_9623	240	4.06 - 4.30	4.53 - 5.08	15EP4, 15EP5
7	SSWT	chr7A	711 - 730	4551774_7al_1331	241	4.06 - 4.56	4.71 - 5.08	CVI16, 15EP4, 15EP5

†Abbreviation of traits: Yield (YLD), thousand kernel weight (TKW), kernels spike^{-1} (KPS), spikes m^{-2} (SPM), harvest index (HI), hand harvest dry grain (HHY), head dry weight (HDWT), single stem weight (SSWT), single seed dry weight with glume (SHDW), biomass er culm (BMPC), height (HEIGHT), test weight (TW), heading date (HEADING).
‡-log(p-value).
§Abbreviation of environments: Chillicothe, TX in 2017 (CH17), Bushland, TX dryland and irrigated land in 2017 and 2016 (BI17, BD17, BD16, and BI16), Dumas, TX irrigated area in 2017 and 2016 (DMS17 and DMS16), Clovis, NM irrigated area in 2016 and 2017 (CVI17 and CVI16), McGregor, TX irrigated locations in 2016 (MCG16), and three irrigated levels (50%, 75%, and 100%) in Etter, TX in 2015 (15EP3, 15EP4, and 15EP5).

significant association with height and harvest index. The markers, identified the QTL on chromosome 4A, were referenced on the physical position of 640 to 727 Mbp. This 4A QTL was shown significant interaction with thousand kernel weight, kernels spike^{-1} and test weight. For the QTL on chromosome 4B, which significantly influenced harvest index, height, single stem weight, and single head dry weight, the closely linked markers were located onto the physical map 37 to 95 Mbp range. The QTL on chromosome 5B linked with the traits biomass per culm and single stem weight, and associated markers for this QTL was referenced at 700 to 702 Mbp. The markers detected the QTL on chromosome 6B was significantly associate with spikes m^{-2} and test weight. The markers were mapped on the physical map at 20 to 64 Mbp. The marker of the QTL for single stem weight and single head dry weight on chromosome 7A were located on the 711 to 730 Mbp position of physical map.

4.4 Discussion

Ten thousand years of domestication, and modern breeding, have increased the tolerance of wheat crops to environmental stresses but resulted in the loss of 69% of its genetic diversity (Reif et al., 2005). Nowadays, narrow genetic basis and continuous pressure from abiotic and biotic stress pose a huge challenge of achieving sustainable food security for wheat (Hubert et al., 2010). Furthermore, global food demand is expected to be double by 2050. Modern wheat improvement heavily relied on crossing between elite varieties (Hao et al., 2011). SHW represents a promising source for improving qualitative and quantitative traits in present day wheat breeding. Even though many studies have shown SHW is among one of the options to introduced genetic diversity into the genome of common wheat (Ogbonnaya et al., 2013) and showed increased resilience to environments stress including biotic and abiotic factors

(Ogbonnaya et al., 2013), the SHW has displayed a very poor performance of agronomic aspects and end-use quality. As a result, repeatedly processes of backcrossing to elite common wheat generated SDW, which has been reported to have better agronomic performance and end-use quality (Mujeeb-Kazi et al., 2008; Lopes and Reynolds, 2011). Studies also demonstrated potential for yield improvement in SDW (Ogbonnaya et al., 2013). Molecular analysis of these SDW lines has indicated improvement in the genetic diversity of bread wheat genome (Dreisigacker et al., 2008). SDW is characterized by higher grain yield than elite varieties primarily due to improvement in yield component (Warburton et al., 2006). Thus, the dissection of the genetic architecture underlying complex yield and yield components traits in large number of SDW lines is helpful to improve the utilization of these germplasms, and to provide a clue for MAS in wheat breeding process. In this study, we describe the application of the whole genome association mapping to evaluate yield, ten yield components, and three agronomic traits in a collection of 420 SDW lines. GWAS results are strongly influenced by the phenotypic information, especially for grain yield, which is a complex quantitative trait. Significant genetic variations for each of these traits were identified between lines, as well as between the environments. Most of the traits assessed in this study expressed high heritability.

Population structure is one of the most confounding factors in GWAS. The presence of population stratification and an unequal distribution of alleles within a population can result in nonfunctional, spurious association (Knowler et al., 1988). In this study, the 419 accessions were subgrouped into two major cutlers by STRUCTURE based on genotypic data. Highly consistent with the pedigree information, the population structure is largely dependent on the maternal parents of the hybrid cross. Although the accessions included in this study were based on synthetic hexaploid wheat crossing with two elite TAM varieties, the partitioning of the global

genetic diversity in synthetic hexaploid wheat remains a distinct feature of this diverse panel. In fact, for the majority of crop species, particularly for self-pollinating cereals like wheat, the presence of non-random 'background' co-ancestry among accessions, for example, population structure and familial relationship, is a common feature of advanced breeding materials (Flint-Garcia et al., 2005; Maccaferri et al., 2005; Cockram et al., 2008). Since population structure greatly affects type I and type II errors in marker-trait associations, the genetic effects due to the population structure need to be appropriately accounted for (Pritchard and Rosenberg, 1999). The MLM model by fitting a population structure (Q) and kinship effect (K) was performed on both GAPIT and TASSLE platform. With the increased stringency and threshold of the models, the power of detecting small effect SNPs will be reduced. However, reducing the stringency of the model would increase the variation explained by the marker, but at the same time would result in more false positives, especially in inbreeding crops like wheat, it is difficult to preclude completely the effect of relationship among genotypes by applying simpler models. Hence, GWAS in highly structured populations of inbreeding crops such as wheat will depend on the careful optimization of the model based on the sensitivity and selectivity.

Even the best associations identified in this study, most of the traits including yield, yield components, and agronomic traits showed only modest corresponding R^2 values, which means the percentage of the phenotypic variations explained by the genetic locus, suggesting low variance predicted by each GBS marker. Many GWAS results in plants have reported low R^2 values, which are usually ranged around 5 %, and correspond well with this study, and the rest of the unexplained variation is termed as "unexplained missing heritability" (Pasam et al., 2012). Possible explanations including the insufficient marker coverage, resulting in the causal polymorphism is not in the perfect LD with the genotyped marker. Consequently, it reduces the

power to detect association and the variation explained by such specific a marker. However, in this study, one of our primary motivations for performing GBS is to enable GWAS, which requires a large number of sequencing markers to provide adequate coverage of the entire wheat genome, up to 188K of GBS markers should be sufficient to offer exhaustive coverage of the wheat genome and ensure each causative polymorphism stands a reasonable chance of being in LD with at least one markers. Another possible reason is that rare alleles (MAF less than 5 %) with a major genetic effect have been dropped from the following GWAS analysis and will go undetectable for their trait associations. The most rational explanation is because the variation expressed of a trait strongly depends on a large number of genes/QTL with small individual effects where insufficient statistical power to detect the significant marker-trait associations. Yield and yield-related traits is under genetic, developmental and also environmental influence. Many QTL studies results show QTL associated with yield and yield-related traits have been identified on almost all wheat chromosomes. Evaluating QTL across several environments conditions is essentials to achieve stable and validated QTL, which is the important basis for dissecting the candidate genes further. In this study, QTL associated with each trait have been included in at least two environments. Besides, wheat genome has large repetitive and non-coding sequence (Bennetzen et al., 2005). Compared with 90K SNP array data, the proportion of gene-based markers identified from ddRAD-seq should be lower than that from 90K wheat SNP array. The non-coding elements controlling the traits should have more probability to be identified in GWAS. Several other arguments should also be taken into consideration for explaining the small effect on GWAS study: insufficient statistic tools to analyze the epistatic effect. GWAS studies depend on the maker-trait association. Epistasis, or interactions between genes/loci, has long been recognized as fundamentally important to understanding the structure

and function of genetic pathways and the evolutionary dynamics of complex genetic traits. However, the effects of many QTLs might be obscured by interactions with other loci, which can make mapping or GWAS difficult to perform and replicate (Phillips, 2008).

4.5 References

Bates, D., M. Maechler, B. Bolker, and S. Walker. 2014. lme4: Linear mixed-effects models using Eigen and S4. R package version 1.1-14. http://CRAN.R-project.org/package=lme4/index.html (accessed 29 Sep. 2017).

Bennetzen, J.L., J.X. Ma, and K.M. Devos. 2005. Mechanisms of recent genome size variation in flowering plants. Ann. Bot. 95: 127-132. doi: 10.1093/aob/mci008

Bradbury, P.J., Z. Zhang, D.E. Kroon, T.M. Casstevens, Y. Ramdoss, and E.S. Buckler. 2007. TASSEL: software for association mapping of complex traits in diverse samples. Bioinformatics 23: 2633-2635. doi: 10.1093/bioinformatics/btm308

Dreisigacker, S., R. Tiwari, and S. Sheeran. 2013. ICAR-CIMMYT molecular breeding course in wheat laboratory manual. http://repository.cimmyt.org/xmlui/bitstream/handle/10883/3221/98133.pdf (accessed 28 Jun. 2015).

Hao, C., L. Wang, H. Ge, Y. Dong, and X. Zhang. 2011. Genetic diversity and linkage disequilibrium in Chinese bread wheat (Triticum aestivum L.) revealed by SSR markers. PLoS one 6: e17279. doi: 0.1371/journal.pone.0017279

Hubert, B., M. Rosegrant, M.A.J.S. van Boekel, and R. Ortiz. 2010. The future of food: scenarios for 2050. Crop. Sci. 50: S33-S50. doi:10.2135/cropsci2009.09.0530

Jafarzadeh, J., D. Bonnett, J.L. Jannink, D. Akdemir, S. Dreisigacker, and M.E. Sorrells. 2016. Breeding Value of Primary Synthetic Wheat Genotypes for Grain Yield. PloS one 11: e0162860. doi: 10.1371/journal.pone.0162860

Kosambi, D.D. 1943. The estimation of map distances from recombination values. Ann. Hum. Genet. 12: 172-175. doi: 10.1111/j.1469-1809.1943.tb02321.x

Lipka, A.E., F. Tian, Q. Wang, J. Peiffer, M. Li, P.J. Bradbury, M.A. Gore, E.S. Buckler, and Z. Zhang. 2012. GAPIT: genome association and prediction integrated tool. Bioinformatics 28:2397-2399. doi: 10.1093/bioinformatics/bts444

Lopes, M.S. and M.P. Reynolds. 2011. Drought adaptive traits and wide adaptation in elite lines derived from resynthesized hexaploid wheat. Crop. Sci. 51: 1617-1626. doi: 10.2135/cropsci2010.07.0445

Mujeeb-Kazi A., V. Rosas, and S. Roldan. 1996. Conservation of the genetic variation of Triticum tauschii (Coss.) Schmalh. (Aegilops squarrosa auct. non L.) in synthetic hexaploid wheats (T. turgidum L. s.lat. x T. tauschii; 2n = 6x = 42, AABBDD) and its potential utilization for wheat improvement. Genet. Resources Crop. Evol. 43: 129-134. doi: 10.1007/BF00126756

Mujeeb-Kazi, A., G. Fuentes-Davila, R. Delgado, V. Rosas, S. Cano, A. Cortes, L. Juarez, and J. Sanchez. 2000. Current status of D-genome based, synthetic, hexaploid wheats and the characterization of an elite subset. Ann Wheat Newsl. 46: 76-79.

Mujeeb-Kazi A., A. Gul, M. Farooq, S. Rizwan, and I. Ahmad. 2008. Rebirth of synthetic hexaploids with global implications for wheat improvement. Aust. J. Agric. Res. 59: 391-398. doi: 10.1071/AR07226

Mujeeb-Kazi, A. and R. Delgado. 2001. A second, elite set of synthetic hexaploid wheats based upon multiple disease resistance. Ann Wheat Newsl. 47: 114-115.

Ogbonnaya, F. C., O. Abdalla, A. Mujeeb-Kazi, S. Xu , N. Gosman, E. S. Lagudah, D. Bonnett, M. E. Sorrells, and H. Tsujimoto. 2013. Synthetic hexaploids: harnessing species of the primary gene pool for wheat improvement. Plant Breeding Reviews. John Wiley & Sons, Inc., Hoboken, NJ. 37: 35-122. doi: 10.1002/9781118497869

Ogbonnaya, F.C., G.Y. Ye, R. Trethowan, F. Dreccer, D. Lush, J. Shepperd, and M. Van Ginkel. 2007. Yield of synthetic backcross-derived lines in rainfed environments of Australia. Euphytica 157: 321-336. doi: 10.1007/s10681-007-9381-y

Patel, R.K. and M. Jain. 2012. NGS QC Toolkit: A Toolkit for Quality Control of Next Generation Sequencing Data. PLoS One 7: e30619. doi:10.1371/journal.pone.0030619

Pasam, R.K., R. Sharma, M. Malosetti, F.A. van Eeuwijk, G. Haseneyer, B. Kilian, and A. Graner. 2012. Genome-wide association studies for agronomical traits in a world wide spring barley collection. BMC plant boil. 12: 16. doi: 10.1186/1471-2229-12-16

Phillips, P.C. 2008. Epistasis—the essential role of gene interactions in the structure and evolution of genetic systems. Nat. Rev. Genet. 9: 855-867. doi: 10.1038/nrg2452

Poland, J.A., P.J. Brown, M.E. Sorrells, and J.L. Jannink. 2012. Development of high-density genetic maps for barley and wheat using a novel two-enzyme genotyping-by-sequencing approach. PLoS one 7: e32253. doi: 10.1371/journal.pone.0032253

Pritchard, J.K., M. Stephens, and P. Donnelly. 2000. Inference of population structure using multilocus genotype data. Genetics 155: 945-959.

Reif, J.C., P. Zhang, S. Dreisigacker, M.L. Warburton, M. van Ginkel, D. Hoisington, M. Bohn, and A.E. Melchinger. 2005. Wheat genetic diversity trends during domestication and breeding. Theor. Appl. Genet. 110: 859-864. doi:10.1007/s00122-004-1881-8

Schwarz, G. 1978. Estimating the dimension of a model. Ann. Stat. 6: 461-464. doi: 10.1214/aos/1176344136

Sehgal, D., E. Autrique, R. Singh, M. Ellis, S. Singh, and S. Dreisigacker. 2017. Identification of genomic regions for grain yield and yield stability and their epistatic interactions. Sci. Rep. 7: 41578. doi: 10.1038/srep41578

Van Ginkel, M. and F. Ogbonnaya. 2007. Novel genetic diversity from synthetic wheats in breeding cultivars for changing production conditions. Field Crop. Res. 104: 86-94. doi: 10.1016/j.fcr.2007.02.005

Van Ooijen, J.W. 2004. MapQTL® 5, Software for the mapping of quantitative trait loci in experimental populations. Kyazma BV, Wageningen, Netherlands.

Van Ooijen, J.W. 2006. JoinMap 4, Software for the calculation of genetic linkage maps in experimental populations. Kyazma BV, Wageningen, Netherlands.

Varshney, R.K., R. Terauchi, and S.R. McCouch. 2014. Harvesting the Promising Fruits of Genomics: Applying Genome Sequencing Technologies to Crop Breeding. PLoS Biol. 12: e1001883. doi: 10.1371/journal.pbio.1001883

Lynch, M. and B. Walsh. 1998. Genetics and Analysis of Quantitative Traits. Sinauer Associates, Inc, Sunderland, MA.

Wang, S., D. Wong, K. Forrest, et al. 2014. Characterization of polyploid wheat genomic diversity using a high-density 90 000 single nucleotide polymorphism array. Plant Biotechnol. J. 12: 787-796. doi: 10.1111/pbi.12183

Yu, J., G. Pressoir, W.H. Briggs, I.V. Bi, M. Yamasaki, J.F. Doebley, M.D. McMullen, B.S. Gaut, D.M. Nielsen, J.B. Holland, and S. Kresovich. 2006. A unified mixed-model method for association mapping that accounts for multiple levels of relatedness. Nat. Genet. 38: 203-208. doi: 10.1038/ng1702

Zhang, D., G. Bai, C. Zhu, J. Yu, and B.F. Carver. 2010. Genetic diversity, population structure, and linkage disequilibrium in U.S. elite winter wheat. Plant Genome 3:117-127. doi: 10.3835/plantgenome2010.03.0004

Zhu, C., M. Gore, E.S. Buckler, and J. Yu. 2008. Status and Prospects of Association Mapping in Plants. Plant Genome 1: 5-20. doi: 10.3835/plantgenome2008.02.0089

CHAPTER V

SUMMARY AND CONCLUSIONS

This dissertation focused on stripe rust resistance, yield and yield components of wheat breeding using a high- saturated genetic map constructed by 90K SNP array and GBS. We used RIL derived from bi-parental population and synthetic derived lines to map significant QTL associated with the target traits and characterized these QTL or candidate genes to applied in MAS.

In chapter II, A mapping population of 124 F_6 recombinant inbred lines (RILs) developed from the cross "TAM 112/TAM 111" was developed. A set of 9928 markers forming 80 chromosome fragments and covering all 21 chromosomes, including 19 SSR and STS, 5094 GBS, 4815 SNPs from 90K were used for QTL analyses. The largest and most consistent stripe rust resistance QTL was identified on the long arm of chromosome 2B, explained for 9% to 49.2% of the phenotypic variance in Infection type (IT) and 3.1% to 28.5% of the variance in disease severity (DS) across the environment. Five tightly linked SNP markers were converted to Kompetitive allele specific PCR (KASP) marker for high throughput screening and used to estimate the effects of these genes/QTL. IWB47487, IWB26631, and IWB29391 are the closest markers and are found to be very effective in predicting stripe rust resistance allele from TAM 111. These markers can be used together to increase selection accuracy. *QYr.tamu-2A* was involved in three out of six epistatic interactions for DS, one of which with the major QTL *QYr.tamu-2BL*. This pair of QTL was also found to impart significant interaction for IT. Significant epistasis by environment interactions for DS, existed between *QYr.tamu-2A* and *QYr.tamu-2BL*, was showed in seven out of twelve environments, and this pair QTL has the

largest epistasis effect. These QTL should be considered as effective major genes which enhance the stripe rust resistance, and corresponding diagnostic markers should be applied through marker-assisted breeding. Some minor QTL or epistatic effects can be used in pyramiding the major stripe rust resistance QTL with other resistance genes to achieve an increased level of durable resistance.

In chapter III, the wheat 90K Infinium iSelect SNP array and GBS were used in construction of high-saturated genetic map for QTL mapping associated with grain yield and yield components. Different QTL mapping results were provided using single trait with single environment from MapQTL, single trait with multiple environment through genome-wide scan from GenStat, and additive effect, additive by environment interaction, epistatic effect, and epistatic by environment interaction from QTLNetwork. Mega-environmental analysis was conducted with single environment testing to maximize the genetic effects of each individual trait. Then comparative analysis was conducted to identify four common and consistent QTL from different software and different environments analysis. Those four QTL were mapped onto the chromosome 1D2, 2D1, 4D, and 7D1. Closely associated markers of those common QTL underlying different yield traits were blasted for potential gene function annotation. The marker IWA1247 linked to 7D1 QTL for several traits was annotated as wheat starch synthase I gene. This study provides an excellent opportunity for increasing the efficiency and accuracy of MAS and future genetic studies of functional analysis, and highly-saturated genetic map used in this work directly support map-based gene cloning of candidate gene in the future.

The fourth chapter focused on SDW, which has been reported to produce more yield than cultivated wheat. To understand the genetics of marker-trait associations underlying yield performance in SDW lines, field trials were conducted at nine locations over three years. Yield,

eight yield components, and two agronomic traits including height and heading date were measured on a panel of 419 diverse SDW lines. We employed GBS to identify the genetic loci for yield traits though GWAS. All accessions clustered into two subgroups, which is highly consistent with their pedigree that eight derived from synthetic spring lines crossing with TAM 111 or TAM 112. After correcting for population structure and using mixed linear model, the results of this study uncovered 45 loci associated with yield, yield components, and agronomic traits in individual environment respectively based on best linear unbiased predication values. Of these, ten loci on chromosomes 1A, 1B, 2A, 2B, 2D, 4A, 4B, 6D, and 7D had pleiotropic effects. Candidate genes were analyzed for co-localized with such QTL, thereby providing potential targets for selection. This study will enable wheat breeders to effectively introgress several desirable alleles into locally adapted germplasm in developing wheat varieties with high yielding potential.